Bend-Optimization for Ortho-Radial Drawings

Master Thesis of

Noah Zuch

At the Department of Informatics and Mathematics
Chair of Theoretical Computer Science

Reviewers:	Prof. Dr. Ignaz Rutter
	Prof. Dr. Christian Bachmaier
Advisors:	Prof. Dr. Ignaz Rutter
	Simon Dominik Fink

Time Period: 26st December 2022 – 26st June 2023

Statement of Authorship

I hereby declare that this document has been composed by myself and describes my own work, unless otherwise acknowledged in the text.

Passau, May 31, 2023

Abstract

An ortho-radial drawing is a straight-line drawing of a graph with right angles between edges drawn on the ortho-radial grid. This grid is composed of increasingly growing concentric rings around a center point and evenly spaced spokes emanating from the center. An ortho-radial drawing can be created by finding a valid ortho-radial representation of the graph in the TSM framework. Up to now, no efficient algorithm for finding such a representation is known except for an optimized Integer-Linear Program, which still may require an exponential amount of time. This work shows that for plane 4-graphs, the problem of finding a bend-free valid ortho-radial drawing is NP-complete by reducing the 3-Sat-problem to it. The decisive property of ortho-radial representations used by the reduction is the global condition that every simple essential cycle must contain edges of specific labels. Further, when restricting oneself to consider series-parallel plane 3-graphs, a quadratic runtime can be achieved for findin a bend-free valid ortho-radial representation if one exists. For so-called 2-legged series-parallel plane 3-graphs, even a linear runtime is possible for bend-minimum valid ortho-radial representations.

Deutsche Zusammenfassung

Eine ortho-radiale Zeichnung eines Graphens ist, ähnlich zu orthogonalen Zeichnungen, eine Zeichnung mit rechten Winkeln zwischen geraden Kanten. Der Unterschied liegt darin, dass ortho-radiale Zeichnungen auf einem Gitter bestehend aus mehreren größer werdenden konzentrischen Ringen und von der Mitte ausgehende geradlinige Linien gezeichnet werden. Eine ortho-radiale Zeichnung kann mittels einer validen ortho-radialen Repräsentation via dem TSM-Framework erstellt werden. Bisher gab es jedoch keine effiziente Möglichkeit, eine solche Repräsentation zu erstellen. Diese Arbeit zeigt, dass für allgemeine 4-Graphen das Finden einer validen ortho-radialen Repräsentation ohne Knicke NP-vollständig ist, indem es auf das 3-Sat Problem reduziert wird. Ausschlaggebend für diese Reduktion ist die globale Bedingung valider ortho-radialer Repräsentationen, dass jeder einfache essenzielle Kreis Kanten mit gewissen Labeln besitzen muss. Diese Arbeit zeigt außerdem, dass dieses Problem in quadratischer Laufzeit für serien-parallele 3-Graphen lösbar ist und für sogenannte zwei-beinige serien-parallele 3-Graphen sogar eine lineare Laufzeit für das Finden von knick-minimaler valider ortho-radialer Repräsentationen erreichbar ist.

Contents

1 Introduction **1**

2 Preliminaries **5**

3 NP-Completeness For General Plane 4-Graphs **11**
3.1 The Scaffolding 11
3.2 Widgets With Predictable Labels 13
3.3 Clause-Cycles 15
3.4 Synchronizing L-Widgets 16
3.5 Putting Things Together 20

4 Polynomial-Time Algorithm For Series-Parallel 3-Graphs **25**
4.1 2-Legged Series-Parallel 3-Graphs 26
4.1.1 Creating Decomposition Trees 26
4.1.2 Finding Bend-Free Ortho-Radial Representations 28
4.1.3 Finding Bend-Minimum Ortho-Radial Representations 46
4.2 Non-st-Outwards Ortho-Radial Representations 50
4.2.1 General Step Values 50
4.2.2 Creating Ortho-Radial Representations 57
4.3 General Series-Parallel 3-Graphs 82

5 Conclusion **89**

Bibliography **91**

1. Introduction

Orthogonal drawings naturally arise from the desire to make the information encoded in a graph accessible to a human reader. Their angles of strict 90 degrees and edges having similar lengths make it easy to trace paths and group information. An orthogonal drawing is an embedding of the graph into the standard grid, where vertices are mapped to points and edges are composed of the vertical and horizontal paths between them. The two arguably most important aesthetic criteria for orthogonal drawings are planarity, meaning no edges cross except at their endpoints, and the number of bends required to place edges only on the lines of the grid. Great work has gone into minimizing the number of bends in a planar orthogonal drawing [GT97, CK12, BBR14, BK94, BKRW11, BLR15, REN06, ZN05, DKLO22, DBLV98]. A natural extension to orthogonal drawings are *ortho-radial* drawings, which are drawings embedded on the *ortho-radial grid* consisting of increasingly growing concentric rings around a center point and evenly spaced spokes emanating from the center. Vertices are placed on the intersection of these lines and edges are composed of the paths between them. Ortho-radial drawings can arguably, compared to orthogonal drawings, put better emphasis on the part of the graph placed in the center of the grid and can better represent the layered nature of a graph. Moreover, ortho-radial drawings have the possibility to reduce the required number of bends compared to an orthogonal drawing as seen in Figure 1.1.

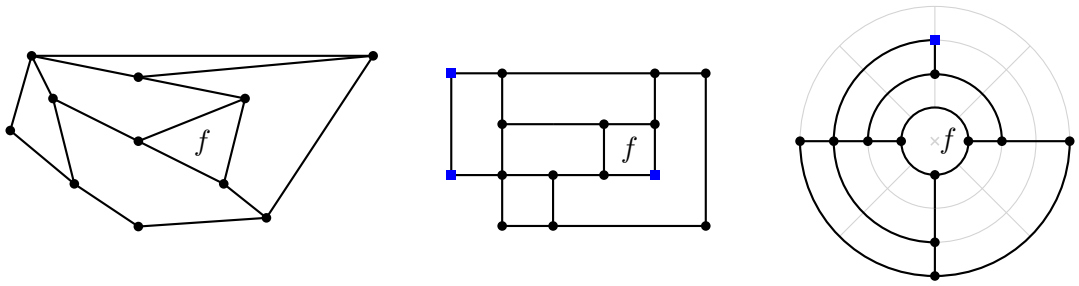

(a) (b) (c)

Figure 1.1: A plane graph (a) and an orthogonal drawing (b) as well as an ortho-radial drawing (c) of it. Both representations have bends indicated by square vertices. The orthogonal drawing is bend-minimum with 3 bends, while the ortho-radial drawing only has 1 bend.

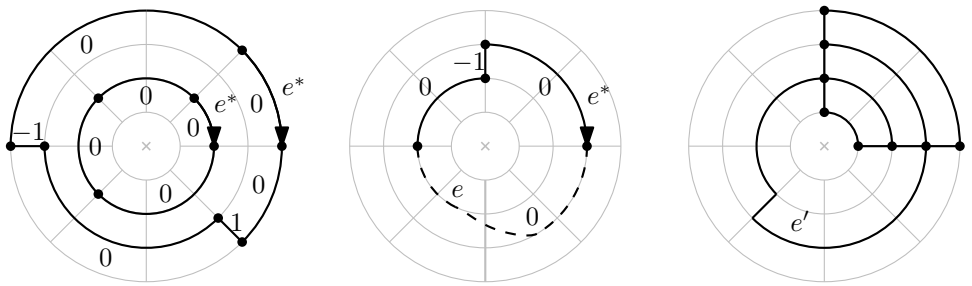

Figure 1.2: An ortho-radial drawing of two cycles (a) and an ortho-radial representation of a cycle that is not drawable (b) because the edge e changes concentric cycles without bending. Nevertheless, the sum of angles around each vertex is 360° and all faces have the same total rotation of 0 in both representations. A bend-minimum ortho-radial drawing (c), having an edge e' that bends both to the left and to the right.

Many algorithms for finding orthogonal drawings use the seminal work of Tamassia [Tam87], where this process is split up into three steps known as the *topology-shape-metric framework* (TSM). The topology step chooses a planar embedding of the graph to eliminate crossing edges. The shape step finds an orthogonal representation, which only describes the angles between edges and excludes the concrete lengths of an edge. The metric step finally assigns a length to each edge, resulting in an orthogonal drawing. Barth et al. [BNRW21] have recently adapted this three-step idea to ortho-radial drawings by introducing the notion of ortho-radial representations. However, their work only covers parts of the framework and a result about the runtime of finding such a valid ortho-radial representation is not included. Compared to orthogonal representations, ortho-radial representations have to be so-called *valid* to always imply an ortho-radial drawing of the graph. This validity condition is not local to a vertex or face of the graph, but a global one, resulting from the possibility of drawing connected cycles around the center. Here, the situation may arise that this cycle does not reconnect to its starting point because it ends at a different concentric ring. Figure 1.2 shows this problem based on an example. It also illustrates that a bend-minimum ortho-radial representation may have both a left and right bend in a single edge. A situation, that would never occur in bend-minimum orthogonal representations. Adapting the efficient network-flow technique used to find orthogonal representations [CK12] is unlikely to succeed since encoding the global condition of ortho-radial representations in these networks is difficult. In this work, we show that finding a bend-free valid ortho-radial representation is in general NP-complete, even if a fixed embedding of the graph is assumed. A polynomial runtime can be achieved though, when restricting the graph to be a series-parallel plane 3-graph. Specifically, we define the problem Bend-Free-Ortho-Radial as, given a plane 4-graph $(G, \mathcal{E})$, with a fixed embedding $\mathcal{E}$, a fixed outer face f_o, and a fixed inner face f_c, to check if G admits a valid bend-free ortho-radial representation of G using the fixed embedding $\mathcal{E}$ as well as the outer face f_o and inner face f_c. The existence of such a representation is then equivalent to the existence of an ortho-radial drawing [BNRW21].

Related Works: The complexity of finding planar orthogonal drawings has been widely studied and can roughly be grouped into results considering planar graphs, where the drawing may use any planar embedding of the graph, and plane graphs, where the planar embedding is fixed. In the case of plane graphs, Garg et al. [GT97] give an approach using a minimum cost flow network to find a bend-minimum orthogonal representation in $\mathcal{O}(n^{7/4}\sqrt{\log(n)})$ time by using the TSM framework of Tamassia [Tam87]. Later, Cornelsen et al. [CK12] improved this bound to $\mathcal{O}(n^{3/2})$ by taking advantage of the planarity of

the used flow network. Only for planar graphs is the problem of finding a bend-free, and therefore also bend-minimum, orthogonal representation NP-complete [GT01]. Another modification making bend-minimum orthogonal drawings of plane graphs NP-complete is using the Kandinsky-Model [BBR14], where a vertex may have multiple outgoing edges in the same direction and the degree of a vertex is no longer limited to 4. A k-embedding is an orthogonal drawing of a planar graph where each edge separately has at most k bends. A 2-embedding exists for all planar 4-graphs except the octahedron graph [BK94] and the existence of a 0-embedding, being equivalent to a bend-free orthogonal drawing is, as previously said, NP-complete. A 1-embedding can be found in polynomial time [BKRW11] and an FPT-algorithm can be formed with respect to k being the number of edges that require 0 bends and having an endpoint with degree 4 [BLR15].

Rahman et al. [REN06] use the recursive structure of series-parallel graphs to test in linear time whether a planar series-parallel 3-graph admits a bend-free orthogonal drawing and, in the case one exists, to find one. In case no orthogonal drawing with zero bends exists, Zhou et al. [ZN05] use a similar approach to then also find a drawing with the minimum number of bends. Recently, Didimo et al. [DKLO22] gave a linear-time algorithm for computing a bend-minimum orthogonal drawing for a plane series-parallel 4-graph. Di Battista et al. [DBLV98] analyzed the complexity of finding a bend-minimum orthogonal drawing for plane graphs and achieved a polynomial-time algorithm for general 3-graphs as well as series-parallel 4-graphs.

The problem of finding an ortho-radial drawing of a planar graph using C-shapes was investigated by Hasheminezhad et al. [HHT09], who found that different to P-shapes for orthogonal representations, the existence of a C-shape for a graph is not equivalent to the existence of an ortho-radial drawing. Barth et al. [BNRW21] use the TSM framework to show that the existence of a valid ortho-radial representation is equivalent to the existence of an ortho-radial drawing. Moreover, they show that creating an ortho-radial drawing given a valid ortho-radial representation is possible in quadratic time. Niedermann et al. [NR20] give an Integer-Linear-Program to search for a valid ortho-radial representation of a given plane 4-graph, which can still has an exponential runtime. Up to now, no other results about finding ortho-radial representations exist. This work now uses the notion of ortho-radial representations and shows that the problem of finding a bend-free ortho-radial drawing is NP-complete. It also gives the first sub-exponential algorithm of finding bend-free and bend-minimum valid ortho-radial representations for series-parallel 3-graphs.

Contribution and Outline: The preliminaries in Chapter 2 introduce basic definitions and facts about ortho-radial and orthogonal representations, as well as small changes to their definition compared to other literature. Chapter 3 covers the proof that finding a bend-free ortho-radial drawing is NP-complete for general graphs, while Chapter 4 shows algorithms to find such a representation for series-parallel 3-graphs. Specifically, Section 4.1 gives a linear-time algorithm to find a bend-minimum valid ortho-radial representation, if one exists, for so-called 2-legged series-parallel 3-graphs, and Section 4.3 generalizes this to normal series-parallel 3-graphs resulting in a quadratic runtime to search for bend-free valid ortho-radial representations.

2. Preliminaries

A graph of maximum degree n is called an *n-graph*. For an oriented edge $\vec{e}$, we use the notation $\overleftarrow{e}$ to represent the edge in its reversed orientation. Paths and cycles contain edges in its undirected form, but the traversal of one implies an orientation of its edges. We assume that a path in a graph is always simple, meaning it contains a vertex at most once. Cycles, on the other hand, can contain vertices multiple times. For a path P, we use the notation $P[u, v]$ to mean the subpath of P between vertices u and v on the path. For edges e and f on the path, $P[e, f]$ represents the subpath of P between e and f including their endpoints and $P(e, f)$ represents this subpath excluding their endpoints. The length of a path represents the number of vertices contained in it. The concatenation of two paths is represented by $P + Q$, and the reverse of a path P is $\overline{P}$.

A *planar drawing* of a graph G is a straight-line drawing of G on the plane where no two edges cross except at their endpoints, and a graph is called *planar* if it admits such a drawing. A planar drawing partitions the plane into disjunct faces, where each face is represented by the cycle formed by its incident edges. An *embedding* $\mathcal{E}$ of a graph G represents an equality class of planar drawings of G that all partition the plane into the same set of faces. A *rotation scheme* $[v_1, \ldots, v_k]$ around a vertex v is a cyclic ordering of its adjacent vertices, and an embedding is uniquely described by a rotation scheme for each vertex. A graph G embedded in a plane with a specific fixed embedding $\mathcal{E}$ is called a *plane graph* $(G, \mathcal{E})$. A simple cycle C in a plane graph separates the set of faces into two disjunct subsets. When selecting one face to be the *outer face* f_o of the plane graph, one of the subsets must contain this outer face. We call the edges and vertices that are incident to a face in this subset the *exterior* of C. The incident edges and vertices to a face in the other subset is called the *interior* of C. By definition, C is contained in both its interior and exterior. When traversing a simple cycle C, its cyclic list of edges is, unless stated otherwise, traversed such that its interior lies locally to the right of it. We then say that we traverse C *clockwise*. If we traverse C in the other direction, we traverse it *anticlockwise*. The notation of subpaths can now also be used for a simple cycle C, where $C[u, v]$ represents the path contained in C starting at u and traversing C clockwise to v.

Let G be a planar 4-graph and let $\mathcal{E}$ be an embedding of G. Between two adjacent edges uv and vw let the angle $\alpha \in \{90°, 180°, 270°, 360°\}$ represent the angle over the right-hand side of uvw. The *rotation* from u to w over v is defined as $\text{rot}(uv, vw) = 2 - \alpha/90°$. The rotation is therefore 1 for a 90° angle, 0 if the angle is 180°, and -1 if the angle is 270°. If $u = w$, then the angle is 360° and the rotation is -2. Figure 2.1a shows an edge uv

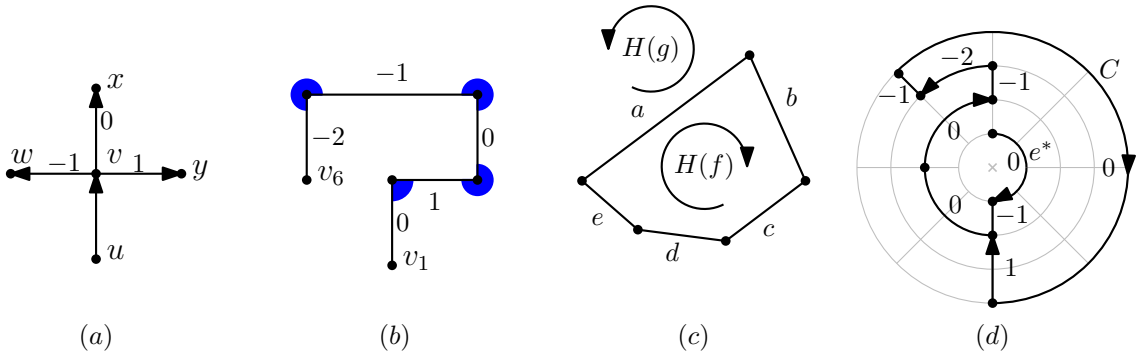

(a) (b) (c) (d)

Figure 2.1: (a) An edge uv with the rotations $\text{rot}(uv, vw)$, $\text{rot}(uv, vx)$, and $\text{rot}(uv, vy)$ written along the corresponding edge. (b) A path from v_1 to v_6 with rotation -2. The summed up rotations up to each edge are shown next to the edges. (c) An angle assignment for the faces f and g with and its incident edges. (d) An ortho-radial representation with reference edge e^* and an essential cycle C with rotation 0. The label $\ell_C(e)$ of each edge e in C is shown next to each edge.

and its rotations to its adjacent edges. A rotation of 1 represents a right turn, a rotation of -1 a left turn, and a rotation of 0 represents no turn at all. We define the rotation of a path $P = v_1 \dots v_k$ as $\text{rot}(P) = \sum_{i=2}^{k-1} \text{rot}(v_{i-1}v_i, v_iv_{i+1})$, which is the sum of the rotations along the path (see Figure 2.1b). It then follows that $\text{rot}(\overline{P}) = -\text{rot}(P)$, and for any edge e in $P = s \dots t$, it follows that $\text{rot}(P) = \text{rot}(P[s, e]) + \text{rot}(P[e, t])$. We also define the rotation for a cycle $C = v_1 \dots v_k v_1$ with $v_k = v_0$ as $\text{rot}(C) = \sum_{i=1}^{k} \text{rot}(v_{i-1}v_i, v_iv_{i+1})$. This also includes the last rotation back to the starting vertex v_1. For a face f, the incident edges form a cycle C_f around f. We then define the rotation of f as $\text{rot}(f) = \text{rot}(C_f)$.

An *angle assignment* $\mathcal{A}$ of a plane 4-graph $(G, \mathcal{E})$ contains a list $H(f)$ for every face f in $\mathcal{E}$. Each $H(f)$ is a circular list of pairs (e, a) containing the incident edges of f in a clockwise order together with an angle $a \in \{90°, 180°, 270°, 360°\}$ representing the inner angle between e and the succeeding edge in the list. An edge e may have multiple entries in $H(f)$ if e is incident to f on both of its sides. An angle assignment for the graph in Figure 2.1c could be formed by $H(f)$ containing the entries $(a, 90°)$, $(b, 90°)$, $(c, 180°)$, $(d, 90°)$, and $(e, 90°)$, and $H(g)$ containing the entries $(a, 270°)$, $(e, 270°)$, $(d, 180°)$, $(c, 270°)$, and $(b, 270°)$. We call $\mathcal{H} = (\mathcal{A}, f_o)$ an *orthogonal representation* with angle assignment $\mathcal{A}$ and outer face f_o if the following holds.

1. The sum of the angles in $\mathcal{A}$ at each vertex is 360°.
2. For each face f, it holds that
   a) either $\text{rot}(f) = 4$ if f is a regular face,
   b) or $\text{rot}(f) = -4$ if f is the outer face.

The previously mentioned angle assignment for Figure 2.1c forms an orthogonal representation with $f_o = g$. Our definition of orthogonal representations is different to the one by Tamassia [Tam87], where each entry in $H(f)$ also contains an edge descriptor indicating the internal bends of e. As we will represent bends of edges by bend-vertices added to an edge, we use the simpler definition above. We know that G admits an orthogonal representation if and only if G admits a straight-line orthogonal drawing [Tam87]. A graph G is called *rectilinear-planar* if it admits an orthogonal straight-line drawing, which is equivalent to admitting an embedding $\mathcal{E}$ and an orthogonal representation $\mathcal{H}$ using this embedding. A plane graph $(G, \mathcal{E})$ is called *rectilinear-plane* if it admits an orthogonal representation using

the fixed embedding $\mathcal{E}$. We define $\Omega(G, \mathcal{E})$ to be the set of all orthogonal representations of the plane graph $(G, \mathcal{E})$.

The definition of an ortho-radial representations not only contains an outer face f_o, but also a *central face* f_c that should be placed in the middle of the drawing and will contain the center-point of the ortho-radial grid. This also implies that, at least without manual modification, no vertex of the graph will be placed at the center-point. For a plane 4-graph G we call $\mathcal{T} = (\mathcal{A}, f_c, f_o)$ an *ortho-radial representation* with angle assignment $\mathcal{A}$, *central face* f_c and *outer face* f_o if the following holds.

1. The sum of the angles in $\mathcal{A}$ at each vertex 360°.
2. For each face f, it holds that

$$\text{rot}(f) = \begin{cases} 4 & \text{if } f \text{ is a normal face} \\ 0 & \text{if } f \text{ is the outer or central face but not both} \\ -4 & \text{if } f \text{ is both the outer and central face} \end{cases}$$

Having G admit an ortho-radial representation is not yet equivalent to having G admit an actual ortho-radial drawing. A cycle C is called an *essential cycle* if it separates the central and the outer face. An essential cycle in an ortho-radial representation may not connect back up, as the starting and end vertex could be placed on different concentric rings. See again Figure 1.2b where this results in the representation not being drawable.

To exclude this problem, Barth et al. [BNRW21] introduce the notion of a *reference edge* e^*, which we define as an oriented edge incident to f_c. This special edge must explicitly be drawn in a clockwise direction on a concentric ring of the ortho-radial grid, also fixing the orientation of every other edge in the representation. Our definition of a reference edge is different to the one by Barth et al., who require e^* to be incident to the outer instead of the central face. When looking at the so-called flipped ortho-radial representation [BNRW21, Lemma 6] one can see that both placements of a reference edge are equivalent. The placement of e^* incident to f_c is chosen to help in the construction of recursive algorithms that build up an ortho-radial representation from the center outwards. Let e and e' be two undirected edges in an ortho-radial representation and let $\vec{e} = xy$ and $\vec{e'} = uv$ be an orientation of e and e'. A path P from x or y to u or v is called a *reference path* from e' to e if it does not contain e or e'. With a reference path the *combinatorial direction* of $\vec{e}$ with respect to $\vec{e'}$ over P is defined as

$$\text{dir}(\vec{e'}, P, \vec{e}) = \begin{cases} \text{rot}(\vec{e'} + P + \vec{e}) & \text{if } P \text{ starts at } v \text{ and ends at } x, \\ \text{rot}(\overleftarrow{e'} + P + \vec{e}) - 2 & \text{if } P \text{ starts at } u \text{ and ends at } x, \\ \text{rot}(\vec{e'} + P + \overleftarrow{e}) + 2 & \text{if } P \text{ starts at } v \text{ and ends at } y, \\ \text{rot}(\overleftarrow{e'} + P + \overleftarrow{e}) & \text{if } P \text{ starts at } u \text{ and ends at } y. \end{cases}$$

With two reference paths P and Q, it holds that $\text{dir}(e', P, e) \equiv \text{dir}(e', Q, e) \pmod 4$. Moreover, $\text{dir}(e', P, e) = \text{dir}(e', Q, e)$ if there exist simple essential cycles C and C' such that

1. C lies in the exterior of C',
2. e lies on C and e' lies on C',
3. and P and Q lie in the exterior of C' as well as in the interior of C.

Our definition of combinatorial direction and the above implications are again slightly different to the ones by Barth et al. [BNRW21, Lemma 3] in the way that the signs of the

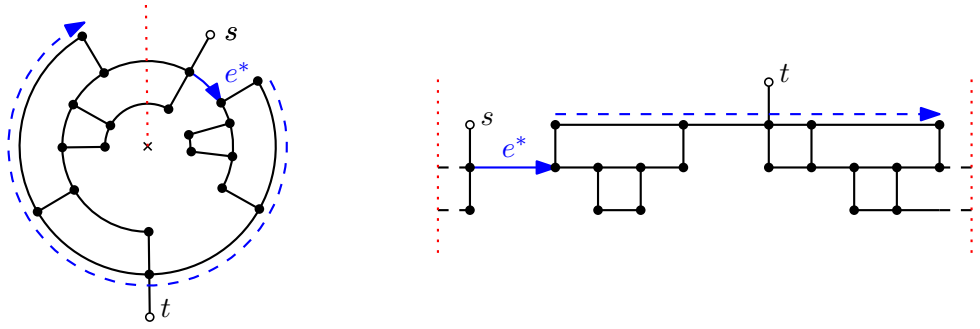

Figure 2.2: On the left, an ortho-radial drawing of a graph around the center point indicated with a cross. On the right, the same drawing cut at the red-dotted line and unwrapped into a rectangular form. The clockwise-facing dashed arrow becomes a rightwards-facing straight-line arrow. Similarly, the clockwise facing reference edge e^* on the left is horizontal and rightwards-facing on the right.

constants 2 and -2 in the definition of combinatorial direction are flipped and that the usage of exterior and interior is flipped in the conditions for equality of two combinatorial directions. This is a consequence of placing the reference edge incident to f_c instead of f_o. We are now interested in the combinatorial direction of edges with respect to the reference edge e^*. The value $\text{dir}(e^*, P, \vec{e}) \pmod 4$ indicates that the oriented edge $\vec{e}$ either points clockwise (0), inwards (1), anticlockwise (2), or outwards (3). For a simple essential cycle C, a reference path from some edge e' to an edge $e \in C$ is said to *respect* C if the path is contained in the interior of C. If two reference paths P, Q from the reference edge e^* to $e \in C$ both respect C, it follows that $\text{dir}(e^*, P, e) = \text{dir}(e^*, Q, e)$. Let e be an edge on a simple essential cycle C and let P be a reference path from e^* to e that respects C. Then the *label of e in C* is defined as $\ell_C(e) = \text{dir}(e^*, P, e)$. Figure 2.1d depicts an ortho-radial representation with reference edge e^* and the label for every edge e on the simple essential cycle C. A simple essential cycle also always has rotation 0. A simple essential cycle is called *valid* if

1. there either exist two edges $e_+, e_- \in C$ such that $\ell_C(e_+) > 0$ and $\ell_C(e_-) < 0$
2. or every edge in C has exactly label 0,

and the cycle is *invalid* otherwise. An ortho-radial representation $\mathcal{T}$ of a graph G is called *valid* if every simple essential cycle in G is valid. It now holds that G admits an ortho-radial drawing if and only if it admits a valid ortho-radial representations [BNRW21]. A graph G is called *orthoradial-planar* if it admits an ortho-radial drawing, which is equivalent to admitting an embedding $\mathcal{E}$ and a valid ortho-radial representation $\mathcal{T}$ using this embedding. A plane graph $(G, \mathcal{E})$ is called *orthoradial-plane* if it admits a valid ortho-radial representation using the fixed embedding $\mathcal{E}$. We define $\Theta(G, \mathcal{E})$ to be the set of all valid ortho-radial representations of the plane graph $(G, \mathcal{E})$.

Throughout this work, ortho-radial representations are rarely drawn in their circular shape. As the center point of the ortho-radial grid never contains a vertex of the graph, the representation can be cut at an arbitrary emanating spoke of the ortho-radial grid. This cuts every essential cycle, and the representation can then be unwrapped into a rectangle. See Figure 2.2 for an illustration of this process. In this rectangle, edges that cross this vertical cut are represented with dashed lines on both sides. These dashed lines vertically line up for a valid simple essential cycle and do not for an invalid one.

In the following, some general mathematical notations. Let $\mathbb{P}$ be the set of all boolean expressions. We define $[\cdot] : \mathbb{P} \to \{0, 1\}$ to be the *Iversion bracket notation* with

$$[P] = \begin{cases} 1 & \text{if } P, \\ 0 & \text{if } \neg P. \end{cases}$$

We sometimes define an interval without knowing which of the bounds is the upper and which is the lower one. To eliminate excessive case distinctions we use the following definition. Given two whole numbers $x, y \in \mathbb{Z}$, the *signed closed interval* $[x, y]_s$ *between* x *and* y is defined as

$$[x, y]_s \coloneqq \begin{cases} [x, y] & \text{if } [x, y] \neq \emptyset, \\ [y, x] & \text{otherwise.} \end{cases}$$

and the *signed open interval* $[x, y)_s$ *between* x *and* y is defined as

$$[x, y)_s \coloneqq \begin{cases} [x, y) & \text{if } [x, y] \neq \emptyset, \\ (y, x] & \text{otherwise.} \end{cases}$$

3. NP-Completeness For General Plane 4-Graphs

This section shows that the Bend-Free-Ortho-Radial-problem is NP-complete for general plane 4-graphs. This stands in contrast to the sub-quadratic runtime achievable for orthogonal representations [CK12].

To show NP-completeness, the well-studied 3-Sat problem is reduced to Bend-Free-Ortho-Radial. An instance $\mathcal{I} = (\mathcal{V}, \mathcal{C})$ of 3-Sat consists of a set of *variables* $\mathcal{V} = \{x_0, \ldots, x_{n-1}\}$ and a set of boolean *clauses* $\mathcal{C} = \{c_0, \ldots, c_{m-1}\}$. Each clause must be of the form $c_j = l_{0j} \vee l_{1j} \vee l_{2j}$ where each l_{ij} is a literal, x or $\neg x$, of a variable x in $\mathcal{V}$. A *variable-assignment* $\mathcal{A}$ is an assignment of the variables in $\mathcal{V}$ to boolean values. The problem is then to check if there exists a variable-assignment $\mathcal{A}$ such that every clause in $\mathcal{C}$ is satisfied (evaluates to *true*). We then say that $\mathcal{A}$ *satisfies* $\mathcal{I}$ and $\mathcal{I}$ is *satisfiable*. An example of a 3-Sat-instance would be the variable set $\mathcal{V} = \{w, x, y, z\}$ together with the four clauses $c_1 = \neg x \vee \neg y \vee z$, $c_2 = w \vee y \vee \neg z$, $c_3 = \neg w \vee \neg x \vee z$, and $c_4 = w \vee x \vee \neg y$ making up the set $\mathcal{C}$. This instance is satisfiable since the variable-assignment $(w, x, y, z) = (\mathit{true}, \mathit{false}, \mathit{true}, \mathit{true})$ results in all clauses evaluating to *true*.

Our reduction from 3-Sat to Bend-Free-Ortho-Radial creates in polynomial time a plane graph $(G_\mathcal{I}, \mathcal{E}_\mathcal{I})$ given an arbitrary 3-Sat-instance $\mathcal{I}$ such that there exists a valid ortho-radial representation of $G_\mathcal{I}$ if and only if $\mathcal{I}$ is satisfiable. The idea of the reduction is to represent a literal of a variable in $\mathcal{V}$ as a vertical segment of the ortho-radial grid and a clause as a simple essential-cycle traversing every segment. See Figure 3.1 for an illustration. Each segment contains a widget per traversing cycle representing the occurrence of the literal in the respective clause. Such a widget has two states for the two possible boolean values a literal can assume. These states are constructed such that the validity constraint of a simple essential cycle models satisfied and unsatisfied clauses. The state assumed by a single widget also has to be transferred to all other widgets in the same segment as well as, in its inverted state, to the widgets of the segment representing the negated literal. For this, widgets in the same segment are connected via vertical synchronization-widgets, and a pair of matching segments is connected via two more special essential cycles.

3.1 The Scaffolding

As a start, we define the scaffolding $\mathcal{S}_{(n,m)}$, which divides the ortho-radial grid in the aforementioned segments and is a holding structure for the widgets. An example of $\mathcal{S}_{(n,m)}$

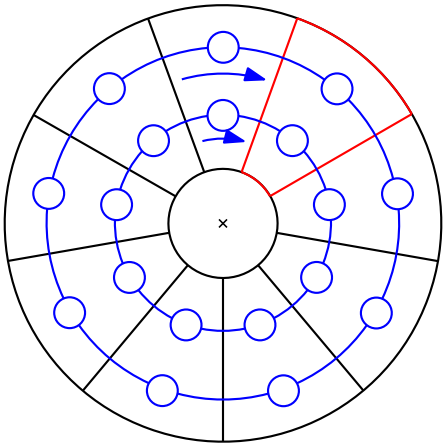

Figure 3.1: An abstract view of the NP-completeness reduction. One vertical segment, which represent a single literal of the 3-SAT-instance, is highlighted red. The blue essential cycles contain a widget per segment and represent the clauses.

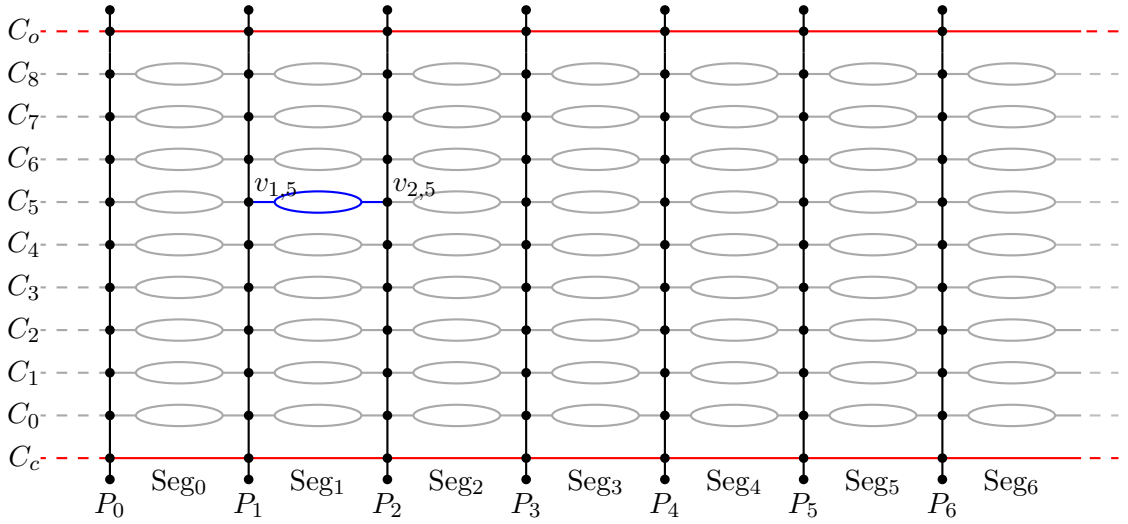

Figure 3.2: The scaffolding $\mathcal{S}_{(3,2)}$. The cycles C_c and C_o are colored red and the paths P_i are colored black. The gray subgraphs indicate widgets placed inside the scaffolding forming the clause-cycles C_j. The widget $w_{1,5}$ is highlighted in blue and placed between the vertices $v_{1,5}$ and $v_{2,5}$.

for $n = 3$ and $m = 3$ is shown in Figure 3.2. Formally, the scaffolding consist of the simple cycle C_c called the *central cycle* and the simple cycle C_o called the *outer cycle*, both having length $2n + 1$, as well as $2n + 1$ simple paths P_i with $i \in [0, 2n]$ each of length $2n + m + 4$. A path P_i is joined to both cycles by identifying the i-th vertex of C_c with the second vertex from P_i and the i-th vertex of C_o with the second-to-last vertex of P_i. The scaffolding is embedded such that the last vertex of each path P_i is on one side of C_o and the rest of the path on the other side. We define the outer face f_o to be the face created by C_o and the last vertices of each path. Then the rest of the paths (including C_c) are contained in the interior of C_o. To complete the embedding, the first vertex of each path is placed in the interior of C_c and they, together with C_c, form the central face f_c. We label the vertices of the paths with $v_{i,j},\ i \in [0, 2n],\ j \in [-2, 2n + m + 1]$ representing the $(j + 2)$-th vertex in P_i. The shift in the index j is used so that now for a path P_i, the $2n + m$ vertices from $v_{i,0}$ to $v_{i,2n+m-1}$ lie between C_c and C_o. As these vertices will be the places where widgets get attached, this index scheme helps in clearly describing where which widget is placed. We call for some $i \in [0, 2n]$ the face of $\mathcal{S}_{(n,m)}$ incident to C_c, C_o, P_i, and P_{i+1} the *segment* Seg_i. When associating P_{2n+1} with P_0, there exist $2n + 1$ segments. Given a 3-SAT instance $\mathcal{I}$ with $n \coloneqq |\mathcal{V}|$ and $m \coloneqq |\mathcal{C}|$, the scaffolding $\mathcal{S}_{(n,m)}$ will be used in the graph $G_\mathcal{I}$ and has enough space for one essential cycle per clause and two special cycles per variable. The following lemma shows that, once all widgets are in place, the scaffolding can only have one specific valid ortho-radial representation.

Lemma 3.1. *A scaffolding $\mathcal{S}_{n,m}$ only admits a single ortho-radial representation if the representation is required to have rotation* $\text{rot}(v_{i,j}v_{i,j+1}, v_{i,j+1}v_{i,j+2}) = 0$ *for all* $i \in [0, 2n], j \in [0, 2n + m - 2]$. *This representation is valid and in it, the cycles C_c and C_o are lying totally on concentric rings around the center and each P_i is totally lying on a spoke radiating from the center.*

Proof. As C_c and C_o only contain vertices of degree 4, the rotations around their vertices are already fixed. The same can be said about the degree-1 vertices on the ends of each path. Together with the restriction on the rotations in the statement, every rotation is fixed and so there exists exactly one angle assignment of the graph. It is easy to see that this angle assignment forms a valid ortho-radial representation when using an arbitrary reference edge $e^* \in C_c$ as also illustrated in Figure 3.2. This representation has the property that C_c and C_o totally lie on concentric rings and each P_i totally lies on a spoke radiating from the center. □

We now associate each literal of the 3-SAT-instance with a segment in the scaffolding. Specifically, the positive literal x_i of variable $x_i \in \mathcal{V}$ is associated with the segment Seg_{2i+1} and the negative literal $\neg x_i$ is associated with the segment Seg_{2i+2} (see again Figure 3.2). This specifically leaves Seg_0 without any associated literal. Why this segment is important will be explained in Section 3.3.

3.2 Widgets With Predictable Labels

We introduce the four widgets E, R_+, R_-, and L that, when placed between vertices $v_{i,j}$ and $v_{i+1,j}$ of the scaffolding, have predictable labels. Having predictable labels means that for an arbitrary simple essential cycle traversing the widget from $v_{i,j}$ to $v_{i+1,j}$, the widget contains in every possible ortho-radial representation either only a label of zero (E-widget), only non-negative labels (R_+-widget), only non-positive labels (R_--widget), or can switch between non-negative and non-positive labels (L-widget). First of all, the *E-widget* is simply a single edge e, which when placed between two vertices $v_{i,j}$ and $v_{i+1,j}$ obviously has label 0. We now define the *R_+- and R_--widgets* as also seen in Figures 3.3a and 3.3b.

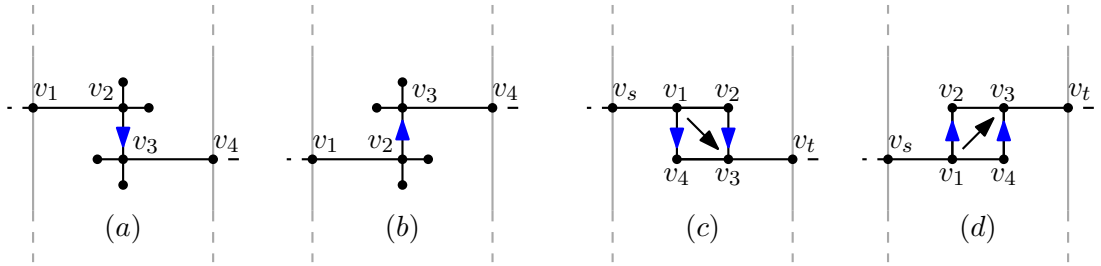

Figure 3.3: An R_+-widget (a) and an R_--widget (b) as well as the two representations of an L widget connected inside a segment. One L-widget is oriented downwards (a), while the other one is oriented upwards (b). A diagonal arrow is placed inside each L-widget to better indicate its orientation. The blue arrows indicate positive and negative labels in the respective representations.

Definition 3.2. *Let R be the planar graph consisting of a 4-path $v_1v_2v_3v_4$ where both v_2 and v_3 get two extra degree-1-vertices attached making them have degree 4. Then the R_--widget is defined as the plane graph $(R, \mathcal{E}_-)$ with start-vertex v_1 and end-vertex v_4 where the rotation scheme at v_2 contains the sublist $[v_1, v_3]$ and the rotation scheme at v_3 contains the sublist $[v_4v_2]$, resulting in $\mathrm{rot}(v_1v_2, v_2v_3) = -1$ and $\mathrm{rot}(v_2v_3, v_3v_4) = 1$ for every angle assignment of R_-. The R_+-widget is defined as the plane graph $(R, \mathcal{E}_+)$ with start vertex v_1 and end vertex v_4 where the rotation scheme at v_2 contains the sublist $[v_3, v_1]$ and the rotation scheme at v_3 contains the sublist $[v_2v_4]$, resulting in $\mathrm{rot}(v_1v_2, v_2v_3) = 1$ and $\mathrm{rot}(v_2v_3, v_3v_4) = -1$ for every angle assignment of R_+.*

Observation 3.3. *Consider an R_+- or R_--widget connected inside a segment of a scaffolding by identifying vertices $v_{i,j}$ and $v_{i+1,j}$ with the start- and end-vertex of the widget. The widget then has only one possible ortho-radial representation. In this representation, a simple essential cycle, starting with label 0 when traversing an R_+-widget from $v_{i,j}$ to $v_{i+1,j}$, contains a positively-labelled edge but no negatively-labelled ones. Conversely, if such a simple essential cycle traverses an R_--widget, it contains a negatively-labelled edge but no positively-labelled ones.*

The R_+- and R_--widgets will ensure the existence of an edge in every simple essential cycle with either a positive or a negative label. The cycle then needs an edge with a label of the opposite sign in some other widget for it to be valid. These widgets are called *L-widgets* and represent the literals in the clauses. Similar to a literal, an L-widget has exactly two possible states. The following definition formally introduces L-widgets, which are also depicted in their two states in Figures 3.3c and 3.3d.

Definition 3.4. *An L-widget is a plane graph consisting of a 4-cycle $v_1v_2v_3v_4$ with extra degree-1 vertices v_s and v_t where v_s is connected to v_1 and v_t is connected to v_3. The embedding is such that the rotation scheme at v_1 is $[v_2, v_4, v_s]$ and the rotation scheme at v_3 is $[v_t, v_4, v_2]$. The start-vertex of L is set to v_s and the end-vertex is set to v_t.*

Observation 3.5. *Consider an L-widget connected inside a segment of a scaffolding by identifying vertices $v_{i,j}$ and $v_{i+1,j}$ with the start- and end-vertex of the widget. This L-widget has exactly two ortho-radial representations. In one representation, every simple essential cycle, starting with label 0 when traversing the L-widget from $v_{i,j}$ to $v_{i+1,j}$, contains only zero- and positively-labelled edges. We then call the L-widget* downwards-oriented *(see Figure 3.3c). In the other representation, such a simple essential cycle contains only zero- and negatively-labelled edges and here we call the L-widget* upwards-oriented *(see Figure 3.3d).*

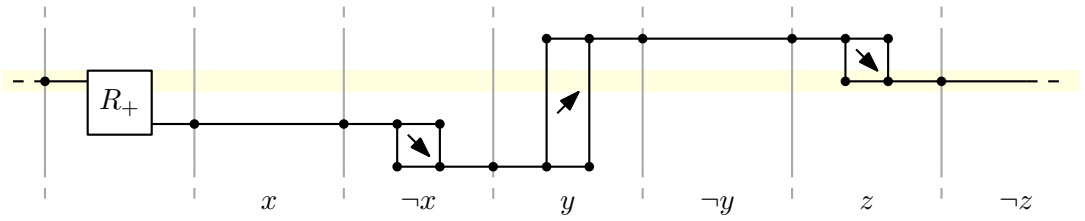

Figure 3.4: A clause-cycle representing the clause $\neg x \vee y \vee z$. The cycle is valid since the L widget in the y-segment is oriented upwards. The yellow bar helps in seeing that the clause-cycle ends up where it started.

With an L-widget having exactly two possible representations, we map the boolean values of a literal to orientations of the widget. An L-widget being upwards-oriented represents a literal taking on the boolean value *true* and conversely, a downwards-oriented L-widget represents a value of *false* for the literal.

3.3 Clause-Cycles

Multiple widgets are connected to form a so-called *clause-cycle* C_j around the center. A clause cycle C_j contains $2n+1$ widgets $w_{i,j},\ i \in [0, 2n]$, where each $w_{i,j}$ is placed inside the segment Seg_i by identifying vertices $v_{i,j}$ and $v_{i+1,j}$ with the start- and end-vertex of the widget. See again Figure 3.2, where the positions of vertices $v_{1,5}$ and $v_{2,5}$ as well as the widget $w_{1,5}$ between them are highlighted. We set $w_{0,j}$ to either be an R_+- or an R_--widget and every other widget in the clause-cycle to either be an L- or an E-widget. A clause-cycle is called *normal* when containing an R_+-widget and *inverted* when containing an R_- widget. Figure 3.4 depicts an example of a normal clause-cycle. A clause-cycle always contains multiple simple essential cycles, as there are two possible paths through each L-widget. But since Observation 3.5 states that any cycle traversing an L-widget has the desired property about labels, we will use the term clause-cycle as also meaning an arbitrary simple essential cycle contained in it. The validity constraint of such a cycle now helps to form the condition that a clause must be satisfied. In general, a simple essential cycle is valid if it contains at least one positively- and one negatively-labelled edge or only zero-labelled edges. As $w_{0,j}$ is either an R_+- or an R_--widget, the case that the cycle only contains zero-labelled edges never occurs, and we get the following result.

Lemma 3.6. *Let G be a scaffolding $\mathcal{S}_{(n,m)}$ containing $2n+m$ clause-cycles from C_0 to C_{2n+m-1} and let $\mathcal{T}$ be an ortho-radial representation of G. Then every simple essential cycle in a clause-cycle C_j is valid if and only if*

1. *either C_j is a normal clause-cycle and at least one L-widget in C_j is upwards-oriented*
2. *or C_j is an inverted clause-cycle and at least one L-widget in C_j is downwards-oriented.*

Proof. Every path of the scaffolding $\mathcal{S}_{(n,m)}$ has $2n+m$ vertices between the central cycle C_c and the outer-cycle C_o and G has $2n+m$ clause cycles placed inside the scaffolding. This fixes the rotations along every path of the scaffolding to all be 0 and Lemma 3.1 implies that every ortho-radial representation of G has these paths totally lying on emanating spokes of the ortho-radial grid. Every simple essential cycle contained inside a clause-cycles then traverses a widget $w_{i,j}$ from $v_{i,j}$ to $v_{i+1,j}$ and has label 0 when entering the widget.

The proof is only given for normal clause-cycles, as the proof for inverted ones is analogous. Let C_j be a normal clause-cycle and consider an arbitrary simple essential cycle in C_j.

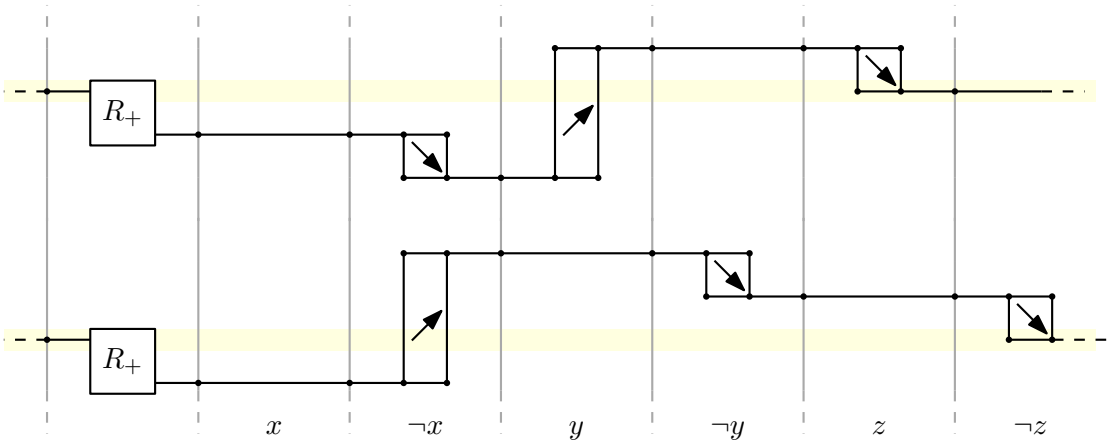

Figure 3.5: Two independent valid clause-cycles in a scaffolding. The two L-widgets inside the $\neg x$-segment have opposing orientations while the L-widgets inside the z- and $\neg z$-segments have the same orientation.

Observation 3.3 implies that a positively-labelled edge is present in the essential cycle inside the R_+-widget $w_{0,j}$. The cycle is therefore valid if and only if a negatively-labelled edge is present in some other part of the cycle. This may only be the case in an L-widget, as E-widgets only contain edges with label 0. Observation 3.5 states that an L-widget contains a negatively-labelled edge if and only if the L-widget is upwards-oriented implying the statement. □

The clause-cycle in Figure 3.4 is valid because the y-segment has an upwards-oriented L-widget. If this widget would also be downwards-oriented, the cycle would not be valid anymore.

Lemma 3.6 implies that clause-cycles can represent two types of clauses. Normal clause-cycles can represent clauses as the ones used in 3-Sat, where literals are connected with *or*-operators. Consequently, we also say that such a clause is *normal*. A normal clause is satisfied if at least one literal has the value *true*. Inverted clause-cycles can represent clauses of the form $\neg(\bigwedge_{i\in[1,k]} l_i)$ for $k \in \mathbb{N}$. We call these *inverted clauses* and an inverted clause is satisfied if at least one literal has the value *false*. We say that a clause-cycle C_j *emulates* a clause c if the type of the clause (normal or inverted) matches the type of the clause-cycle and the widget $w_{i,j}$ for $i \in [1, 2n]$ is set to an L-widget if the corresponding literal of the segment Seg_i is contained in c, and is set to an E-widget otherwise. Clause-cycles emulating clauses in $\mathcal{C}$ are all normal. Inverted clause-cycles are only required for technical reasons as will be seen in the next section.

3.4 Synchronizing L-Widgets

Lemma 3.6 and the definition of emulating clause-cycles can already model a single clause of $\mathcal{C}$ in isolation. But since the orientation of one L-widget does not depend on the orientation of another, every clause-cycle can trivially be made valid as long as it contains at least one L-widget (see Figure 3.5). To handle this problem, L-widgets representing the same variable are *synchronized*. This synchronization happens in two steps. First, we ensure that all L-widgets in a single segment must share the same orientation, and second, we ensure that the L-widgets contained in segments representing the normal and negated literal of a variable are always oriented in opposing directions.

We start with the first problem of synchronizing all L widgets in a single segment. Observe that switching between the two orientations of an L-widget in a sense rotates the central 4-cycle of L by 90 degrees (see again Figures 3.3c and 3.3d). To synchronize all L-widgets,

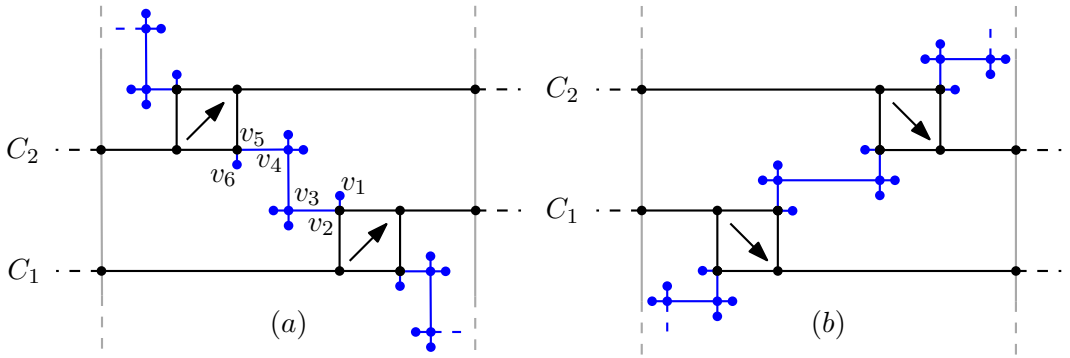

Figure 3.6: Two L widgets in one segment connected via a blue *Sync* widget. In (a) both L-widgets are upwards-oriented and in (b) both are downwards-oriented.

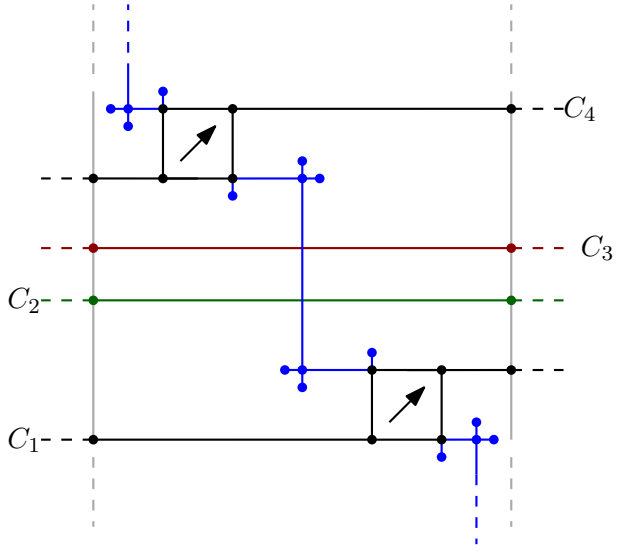

Figure 3.7: Two L-widgets separated by a normal dark-green clause-cycle C_2 and an inverted dark-red clause-cycle C_3. The *Sync*-widget between the two L-widgets creates crossing edges in the embedding.

a special *Sync*-widget transfers the rotation of one widget to the neighboring widgets, which have to rotate in the same direction to still form an ortho-radial representation. The following definition formally introduces *Sync*-widgets, which can also be seen in Figure 3.6, where they are highlighted in blue.

Definition 3.7. *A Sync-widget is the plane graph consisting of a* 6*-path* $v_1v_2v_3v_4v_5v_6$ *with two degree-*1 *vertices attached to each of the two inner vertices* v_3 *and* v_4 *of the path. The embedding of the Sync-widget is defined such that the rotation scheme for* v_3 *contains the sublist* $[v_4, v_2]$ *and the rotation scheme for* v_4 *contains the sublist* $[v_3, v_5]$*. This results in the rotations* $\mathrm{rot}(v_2v_3, v_3v_4) = 1$ *and* $\mathrm{rot}(v_3v_4, v_4v_5) = -1$ *for every angle assignment of the Sync-widget.*

Two neighboring L-widgets $w_{i,j}$ and $w_{i,j+1}$ are so-called *synchronized* by connecting both to a *Sync*-widget. See Figure 3.6 for an example. The widgets are connected by identify the vertex v_2 of the *Sync*-widget with the vertex v_2 of $w_{i,j}$ (see again Definition 3.4) and by identifying the vertex v_5 of the *Sync*-widget with the vertex v_4 of $w_{i,j+1}$. These connection points are embedded such that the rotation scheme of v_2 first contains v_3 and v_1 and then the other two vertices of the L-widget, while the rotation scheme of v_5 first contains v_4 and v_6 and then the other two vertices of the second L-widget.

Observation 3.8. *Consider a segment* Seg_i *in a scaffolding* $\mathcal{S}$ *containing multiple synchronized L-widgets. Then the segment only admits two ortho-radial representations. In one representation, all the L-widgets are upwards-oriented, and in the other representation, all are downwards-oriented.*

Observation 3.8 however does not consider two L-widgets that are separated by other clause-cycles not containing the corresponding literal. These other clause-cycles contain E- instead of L-widgets in the segment as Figure 3.7 illustrates. In this case, the resulting graph is no longer planar since edges of the *Sync*-widget cross with the E-widgets of the separating clause-cycles. A simple planarization of this graph, by introducing vertices the crossing points of two edges, can result in a situation, where either planarized *Sync*-widgets can no longer rotate freely or the preconditions in Lemma 3.6 no longer hold. We introduce a planarization method that takes both of these problems into account. The key is to planarize crossings with normal clause-cycles differently to crossings with inverted clause-cycles.

If an E-widget of a normal clause-cycle crosses a *Sync*-widget (see Figure 3.8a), the edge of the E-widget gets subdivided into four edges and the central edge of the *Sync*-widget gets subdivided into two. The newly created central vertices of both widgets are then identified with each other to eliminate the crossing.

If an E-widget of an inverted clause-cycle crosses a *Sync*-widget (see Figure 3.8b), the edge of the E-widget also gets subdivided into four edges, but more work has to be done for the *Sync*-widget. Its central edge is replaced by a 5-path $v_1v_2v_3v_4v_5$ where the embedding is chosen similar to the one for a *Sync* widget such that $\mathrm{rot}(v_1v_2, v_2v_3) = -1$ and $\mathrm{rot}(v_3v_4, v_4v_5) = 1$. The central vertex v_3 of the 5-path finally gets identified with the central vertex of the subdivided E-widget.

The result of this planarization can be seen in a more complex example in Figures 3.7 and 3.9a. If we say that two L-widgets are synchronized, we from now on mean the planarized version of the synchronization, and we say that a set of clause-cycles is synchronized if, per segment, all L-widgets contained in this segment are synchronized. As mentioned before, the planarization is designed such that the *Sync*- and connected L-widgets still have two possible orientations and the paths through planarized E-widgets do not compromise the correctness of Lemma 3.6. The following observation and lemma shows this in detail.

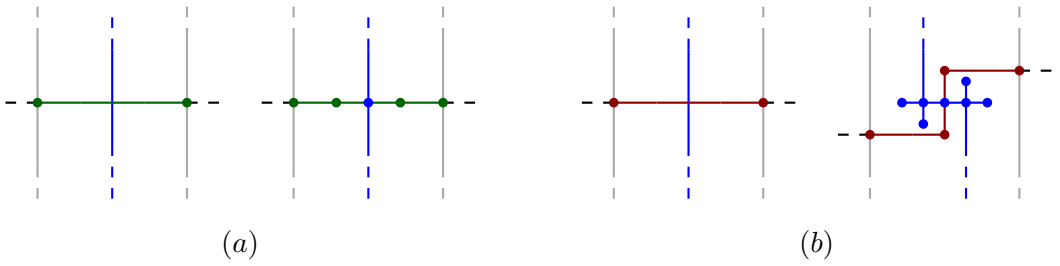

Figure 3.8: The planarization method for the case that a *Sync*-widget crosses an E-widget. The planarization with a normal clause-cycle (a) is different to the one with an inverted clause-cycle (b).

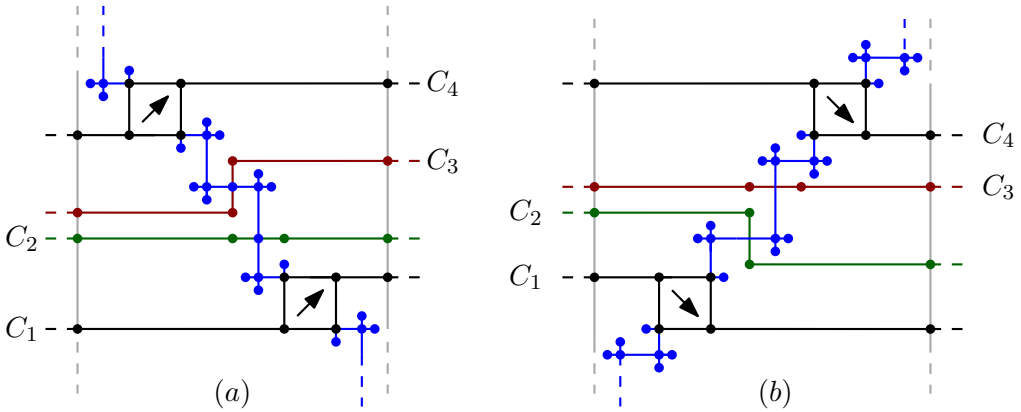

Figure 3.9: The planarized version of Figure 3.7. The synchronization still has exactly two ortho-radial representations.

Observation 3.9. *Consider a segment* Seg_i *of a scaffolding where* $w_{i,j}$ *and* $w_{i,j'}$ *are synchronized L-widgets with* $j' > j+1$ *and* $w_{i,k}$ *for* $k \in [j+1, j'-1]$ *are E-widgets, all associated with either a normal or an inverted clause-cycle. Then the segment admits exactly two ortho-radial representations (see Figures 3.9a and 3.9b) having the same properties as in Observation 3.8. Moreover, in both orientations every simple essential cycle traversing a planarized E-widget* $w_{i,k}$ *from* $v_{i,k}$ *to* $v_{i+1,k}$*, starting with label* 0 *when entering the widget, contains only non-negative labels in* $w_{i,k}$ *if the widget is contained in a normal clause-cycle, and contains only non-positive labels in* $w_{i,k}$ *if the widget is contained in an inverted clause-cycle.*

Lemma 3.10. *Let* G *be a scaffolding* $\mathcal{S}_{(n,m)}$ *containing* $2n+m$ *synchronized clause-cycles and let* C *be a clause-cycle that contains, due to the synchronization, some planarized E-widgets. Then the equivalence of Lemma 3.6 still holds for* C*.*

Proof. Let C be a normal clause-cycle (the proof for inverted cycles follows analogously). The equivalence of Lemma 3.6 is based on the fact that E-widgets only contain zero-labelled edges. In general, this is no longer the case for a planarized E-widget. Due to C being a normal clause-cycle, Observation 3.9 implies that each planarized E-widget in C only contains non-negative labels. As C is normal, it already contains a positive label in its R_+-widget and a possible positive label in a planarized E-widget does not change the correctness of Lemma 3.6. □

What is left is to ensure that the L-widgets contained in segments associated with the normal and negated literal of a variable are always oriented in opposing directions. Stated

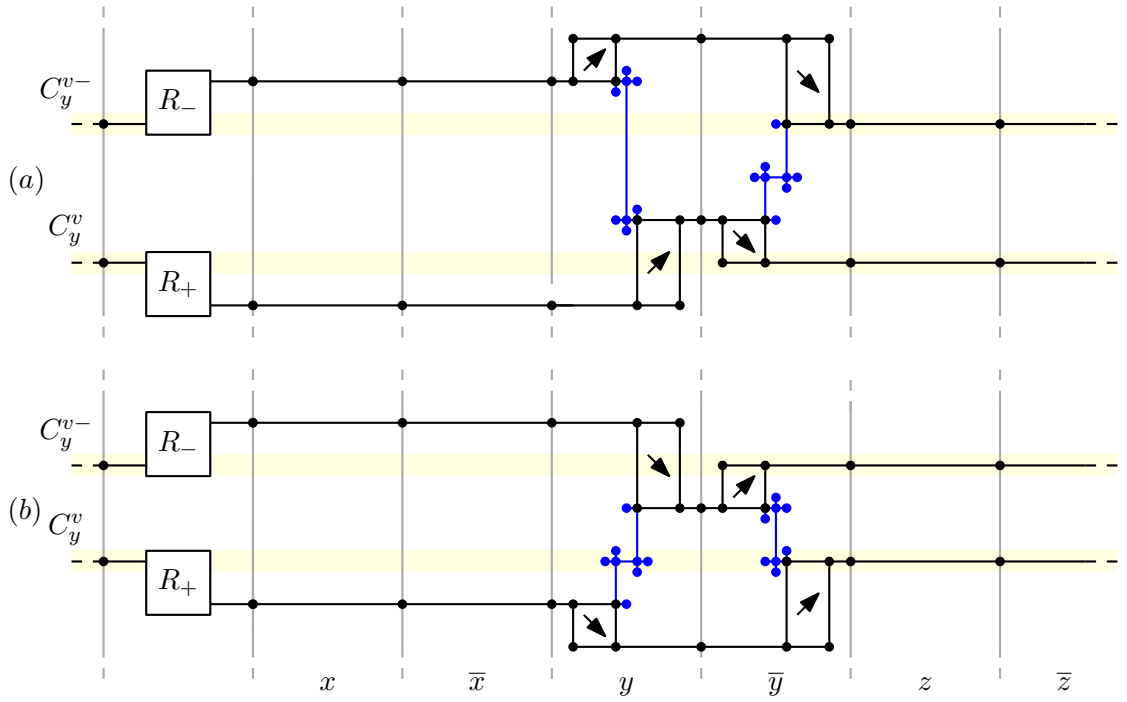

Figure 3.10: The only two valid ortho-radial representations of the synchronized clause-cycles C_y and C_y^- in a scaffolding. In both representations, the y- and $\overline{y}$-segments contain L-widgets of different orientations. In one, all L-widgets in the y-segment are upwards-oriented (a) and in the other, they are downwards-oriented (b).

differently, we aim to exclude ortho-radial representations where these L-widgets are either both upwards-oriented or both downwards-oriented. This can also be done via clause-cycles. Let x_i be a variable in $\mathcal{V}$ and to better indicate that the literal-segments are independent of each other we call the negative literal $\overline{x_i}$ for now. We define the two *variable-clauses* $c_i^v = x \vee \overline{x}$ and $c_i^{v-} = \neg(x_i \wedge \overline{x_i})$ and represent them via the following clause-cycles (see also Figure 3.10). The first variable-clause c_i^v can be represented by a normal clause-cycle and ensures that not both L-widgets of x_i and $\overline{x_i}$ are downwards-oriented. The second variable-clause c_i^{v-} can be represented by an inverted clause-cycle, as the clause follows the form $\neg(\bigwedge_{i\in[1,k]} l_i)$. This clause-cycle ensures that not both L-widgets are upwards-oriented. Due to them also being synchronized, there only exist two valid ortho-radial representations of this graph representing the two values (*true* or *false*) of y.

3.5 Putting Things Together

Definition 3.11. *Let $\mathcal{I} = (\mathcal{V}, \mathcal{C})$ be a 3-SAT-instance. Then the graph $G_\mathcal{I}$ consists of a scaffolding $\mathcal{S}_{(n,m)}$ and $2n + m$ synchronized clause-cycles such that for $i \in [0, m-1]$ C_i emulates $c_i \in \mathcal{C}$ as well as for $i \in [0, n]$ C_{m+2i} emulates c_i^v and C_{m+2i+1} emulates c_i^{v-}.*

With the definition of the graph $G_\mathcal{I}$ we now show the equivalence required for the reduction.

Lemma 3.12. *Let $\mathcal{I} = (\mathcal{V}, \mathcal{C})$ be a 3-SAT-instance and consider the graph $G_\mathcal{I}$. Then $\mathcal{I}$ is satisfiable if and only if there exists a valid ortho-radial representation of $G_\mathcal{I}$.*

Proof. We start with the "$\Longleftarrow$"-direction, so consider the case that a valid ortho-radial representation $\mathcal{T}$ of $G_\mathcal{I}$ exists. For every variable x_i, the clause-cycles C_{m+2i} and C_{m+2i+1}

emulating c_i^v and c_i^{v-} must be valid. Lemma 3.10 implies that one of the two L-widgets in C_{m+2i} is upwards-oriented, and one of the two L-widgets in C_{m+2i+1} is downwards-oriented. Both clause-cycles only contain L-widgets in the segments Seg_{2i+1} and Seg_{2i+2}, and as all clause-cycles in $G_{\mathcal{I}}$ are synchronized, Observation 3.9 implies that the L-widgets in a single segment are oriented in the same direction. Therefore, the upwards-oriented L-widget of C_{m+2i} can not be contained in the same segment as the downwards-oriented L-widget of C_{m+2i+1}. This leaves only the scenario where all L-widgets in Seg_{2i+1} are oriented in one direction and all L-widgets in Seg_{2i+2} are oriented in the opposite direction.

Then a variable-assignment $\mathcal{A}$ can be created where the variable x_i has value *true* exactly if all L-widgets in the segment Seg_{2i+1} are upwards-oriented and all L-widgets in the segment Seg_{2i+2} are downwards-oriented. Let c_j be an arbitrary clause in $\mathcal{C}$. As the clause-cycle C_j emulating c_j is normal and valid, there must according to Lemma 3.10 exist a segment Seg_i containing an upwards-oriented L-widget in C_j. This implies that c_j contains the corresponding literal of Seg_i, and as the L-widget is upwards-oriented, the literal evaluates to *true* in the variable-assignment $\mathcal{A}$. Therefore, c_j is satisfied by $\mathcal{A}$. As c_j was arbitrary, $\mathcal{A}$ satisfies all clauses in $\mathcal{I}$ and $\mathcal{I}$ is satisfiable.

Now to the "$\Longrightarrow$"-direction. Consider the case that $\mathcal{I}$ is satisfiable, which implies the existence of a variable-assignment $\mathcal{A}$ satisfying all clauses in $\mathcal{C}$. Let $\mathcal{T}$ be the ortho-radial representation of $G_{\mathcal{I}}$ obtained by Lemma 3.1 and Observations 3.3 and 3.5 such that every L-widget represents the value of the literal in the variable-assignment $\mathcal{A}$ of the segment it is placed in. Then all L-widgets in the same segment must be oriented in the same direction. Observation 3.8 implies that every segment has an ortho-radial representation and $\mathcal{T}$ is well-defined. Now let C be a simple essential cycle in $G_{\mathcal{I}}$. Then there are four possible cases.

Case 1: C is either C_c or C_o of the scaffolding $\mathcal{S}_{(n,m)}$. Then Lemma 3.1 implies its validity.

Case 2: C is fully contained in a clause-cycle emulating some clause $c_j \in \mathcal{C}$. Then, due to c being satisfied by $\mathcal{A}$, there exists a literal l in c that has the value *true*. We know that the segment representing l contains an L-widget in the clause-cycle and that the L-widget is upwards-oriented. Lemma 3.10 then implies that C must be valid.

Case 3: C is fully contained in a clause-cycle emulating either the clause c_i^v or c_i^{v-} of some variable $x_i \in \mathcal{V}$. Then this clause-cycle contains L-widgets for both literals x_i and $\overline{x_i}$. Again due to $\mathcal{T}$ respecting $\mathcal{A}$ we know that one of the two L-widgets is upwards- and the other one is downwards-oriented. Lemma 3.10 again implies the validity of C, no matter which of the two clauses is emulated.

Case 4: C is not fully contained in a clause-cycle and is also not the cycle C_c or C_o of $\mathcal{S}_{(n,m)}$. As C is an essential cycle, it must cross every path in the scaffolding $\mathcal{S}$ at least once. When traversing C, we record the index j of every path vertex $v_{i,j}$ that C traverses, resulting in a cyclic list $(b_0, b_1, \ldots, b_k, b_0)$. We know that not all b_i have the same value, as otherwise we would be in some other case above. So with $b_{\min}$ being the minimum value over all b_i and $b_{\max}$ being the maximal value over all b_i we know that $b_{\min} \neq b_{\max}$. Every clause-cycle C_j of $G_{\mathcal{I}}$ is connected at path vertices $v_{i,j}$ for $i \in [0, 2n]$ and the set of clause-cycles therefore separates the ortho-radial grid into multiple layers similar to the rings on the ortho-radial grid. The part of C from layer $b_{\min}$ to the higher layer $b_{\max}$, then must contain a negatively-labelled edge and the path from $b_{\max}$ back to $b_{\min}$ must contain a positively-labelled edge. Hence, C is valid. □

Theorem 3.13. *The problem* Bend-Free-Ortho-Radial *is NP-complete for general plane 4-graphs.*

Proof. It is well known that the 3-Sat-problem is NP-complete, and the 3-Sat can be reduced to Bend-Free-Ortho-Radial by creating the graph $G_{\mathcal{I}}$ for a given 3-Sat-instance $\mathcal{I}$. This reduction can be done in polynomial time and Lemma 3.12 implies that $\mathcal{I}$ is satisfiable if and only if $G_{\mathcal{I}}$ has a valid ortho-radial representation. Therefore, Bend-Free-Ortho-Radial is NP-hard. As one can test in polynomial time if a given representation is a valid ortho-radial one [BNRW21], it must also be NP-complete. □

Figure 3.11 shows an example of a complete graph $G_{\mathcal{I}}$.

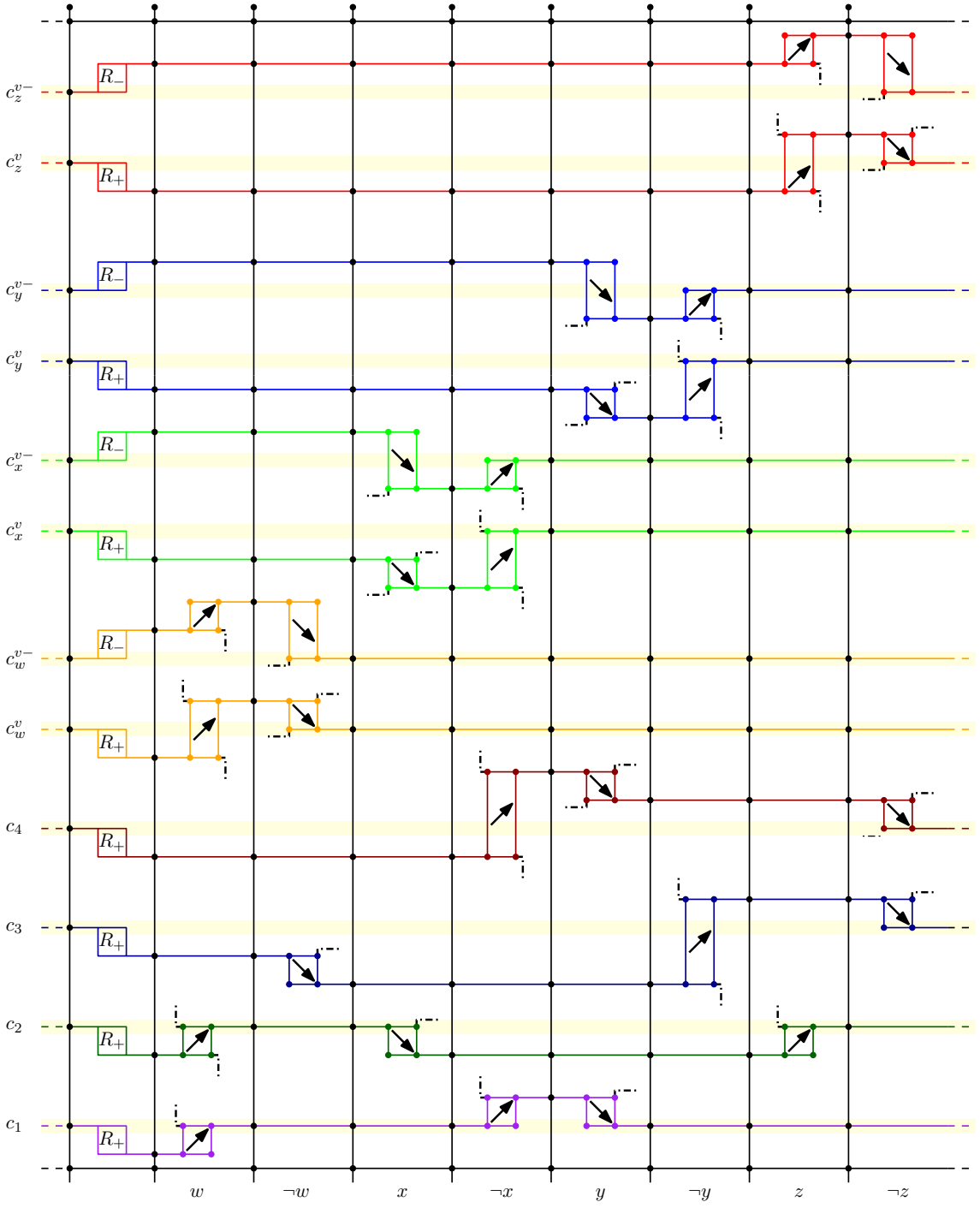

Figure 3.11: A valid ortho-radial representation of the graph $G_{\mathcal{I}}$ for the 3-SAT-instance $\mathcal{I} = (\mathcal{V}, \mathcal{C})$ with $\mathcal{V} = \{w, x, y, z\}$ and the four clauses $c_1 = w \vee \neg x \vee y$, $c_2 = w \vee x \vee z$, $c_3 = \neg w \vee \neg y \vee \neg z$, and $c_4 = \neg x \vee y \vee \neg z$ making up the set $\mathcal{C}$. The variable assignment shown in the representation is $w = \mathit{true}, x = \mathit{false}, y = \mathit{false}, z = \mathit{true}$. Due to space problems, the *Sync*-widgets are not included in the drawing, but are indicated at their connection points by dashed lines.

4. Polynomial-Time Algorithm For Series-Parallel 3-Graphs

Series-parallel graphs have the nice property that many NP-hard problems turn out to have a polynomial-time solution on them. This section shows that also the problem of finding bend-free or bend-minimum valid ortho-radial representations can be solved in polynomial-time for series-parallel graphs, as long as we consider series-parallel 3-graphs.

Definition 4.1. Series-parallel graphs (SP-graphs) *with terminals s and t are recursively defined as follows.*

1. *A single edge $\{s, t\}$ is an SP-graph*
2. *Given two SP-graphs G_1 and G_2 with terminals s_1, t_1 and s_2, t_2, then*
   - *the graph G obtained by identifying t_1 with s_2 is an SP-graph. Such a composition is called a* series composition*. The terminals of G are s_1 and t_2.*
   - *the graph G obtained by identifying s_1 with s_2 and t_1 with t_2 is an SP-graph. Such a composition is called a* parallel composition*. The terminals of G are $s_1 = s_2$ and $t_1 = t_2$.*

Figure 4.1 illustrates these two possible compositions. We call a simple path from s to t in an SP-graph an *st-path* and we use $\mathcal{P}_{st}(G)$ to denote the *set of all st-path of an SP-graph G*. Because st-paths are simple, they for each parallel composition of an SP-graph at most traverse one of its subgraphs. We now show that the Bend-Free-Ortho-Radial-problem can be solved in polynomial time for series-parallel plane 3-graphs

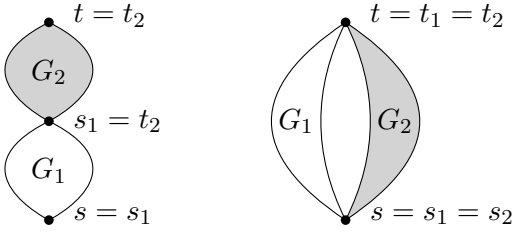

Figure 4.1: A series composition of two SP-graphs on the left and a parallel composition on the right.

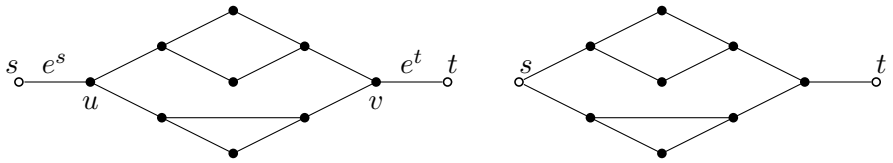

Figure 4.2: On the left, a 2-legged SP-graph with legs e^s and e^t and leg-vertices u, v. On the right, an SP-graph that is not 2-legged as $\deg(s) \neq 1$.

by extending the basic idea of Zhou et al. [ZN05] and Didimo et al. [DKLO22] to the ortho-radial case. We specifically only consider the situation where $f_o \neq f_c$, as otherwise finding a valid ortho-radial representation degenerates to finding a normal orthogonal representation [HHT09].

In Section 4.1 we first consider the subset of 2-legged series-parallel plane 3-graph and show that a bend-minimum valid ortho-radial representation can be computed in $\mathcal{O}(n)$ time as long as one exists. Section 4.2 covers how this approach can be adapted to search for ortho-radial representations with specific propeties. These are then used in Section 4.3 to formulate an algorithm for general series-parallel plane 3-graphs, where a bend-free valid ortho-radial representation can, if one exists, be found in $\mathcal{O}(n^2)$ time.

4.1 2-Legged Series-Parallel 3-Graphs

Definition 4.2. *A series-parallel graph G with terminals s and t is called* 2-legged *if* $\deg(s) = \deg(t) = 1$. *The edges incident to s and t are called* legs *and are named e^s and e^t, respectively. The two vertices adjacent to s and t are called* leg-vertices.

Figure 4.2 shows the difference between a general series-parallel 3-graph and a 2-legged one. We intentionally diverge from the definition of a 2-legged SP-graph by Zhou et al. [ZN05], as in their definition they also require the SP-graph to contain at least three vertices. This would specifically exclude the graph consisting of a single edge from being 2-legged. As that would break the possibility of a recursive decomposition of 2-legged SP-graphs, we use the above slightly different definition.

4.1.1 Creating Decomposition Trees

Using the normal decomposition tree of a series-parallel graph for 2-legged series-parallel 3-graphs is not advisable. In such a tree there would exist series nodes that disconnect the edges e^s and e^t from the inside of the graph and would eventually decompose it into subgraphs that are not 2-legged anymore. With this, recursive algorithms would get complicated. In the case of 2-legged series-parallel 3-graphs, a different deconstruction is possible that preserves the 2-legged-property. Given a 2-legged series-parallel graph G, the graph $G - s - t$ obtained by deleting vertices s and t is a series-parallel graph having the original leg-vertices as the terminals. We decompose G into two 2-legged sub-graphs depending on whether $G - s - t$ is a series or parallel composition similar to the work of Zhou et al. [ZN05].

Lemma 4.3. *Let G be a 2-legged series-parallel 3-graph where $G - s - t$ is a series composition of two subgraphs G'_1 and G'_2. Then G can be deconstructed into two subgraphs G_1 and G_2 that only share a single edge e and are both 2-legged series-parallel 3-graphs.*

Proof. Let w be the single vertex connecting the subgraphs G'_1 and G'_2. Without loss of generality, as $\deg(w) \leq 3$, G'_2 contains only a single edge e incident to w as seen in Figure 4.3. Defining $G_1 \coloneqq G'_1 \cup \{e\}$ and $G_2 \coloneqq G'_2$ we get two 2-legged series-parallel subgraphs. □

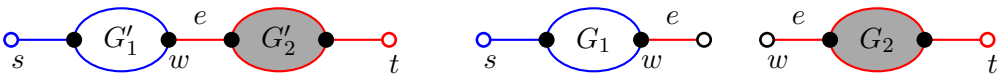

Figure 4.3: On the left, a 2-legged SP-graph consisting of two subgraphs G'_1 in blue and G'_2 in red as by the normal composition rules of SP-graphs. On the right, the subgraphs G_1 and G_2 resulting from the decomposition into 2-legged SP-graphs. For G_1 to be 2-legged, it receives a copy of the edge e.

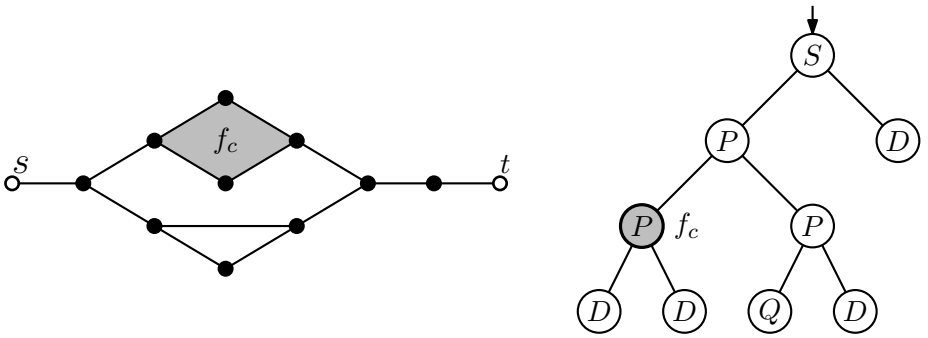

Figure 4.4: A 2-legged SP-graph and its decomposition tree. The order of the children in the tree represents the embedding of the graph and the marked node indicates the parallel composition where f_c is formed.

In this decomposition, we require series nodes to have exactly two children. A series connection of more than two subgraphs has to be represented by a sequence of series nodes. Note that in a normal series composition, the two subgraphs share a single vertex, whereas in the decomposition of Lemma 4.3, the resulting subgraphs share a single edge. When connecting two 2-legged SP-graphs G_1, G_2 in series, e^t of G_1 and e^s of G_2 therefore get merged into a single edge (see edge e in Figure 4.3).

Lemma 4.4. *Let G be a 2-legged series-parallel 3-graph where $G - s - t$ is a parallel composition of multiple subgraphs. Then G can be deconstructed into exactly two subgraphs G_1 and G_2 both of which are 2-legged series-parallel 3-graphs.*

Proof. Let u, v be the two leg-vertices of G. As $\deg(u), \deg(v) \leq 3$ and u, v already have the incident edges e^s and e^t, there are exactly two children in the parallel composition. Each child is connected to v and u with a single edge and is therefore 2-legged. □

With this knowledge, a 2-legged series-parallel 3-graph G can be represented by a decomposition tree similar to general SP-graphs. An $\mathcal{S}$-node represents a series and $\mathcal{P}$-node a parallel composition of two 2-legged subgraphs, where both always have two subgraphs. There also exist two types of leaf nodes. A $\mathcal{Q}$-node, similar to normal decomposition trees, represents a single edge and a $\mathcal{D}$-node represents two connected series edges. Figure 4.4 shows an example of a decomposition tree. Note that the second type of leaf node is required for these kinds of decomposition trees. This is because a $\mathcal{D}$-node (two adjacent edges) is not the result of a series composition of two $\mathcal{Q}$-nodes as would be the case for normal decomposition trees. A series composition of two 2-legged SP-graphs always merges one leg of one subgraph with another leg of the other subgraph into a single edge. Therefore, a series composition with a $\mathcal{Q}$-node is in fact an identity operation. Connecting two $\mathcal{Q}$-nodes serially together would again simply result in another $\mathcal{Q}$-node, so a $\mathcal{D}$-node is necessary. The creation of a decomposition tree for a 2-legged SP-graph is, per step, based on the creation of a normal decomposition tree. Therefore, a linear-time algorithm for constructing a 2-legged decomposition tree can be easily deduced from the literature.

We now also restrict the set of embeddings we consider. Specifically, we require for the given fixed embedding $\mathcal{E}$ that the terminals of G are incident to the outer face f_o. We say that $\mathcal{E}$ is an *outer embedding* of G if this is given. With $\mathcal{E}$ being an outer embedding, the order of the children in the tree completely describe $\mathcal{E}$ as follows. If a vertex v has a degree of 2 or lower, its rotation scheme is already fixed. If its degree is 3, it must be the leg-vertex of some $\mathcal{P}$-node ϕ. The fact that $\mathcal{E}$ is outer together with the ordering of the child nodes implies an order of the incident edges of v and therefore a rotation scheme of v. The embedding described in Figure 4.4 is outer and the order of the children in the decomposition tree reflects the embedding of the graph.

A $\mathcal{Q}$-node is *marked* if at the connection of its children the central face f_c is formed (again see Figure 4.4) and a node contains f_c if it contains the marked node in its subtree. These are exactly all nodes in the direct path from the marked $\mathcal{Q}$-node to the root node. The problem instance of $(G, \mathcal{E}, f_o, f_c)$ can now be completely represented by a decomposition tree of G. From now on, unless specified otherwise, 2-legged SP-graphs always have a maximum degree of 3, an embedding is always outer, and a decomposition tree of a 2-legged SP-graph refers to the above-mentioned new type of decomposition tree. A node ϕ is said to *induce* a 2-legged SP-graph G if G has a decomposition tree with ϕ as its root. Moreover, if G is rectilinear-plane with the fixed embedding of ϕ, we also say that ϕ is rectilinear-plane and if G is orthoradial-plane with the fixed embedding of ϕ, we say that ϕ is orthoradial-plane.

4.1.2 Finding Bend-Free Ortho-Radial Representations

The general idea in this chapter is to traverse the decomposition tree of a 2-legged SP-graph G in a bottom-up fashion while keeping track of which orthogonal or ortho-radial representations are achievable at each node. As only some properties of these representations are important for the recursion, only these are tracked. Before defining which properties are needed, we define the notion of *relative labels*. A relative label is similar to the labelling in an ortho-radial representation but with a variable reference edge. We will use relative labels in the construction of our proofs rather than normal labels since the actual reference edge in the to-be-found valid ortho-radial representation may not yet be present in some steps of the recursion.

Lemma 4.5. *Let $(G, \mathcal{E})$ be a 2-legged series-parallel plane 3-graph, $\mathcal{H}$ an orthogonal representation of G and e^* an edge in G. Let $e \in G$ be an edge for which there exists an st-path P first traversing e^* and then traversing e. Then* $\mathrm{rot}(P[e^*, e])$ *is independent of the choice of P.*

Proof. Let P_1 and P_2 be two st-paths both first traversing e^* and afterwards e. One has to now show that $\mathrm{rot}(P_1[e^*, e]) = \mathrm{rot}(P_2[e^*, e])$. For this, let G' be the subgraph $P_1[e^*, e] \cup P_2[e^*, e] \subseteq G$ consisting only of the two alternative paths between e^* and e. As G' is a subgraph of G, it can be associated with the induced orthogonal representation of $\mathcal{H}$. Then $P_1[e^*, e]$ and $P_2[e^*, e]$ are both so-called spines of G', and $\mathrm{rot}(P_1[e^*, e]) = \mathrm{rot}(P_2[e^*, e])$ follows from the literature [DBLV98, Lemma 4.1]. □

Definition 4.6. *Let $(G, \mathcal{E})$ be a 2-legged series-parallel plane 3-graph, $\mathcal{H}$ an orthogonal representation of G and e^* an edge in G. Let $e \in G$ be an edge for which there exists an st-path P first traversing e^* and then traversing e. Then $\ell_{e^*}(e)$ is called the* label *of e* relative *to e^* in $\mathcal{H}$ and is defined as*

$$\ell_{e^*}(e) \coloneqq \mathrm{rot}(P[e^*, e]).$$

We further define $\ell_s(e) \coloneqq \ell_{e^s}(e)$.

Unless specified otherwise, a relative label of some edge in a 2-legged SP-graph always refers to the label relative to e^s. As relative labels are defined via rotations on paths, we also know that if an st-path contains three edges e, f, g in this order, then

$$\ell_e(g) = \ell_e(f) + \ell_f(g).$$

We now define the specific properties of nodes in the tree that have to be tracked. As will be shown later, it is enough to only define properties for nodes not yet containing f_c. For these nodes, the definition of orthogonal representations and (valid) ortho-radial representations are equivalent. First, we have to make sure that when connecting two subgraphs together, there exist representations of the subgraphs that can be connected to form a representation of the whole graph. To do this, the approach of Didimo et al. [DKLO22] is used. They also find bend-minimum drawings of SP-graphs using decomposition trees but only in the orthogonal case. They found that per node they only have to keep track of the *spirality* of the induced subgraph to tell if and how many bends are required for the parent node to admit an orthogonal representation as well.

The spirality $\sigma(\mathcal{H})$ of an orthogonal representation $\mathcal{H}$ was first introduced by Di Battista et al. [DBLV98]. They define it, at least in the case of 2-legged SP-graphs, as $\sigma(\mathcal{H}) = \text{rot}(P)$ for an st-path $P \in \mathcal{P}_{st}(G)$. For general graphs, the definition is slightly more complicated. Lemma 4.5 also implies that the spirality is indipendent of the concrete st-path. With the definition of relative labels, the spirality of $\mathcal{H}$ could also be defined as $\sigma(\mathcal{H}) = \ell_s(e^t)$. Spirality essentially measures how much a graph is curled up in a given orthogonal representation. The following lemma shows that for 2-legged series-parallel plane 3-graphs, an orthogonal representation of the graph can, intuitively speaking, always be unraveled such that it is less curled up.

Lemma 4.7. *Let $(G, \mathcal{E})$ be a 2-legged series-parallel plane 3-graph for which an orthogonal representation $\mathcal{H}$ of G exists with $\sigma(\mathcal{H}) = x \neq 0$. Then for every $y \in \{0, \dots, x-1\}$, if x is positive, or $y \in \{x+1, \dots, 0\}$, if x is negative, there exists an orthogonal representation $\mathcal{H}_y$ of G with $\sigma(\mathcal{H}_y) = y$.*

Proof. For positive x, this fact is proven by Di Battista et al. [DBLV98, Lemma 5.1, Lemma 5.2] as G is a 3-graph. They later argue that the mirrored result for negative x also holds. □

Lemma 4.7 implies that the set of possible spirality values for a 2-legged SP-graph is an interval. As also done by Didimo et al. [DKLO22], a node keeps track of the maximum and minimum spirality values possible over all orthogonal representations of a graph. We call the minimum possible spirality of the graph its *left bend value* and the maximum possible spirality the *right bend value*.

Definition 4.8. *Let $(G, \mathcal{E})$ be a 2-legged rectilinear-plane series-parallel 3-graph. Then the* left bend value b^l *and the* right bend value b^r *of G are defined as*

$$b^l := -\min\{\sigma(\mathcal{H}) \mid \mathcal{H} \in \Omega(G, \mathcal{E})\} \text{ and}$$
$$b^r := \max\{\sigma(\mathcal{H}) \mid \mathcal{H} \in \Omega(G, \mathcal{E})\}.$$

Intuitively, the value b^l indicates how much the graph can curl up to the left relative to e^s, and b^r indicates how much it can curl up to the right. Figure 4.5 shows two sample graphs and their bend values.

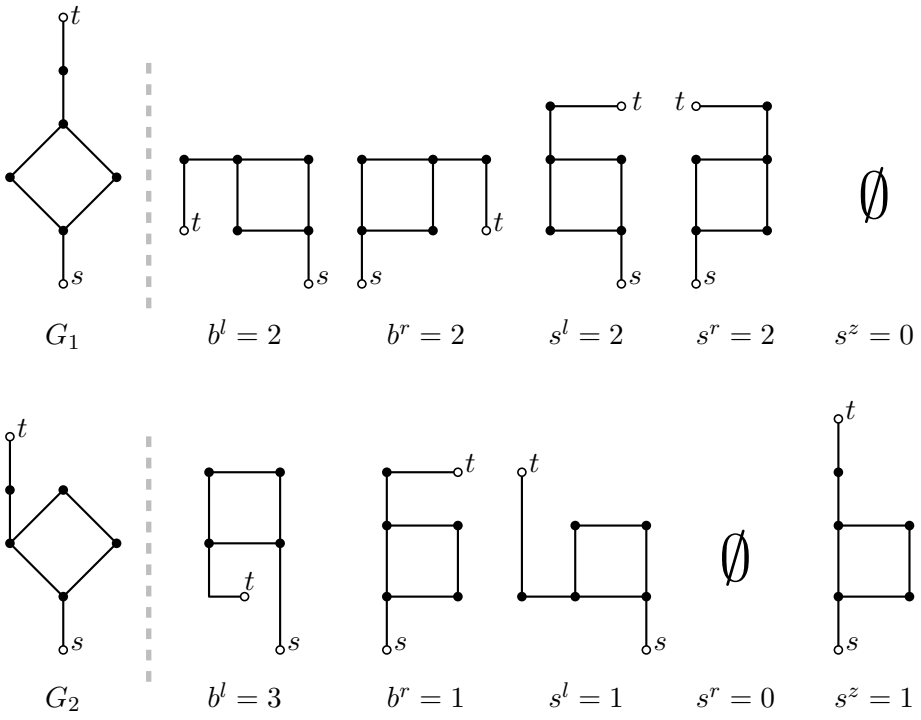

Figure 4.5: Two 2-legged SP-graphs and orthogonal representations corresponding to their bend and step values. If some step value is 0, no matching orthogonal representation exists.

Lemma 4.9. *Let $(G, \mathcal{E})$ be a 2-legged rectilinear-plane series-parallel 3-graph and let b^l and b^r be its step values. We then know that $b^l \geq 0$ and that for every $y \in \{-b^l, \ldots, b^r\}$ there exists an orthogonal representation $\mathcal{H}_y$ of G with $\sigma(\mathcal{H}_y) = y$.*

Proof. Both statements directly follow from Definition 4.8 and Lemma 4.7. □

Bend values would be enough in the orthogonal case, but to satisfy the labeling-constraint of a valid ortho-radial representation more information about the internal structure of each subgraph is required. At some $\mathcal{P}$-nodes in the recursion essential cycles may be formed by connecting two subgraphs in parallel We have to make sure that these do not become invalid cycles. A cycle is valid if it contains a positively- and negatively-labelled edge or if it only consists of edges with label 0. To ensure this, we are interested in a few subsets of special orthogonal representations of each subgraph. Namely, those where in every st-path there exists an edge with a negative (resp. positive) label relative to the starting terminal, and those where an st-path exists consisting of only edges with a relative label of 0. We define these special subsets for a 2-legged rectilinear-plane series-parallel 3-graph $(G, \mathcal{E})$ as

$$\Omega_-(G, \mathcal{E}) \coloneqq \{\mathcal{H} \in \Omega(G, \mathcal{E}) \mid \forall P \in \mathcal{P}_{st}(G) : \exists e \in P : \ell_s(e) < 0\}$$

for the subset of orthogonal representations containing an edge with a negative relative label in every st-path and

$$\Omega_+(G, \mathcal{E}) \coloneqq \{\mathcal{H} \in \Omega(G, \mathcal{E}) \mid \forall P \in \mathcal{P}_{st}(G) : \exists e \in P : \ell_s(e) > 0\}$$

for the subset of orthogonal representations containing an edge with a positive relative label in every st-path. Finally, we use

$$\Omega_z(G, \mathcal{E}) \coloneqq \{\mathcal{H} \in \Omega(G, \mathcal{E}) \mid \exists P \in \mathcal{P}_{st}(G) : \forall e \in P : \ell_s(e) = 0\}$$

for the subset of orthogonal representations where an st-path exists consisting of only edges with relative label 0. The correlation between relative labels and spirality implies that every orthogonal representation in $\Omega_z(G, \mathcal{E})$ has spirality 0. But the orthogonal representations in the other two set are allowed to have different spirality values. Similar to bend values, we need to know the range of spirality values achievable in these subsets. For this, we introduce the notion of *step values*.

Definition 4.10. *Let $(G, \mathcal{E})$ be a 2-legged rectilinear-plane series-parallel 3-graph. We define the following three* step values*.*

1. *The* left step value *s^l is defined as*

$$s^l \coloneqq \max(\{0\} \cup \{\sigma(\mathcal{H}) + 1 \mid \mathcal{H} \in \Omega_-(G, \mathcal{E})\}).$$

2. *The* right step value *s^r is defined as*

$$s^r \coloneqq \max(\{0\} \cup \{-\sigma(\mathcal{H}) + 1 \mid \mathcal{H} \in \Omega_+(G, \mathcal{E})\}).$$

3. *The* zero step value *$s^z \in \{0, 1\}$ is defined as*

$$s^z = \begin{cases} 1 & \text{if } \Omega_z(G, \mathcal{E}) \neq \emptyset, \\ 0 & \text{otherwise.} \end{cases}.$$

Observe that we intentionally add 1 to the spirality in the definition of s^l and s^r. This is done to differentiate between the case $s^l = 0$, which implies that no orthogonal representation in $\Omega_-(G, \mathcal{E})$ exists with a spirality of 0 or greater, and the case $s^l > 0$, where an orthogonal representation $\mathcal{H}$ in $\Omega_-(G, \mathcal{E})$ exists with $\sigma(\mathcal{H}) = s^l - 1 \geq 0$. To get a feel for step values, Figure 4.5 depicts two examples of 2-legged SP-graphs and their corresponding step values. As seen in the figure, the left and right step values may differ. This is due to the fact that we are given a fixed embedding. The benefits of step-values can be seen in the following example. If $s^l = 1$ for some subgraph G, we know that an orthogonal representation $\mathcal{H}$ of G exists with $\sigma(\mathcal{H}) = 0$ and an edge in every st-path with a negative relative label. If an ortho-radial representation of the complete graph exists containing $\mathcal{H}$ and the leg e^s of G is oriented to have label 0, every essential cycle traversing G must completely traverse some st-path of G and therefore contains at least one negatively-labelled edge.

Now, for every tree node ϕ that does not yet contain the central face f_c we keep track of both bend and step values in a tuple $[b^l, b^r, s^l, s^r, s^z]$ called the *structure of ϕ*. For tree nodes that already contain the central face no further information is required. As a base case for the recursion, we assign to every $\mathcal{Q}$-node the structure

$$[b^l, b^r, s^l, s^r, s^z] = [0, 0, 0, 0, 1]$$

and to every $\mathcal{D}$-node the structure

$$[b^l, b^r, s^l, s^r, s^z] = [1, 1, 0, 0, 1].$$

Before actually looking at the recursion itself, further insight into the properties of bend and step values are required. Given some orthogonal representation $\mathcal{H}$ of a graph G we know from Lemma 4.7 that $b^r \geq \sigma(\mathcal{H})$ and $b^l \geq -\sigma(\mathcal{H})$. But sometimes further properties of $\mathcal{H}$ are deducible that improve on these simple inequalities.

Lemma 4.11. *Let $(G, \mathcal{E})$ be a 2-legged rectilinear-plane series-parallel 3-graph and let $\mathcal{H}$ be an orthogonal representation of G with $x \coloneqq \sigma(\mathcal{H})$. Then the following holds.*

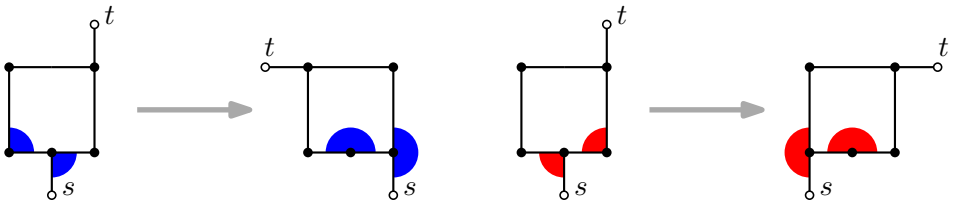

Figure 4.6: On the left, an orthogonal representation that contain a positive rotation in every st-path indicated by a blue angle. Next to it the result of Lemma 4.11, where the spirality of the new representation was decreased by 1. On the right, the same orthogonal representations with negative rotations in every st-path indicated by red angles and similarly the resulting graph with now a higher spirality.

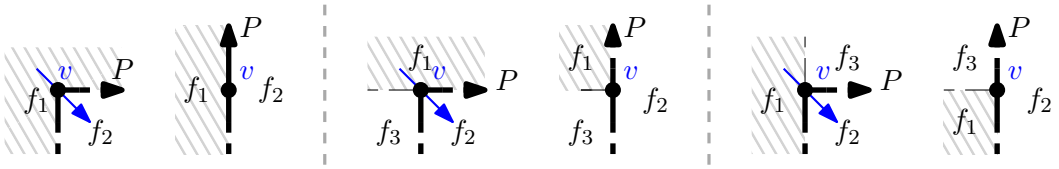

Figure 4.7: The three possibilities of an access from the face f_1 on the left of the st-path P to the face f_2 on the right at the vertex v. For every case the rotation at v along P is positive. Next to each drawing is the result of an elementary transformation using the access v.

- *If in every st-path P there exist adjacent vertices u, v, w such that* $\mathrm{rot}(uv, vw) = 1$*, then there exists another orthogonal representation $\mathcal{H}'$ of G with $\sigma(\mathcal{H}') = x - 1$ and therefore $b^l \geq x + 1$.*
- *If in every st-path P there exist adjacent vertices u, v, w such that* $\mathrm{rot}(uv, vw) = -1$*, then there exists another orthogonal representation $\mathcal{H}'$ of G with $\sigma(\mathcal{H}') = x + 1$ and therefore $b^r \geq x + 1$.*

In both cases, $\mathcal{H}'$ and $\mathcal{H}$ differ per st-path only in the rotation at exactly one vertex v having the above requirements. All other rotations stay the same.

Proof. Only the proof for the first half is given, since the other half is simply the mirrored result. Let $\mathcal{H}$ be an orthogonal representation of G with $\sigma(\mathcal{H}) = x$,where every st-path contains adjacent vertices u, v, w such that $\mathrm{rot}(uv, vw) = 1$ (see Figure 4.6). The following proof is an adaption to the one by Di Battista et al. [DBLV98, Lemma 5.2]. They show that given an orthogonal representation with positive spirality y, an orthogonal representation with spirality $y-1$ can be created by finding a correctly oriented elementary transformation as defined by Tamassia et al. [TTV91]. They show this for general planar 3-graphs and their notation is therefore slightly different. Instead of using st-paths they use the more general notion of splines. In our case though, they are equivalent. Their proof depends on the existence of a so-called access in every st-path of the graph, where the source face of the access is locally to the left of the st-path and the target is to the right. An access is a vertex a with source face f and target face g if one of the following two cases holds.

1. If vertex a has exactly two incident faces f_1 and f_2 and the rotation of face f_1 at a is not 1, then a is an access from f_1 to f_2.
2. If vertex a has three incident faces f_1, f_2, and f_3 and the rotation of face f_1 at a is zero, then a is an access from f_1 to both f_2 and f_3.

Now let v be the vertex in an arbitrary st-path P with the requirements given in the statement (see Figure 4.7). As $\text{rot}(uv, vw) = 1$, then only one incident face of v can lie locally to the right of P. If also $\deg(v) = 2$, then only two faces are incident to v and the other incident face has a rotation of -1 at v. If $\deg(v) = 3$, then exactly one of the now two other incident faces has a rotation of 0 at v. In any case, v is in an access from the left side of P to the right side. As P was arbitrary, every st-path contains a correctly oriented access. Di Battista et al. [DBLV98] only require the orthogonal representation to have a positive spirality in their lemma so they can later argue that every st-path must contain a correctly oriented access. As this is already given in our case, we can, even with having $\sigma(\mathcal{H}) = x \leq 0$, deduce that another orthogonal representation $\mathcal{H}'$ of G must exist with $\sigma(\mathcal{H}) = x - 1$.

The elementary transformation used in the proof by Di Battista et al. [DBLV98] only traverses one access per st-path. As only traversed vertices are changed, all other rotations in $\mathcal{H}$ stay the same. □

Lemma 4.12. *Let $(G, \mathcal{E})$ be a 2-legged rectilinear-plane series-parallel 3-graph having the structure $[b^l, b^r, s^l, s^r, s^z]$. Then $b^r \geq s^l$ and $b^l \geq s^r$.*

Proof. Let $x = s^l > 0$. Then there exists an orthogonal representation $\mathcal{H}$ of G with $\sigma(\mathcal{H}) = x - 1$ and every st-path contains an edge e with $\ell_s(e) < 0$. Let P be an arbitrary st-path. For P to have a relative label of 0 at e^s and a negative label at the edge e with $\ell_s(e) < 0$, there must exist three adjacent vertices u, v, w in P between s and e with $\text{rot}(uv, vw) = -1$. Lemma 4.11 then implies $b^r \geq x = s^l$. For s^r this follows analogously. □

Lemma 4.13. *Let $(G, \mathcal{E})$ be a 2-legged rectilinear-plane series-parallel 3-graph having the structure $[b^l, b^r, s^l, s^r, s^z]$. Then $s^l = 0$ if $b^l = 0$, and $s^r = 0$ if $b^r = 0$.*

Proof. We make a proof by contraposition. Assume $s^l > 0$. Then there exists an orthogonal representation $\mathcal{H}$ of G with $\sigma(\mathcal{T}) = 0$ and an edge with a negative relative label in every st-path of G. Let P be an arbitrary st-path and let e be an edge with a negative relative label in P. Then for $0 = \sigma(\mathcal{T}) = \ell_s(e^t)$ to hold, the labels on the path must go from a negative relative label at e to a relative label of 0 at e^t. So there must exist three adjacent vertices u, v, w between e and e^t with $\text{rot}(uv, vw) = 1$. Lemma 4.11 then implies $b^l \geq 0 + 1 > 0$. For s^r and b^r this follows analogously. □

Lemma 4.14. *Let $(G, \mathcal{E})$ be a 2-legged rectilinear-plane series-parallel 3-graph and let $\mathcal{H}$ be an orthogonal representation of G where every st-path contains an edge with a positive and an edge with a negative relative label. If $\sigma(\mathcal{H}) \leq 0$, then $b^l \geq 2$. Similarly, if $\sigma(\mathcal{H}) \geq 0$, then $b^r \geq 2$.*

Proof. As a start, consider the case $\sigma(\mathcal{H}) = 0$ and let P be an arbitrary st-path in G. Without loss of generality, P contains first an edge e with a negative and then an edge f with a positive label. Then P has to contain adjacent vertices u, v, w between s and e as well as u', v', w' between f and e with $v \neq v'$ and $\text{rot}(uv, vw) = \text{rot}(u'v', v'w') = -1$. Moreover, P must also contain adjacent vertices x, y, z and x', y', z' between e and f with $y \neq y'$ and $\text{rot}(xy, yz) = \text{rot}(x'y', y'z') = 1$. Looking at the vertex v in every path, Lemma 4.11 implies the existence of another orthogonal representation with spirality 1. As in the new orthogonal representation only the rotations at each v may be different, $\text{rot}(u'v', v'w') = -1$ still holds. Therefore, Lemma 4.11 implies the existence of a third orthogonal representation, now with spirality 2, and $b^r \geq 2$ follows. The same argument with y and y' implies $b^l \geq 2$.

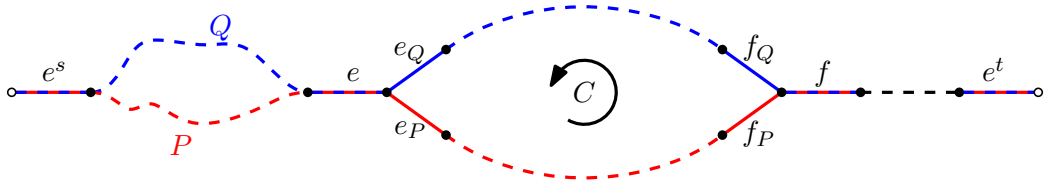

Figure 4.8: Two st-paths P and Q. Between e and f the paths are disjoint and after f the paths coincide. The cycle C is formed by connecting the subpaths $P[e_P, f_P]$ and $\overline{Q[e_Q, f_Q]}$.

Now if $x = \sigma(\mathcal{H}) \geq 1$, there must still exist adjacent vertices u, v, w in every path with $\mathrm{rot}(uv, vw) = -1$. It follows again with Lemma 4.11 that $b^r \geq x + 1 = 2$. The same applies if $\sigma(\mathcal{H}) \leq 1$, where there still exist adjacent vertices x, y, z in every path with $\mathrm{rot}(xy, yz) = 1$. □

Lemma 4.15. *Let $(G, \mathcal{E})$ be a 2-legged rectilinear-plane series-parallel 3-graph. Then*

$$\Omega_-(G, \mathcal{E}) \cup \Omega_+(G, \mathcal{E}) \cup \Omega_z(G, \mathcal{E}) = \Omega(G, \mathcal{E}).$$

Proof. It is clear From the definition of each set that the "$\subseteq$"-direction must hold. To prove the "$\supseteq$"-direction, we show that if an orthogonal representation $\mathcal{H}$ of G is neither contained in $\Omega_-(G, \mathcal{E})$ nor in $\Omega_+(G, \mathcal{E})$, it must be contained in $\Omega_z(G, \mathcal{E})$. Let $\mathcal{H}$ be an orthogonal representation of G with $\mathcal{H} \notin \Omega_-(G, \mathcal{E}) \cup \Omega_+(G, \mathcal{E})$. Then there exists an st-path P in G where $\ell_s(e) \geq 0$ for all $e \in P$. There also exists an st-path Q in G where $\ell_s(e) \leq 0$ for all $e \in Q$. Now as e^t is contained in both P and Q, it follows that $0 \geq \ell_s(e^t) \geq 0$ and therefore $\sigma(\mathcal{H}) = \ell_s(e^t) = 0$. What is left is to prove the existence of an st-path having only zero-labelled edges and in fact, we show that $P = Q$ and this path has the desired property. As e^t is contained in both paths and has relative label 0, we can define f to be the first edge in P and Q at and after which both paths coincide. Just as for e^t we know that f and every edge after f has relative label 0. Now if $f = e^s$, then both paths would coincide in their whole length and the statement would already hold. So assume $f \neq e^s$. Then the following situation, as also seen in Figure 4.8, would arise. There exists a predecessor f_P of f in P and a predecessor f_Q of f in Q with $f_Q \neq f_P$. Let also e be the first edge preceding f_P in P and f_Q in Q that is contained in both paths again, and let e_P be the successor of e in P and e_Q be the successor of e in Q. Then $P[e_P, f_P] + \overline{P[e_Q, f_Q]}$ forms a simple cycle C. The orientation of the cycle implied by the two subpaths may be such that its interior is not locally to the right, but to the left. By the definition of orthogonal representations it follows that $\mathrm{rot}(C)$ is either 4 if the interior is to the right or -4 if it is to the left. Regarding the part $P[e_P, f_P]$ it follows that

$$\begin{aligned}\mathrm{rot}(P[e_P, f_P]) &= \underbrace{\ell_s(e_P) + \ell_{e_P}(f_P) + \ell_{f_P}(f)}_{=\ell_s(f)=0} - \ell_s(e_P) - \ell_{f_P}(f) \\ &= -\ell_s(e) - \mathrm{rot}(e, e_P) - \mathrm{rot}(f_P, f).\end{aligned}$$

Similarly, $\mathrm{rot}(\overline{P[e_Q, f_Q]}) = \ell_s(e) + \mathrm{rot}(e, e_Q) + \mathrm{rot}(f_Q, f)$ follows. As e, e_P, and e_Q share the same incident vertex, it follows from the definition of an orthogonal representation that $\mathrm{rot}(e, e_P)$ and $\mathrm{rot}(e, e_Q)$ are not both 0 at the same time. The same is true for $\mathrm{rot}(f_P, f)$ and $\mathrm{rot}(f_Q, f)$. Then it follows that

$$\begin{aligned}\mathrm{rot}(C) &= \mathrm{rot}(P[e_P, f_P]) + \mathrm{rot}(\overline{P[e_Q, f_Q]}) \\ &= \underbrace{\mathrm{rot}(e, e_Q) - \mathrm{rot}(e, e_P)}_{\in\{-2,-1\}} + \underbrace{\mathrm{rot}(f_Q, f) - \mathrm{rot}(f_P, f)}_{\in\{1,2\}} \in [-1, 1].\end{aligned}$$

This contradicts $\mathrm{rot}(C) \in \{-4, 4\}$ and therefore $e = e^s$, which implies that P is equal to Q and the paths only contain zero-labelled edges. □

Lemma 4.16. *Let $(G, \mathcal{E})$ be a 2-legged rectilinear-plane series-parallel 3-graph having an orthogonal representation $\mathcal{H}$ of G where there exists an st-path containing only edges with relative label 0. Then every other st-path contains both an edge with a positive and an edge with a negative relative label.*

Proof. Let P be the st-path containing only edges with relative label 0 and let Q be an arbitrary other st-path of G. Let v be the vertex where P and Q split up and let w be the vertex where they meet again. These vertices are never the terminals and both paths share a common edge e before v and a common edge f after w. Let also e_P and e_Q be the edges after e in P and Q and let f_P and f_Q be the edges before e in P and Q. We then know that $\ell_s(e) = \ell_s(w) = 0$. As the edges e_P and f_P also have relative label 0 we know that $\ell_s(e_Q) = 1$ if e_Q lies locally to the right of P and $\ell_s(e_Q) = -1$ if e_Q lies locally to the left. Similarly, we know $\ell_s(f_Q) = -1$ if f_Q lies locally to the right and $\ell_s(f_Q) = 1$ if it lies locally to the left. It is impossible that e_Q and f_Q lie locally on different sides of P, as then either s or t is not contained in f_o. This would be a contradiction to $\mathcal{E}$ being an outer embedding and therefore, Q always contains edges with positive and negative relative labels. □

Similar to the work of Didimo et al. [DKLO22], the structure of an inner node can be described with respect to the structures of its children. We now often rely on the Iversion bracket notation to formulate these relationships. When multiplying an Iversion bracket with some other term, the boolean expression in the bracket essentially acts as a condition for the term. If we for example have $(s^l + b^r) \cdot [s^l > 0]$ containing the left step and right bend value we get the following equality.

$$(s^l + b^r) \cdot [s^l > 0] = \begin{cases} (s^l + b^r) & \text{if } s^l > 0, \\ 0 & \text{otherwise} \end{cases}$$

Lemma 4.17. *Let ϕ be an $\mathcal{S}$-node not containing f_c, where its children ϕ_1 and ϕ_2 both are rectilinear-plane. Also, let $[b_1^l, b_1^r, s_1^l, s_1^r, s_1^z]$ be the structure of ϕ_1 and $[b_2^l, b_2^r, s_2^l, s_2^r, s_2^z]$ be the structure of ϕ_2. Then ϕ is also rectilinear-plane and the structure $[b^l, b^r, s^l, s^r, s^z]$ of ϕ satisfies the following.*

$$b^l = b_1^l + b_2^l$$
$$b^r = b_1^r + b_2^r$$

$$s^l = \max \begin{cases} s_2^l, & (4.1) \\ b_2^r \cdot [b_1^l > 0], & (4.2) \\ (s_1^l + b_2^r) \cdot [s_1^l > 0] & (4.3) \end{cases}$$

$$s^r = \max \begin{cases} s_2^r, & (4.4) \\ b_2^l \cdot [b_1^r > 0], & (4.5) \\ (s_1^r + b_2^l) \cdot [s_1^r > 0] & (4.6) \end{cases}$$

$$s^z = s_1^z \cdot s_2^z \quad (4.7)$$

Proof. Let G be the induced graph of ϕ, G_1 be the induced subgraph of ϕ_1, and G_2 the induced subgraph of ϕ_2. Also let s_1, t_1 be the terminals of G_1 and s_2, t_2 the terminals of G_2 as well as $e_1^s, e_2^s, e_1^t, e_2^t$ be the legs of G_1 and G_2. The proof that ϕ is rectilinear and the proof for the equations of b^l and b^r follow from the work of Didimo et al. [DKLO22, Lemma 5].

The equality for s^z is easy to see since there exists an orthogonal representation $\mathcal{H}$ of G with a zero-labelled path if and only if both subgraphs have orthogonal representations with a zero-labelled path.

Regarding the other two step values, we only show equality for s^l, as s^r follows analogously. First, we prove the "$\geq$"-direction where we here have to show that s^l is greater than any of the three Terms (4.1), (4.2), and (4.3) on the right-hand side. For Term (4.1), we know with Lemma 4.9 that an orthogonal representation $\mathcal{H}_1$ of G_1 with $\sigma(\mathcal{H}_1) = 0$ exists. Now let $\mathcal{H}$ be an orthogonal representation of G containing $\mathcal{H}_1$. Then for every edge e in G_2 we know that $\ell_s(e) = \ell_{s_2}(e)$. From Definition 4.10 we see that the left step value of G is at least the left step value of G_2 for such an orthogonal representation $\mathcal{H}$. In other words $s^l \geq s_2^l$ (Term (4.1)). This is represented in the leftmost drawing of Figure 4.9.

Next, assume $b_1^l > 0$ so that the Iversion bracket in Term (4.2) evaluates to 1 (see Figure 4.9b). Then there exists an orthogonal representation $\mathcal{H}_1$ of G_1 with $\sigma(\mathcal{H}_1) = -1$. As an orthogonal representation $\mathcal{H}_2$ of G_2 exists with spirality $\sigma(\mathcal{H}_2) = b_2^r$, it follows for the orthogonal representation $\mathcal{H}$ of G created by combining $\mathcal{H}_1$ and $\mathcal{H}_2$ that

$$\sigma(\mathcal{H}) = \ell_s(e^t) = \underbrace{\ell_s(e_2^s)}_{=-1} + \underbrace{\ell_{s_2}(e_2^t)}_{=\sigma(\mathcal{H}_2)=b_2^r} = b_2^r - 1.$$

In summary, $\mathcal{H}$ contains a negatively-labelled edge, namely e_1^t in every st-path and has $\sigma(\mathcal{H}) = b_2^r - 1$. This implies $s^l \geq b_2^r \cdot [b_1^l > 0]$ (Term (4.2)).

Finally, consider the case $s_1^l > 0$ so that the Iversion bracket in Term (4.3) evaluates to 1 (see Figure 4.9c). By Definition 4.10 there exists an orthogonal representation $\mathcal{H}_1$ of G_1 with $\sigma(\mathcal{H}_1) = \ell_{s_1}(e_1^t) = s_1^l - 1$ that contains an edge in every st-path with a negative relative label. Now as an orthogonal representation $\mathcal{H}_2$ of G_2 with $\sigma(\mathcal{H}_2) = b_2^r$ exists, we get by concatenating $\mathcal{H}_1$ and $\mathcal{H}_2$ an orthogonal representation $\mathcal{H}$ of G, containing a negatively-labelled edge in every st-path and $\sigma(\mathcal{H}) = s_1^l + b_2^r - 1$. This implies that $s^l \geq (s_1^l + b_2^r) \cdot [s_1^l > 0]$ (Term (4.3)).

Now to the "$\leq$"-direction. Here we have to show that in every case s^l is smaller or equal to at least one Term on the left-hand side. As every such term is non-negative, the case $s^l = 0$ is trivial. So suppose $s^l = x > 0$. Then there exists an orthogonal representation $\mathcal{H}$ of G that contains a negatively-labelled edge in every st-path and has total spirality $x - 1$. Now let $e = e_1^t = e_2^s$ be the edge connecting the two components G_1 and G_2 and $\ell_s(e)$ be the relative label of this edge. We distinguish between two cases. **Case 1:** $\ell_s(e) = y < 0$. Then this implies $\sigma(\mathcal{H}_1) < 0$ and therefore $b_1^l > 0$. As $\sigma(\mathcal{H}) = x - 1$ we get for Term 4.1 that

$$b_2^r \cdot [b_1^l > 0] = b_2^r \geq \sigma(\mathcal{H}_2) = \sigma(\mathcal{H}) - \sigma(\mathcal{H}_1) = x - 1 - y \geq x = s^l.$$

Case 2: $\ell_s(e) = y \geq 0$. Then $b_1^r \geq y$ and as the spirality of G is $x - 1$ it follows for G_2 that $b_2^r \geq \max(0, x - y - 1)$. Now, since an edge with a negative relative label has to be present in every st-path and $\ell_s(e) \geq 0$. This edge must be contained in one of the two components. If it is contained in $\mathcal{H}_1$, then $s_1^l \geq y + 1$ and Term (4.3) satisfies

$$(s_1^l + b_2^r) \cdot [s_1^l > 0] \geq y + 1 + \max(0, x - y - 1) \geq x = s^l.$$

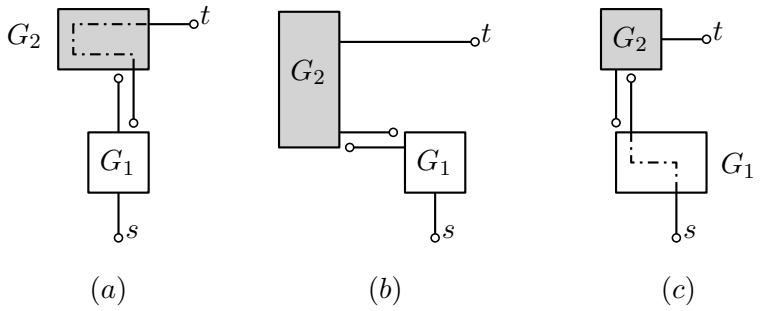

Figure 4.9: An abstract view of creating a non-zero left step value s^l in a series composition of two subgraphs G_1 and G_2.

If it is contained in $\mathcal{H}_2$, then the following situation arises. First, $\mathcal{H}_1$ makes at least y right turns along each st-path to achieve $\ell_s(e) = y > 0$, then $\mathcal{H}_2$ makes $y+1$ left turns along each st-path to the edge with the negative relative label and afterwards makes at least x right turns again to achieve $\sigma(\mathcal{H}) = x-1$. Lemma 4.11 can now be applied to the first y left turns in $\mathcal{H}_2$. This results in an orthogonal representation $\mathcal{H}_2'$ of G_2 with an edge in every st-path having relative label -1 and with the x right turns afterwards the representation still has spirality $x-1$. This implies $s_2^l \geq x$ and Term (4.3) satisfies $s_2^l \geq x = s^l$. □

To formulate a similar result for a $\mathcal{P}$-node, we first introduce more notation.

Definition 4.18. *Let ϕ be a $\mathcal{P}$-node, let G be its induced graph, and let G_1,G_2 be the induced subgraphs of the child nodes ϕ_1 and ϕ_2. Let moreover $e_1^s, e_1^t, e_2^s, e_2^t$ be the legs of G_1 and G_2. For an angle assignment $\mathcal{A}$ of G we define the* rotation values *$r_1^s = \text{rot}(e^s, e_1^s)$, $r_2^s = \text{rot}(e^s, e_2^s)$, $r_1^t = \text{rot}(e_1^t, e^t)$, and $r_2^t = \text{rot}(e_2^t, e^t)$. We call the tuple $[r_1^s, r_1^t, r_2^s, r_2^t]$ a* rotation combination*.*

For an orthogonal or ortho-radial representation we know that r_1^s and r_1^t are in the set $\{-1, 0\}$ and that r_2^s and r_2^t are in the set $\{0, 1\}$. Moreover, r_1^s and r_2^s can not be 0 at the same time and this also holds for r_1^t and r_2^t. Finally, the equations $\text{rot}(e_1^t, e_2^t) = |r_1^t + r_2^t| \in \{0, 1\}$ and $\text{rot}(e_2^s, e_1^s) = |r_1^s + r_2^s| \in \{0, 1\}$ hold.

Lemma 4.19. *Let ϕ be a $\mathcal{P}$-node not containing f_c, where its children ϕ_1 and ϕ_2 both are rectilinear-plane. Also, let $[b_1^l, b_1^r, s_1^l, s_1^r, s_1^z]$ be the structure of ϕ_1 as well as $[b_2^l, b_2^r, s_2^l, s_2^r, s_2^z]$ be the structure of ϕ_2. Then ϕ is rectilinear-plane if and only if*

$$b_1^r + b_2^l \geq 2.$$

Moreover, in the case that ϕ is rectilinear-plane the structure $[b^l, b^r, s^l, s^r, s^z]$ of ϕ satisfies the following.

$$b^l = \min(b_1^l + 2, b_2^l)$$
$$b^r = \min(b_1^r, b_2^r + 2)$$

$$s^l = \max \begin{cases} [b_1^r > 0] \cdot [b_2^l > 0], & (4.8) \\ \min(b_1^r, s_2^l + 1) \cdot [s_2^l > 0] \cdot [b_1^r \geq 2] & (4.9) \end{cases}$$

$$s^r = \max \begin{cases} [b_1^r > 0] \cdot [b_2^l > 0], & (4.10) \\ \min(b_2^l, s_1^r + 1) \cdot [s_1^r > 0] \cdot [b_2^l \geq 2] & (4.11) \end{cases}$$

$$s^z = \max\{[b_1^r \geq 2] \cdot s_2^z, [b_2^l \geq 2] \cdot s_1^z\} \quad (4.12)$$

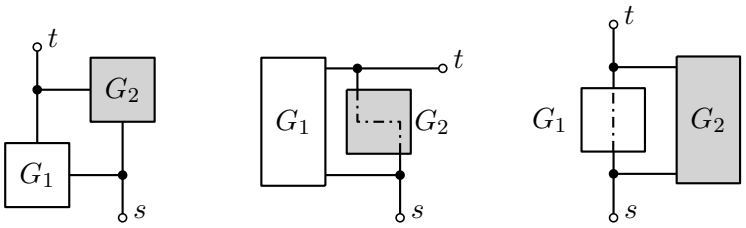

Figure 4.10: Examples of how a parallel connection of subgraphs G_1 and G_2 result in $s^l = 1$ for the left step value (a), in $s^l = 2$ for the left step value (b), and in $s^z = 1$ for the zero step value (c).

Proof. Let G be the induced graph of ϕ, G_1 the induced subgraph of ϕ_1, and G_2 the induced subgraph of ϕ_2. Also let s_1, t_1 be the terminals of G_1 and s_2, t_2 the terminals of G_2 as well as $e_1^s, e_2^s, e_1^t, e_2^t$ be the legs of G_1 and G_2. The proof for having an orthogonal representation as well as the values of b^l and b^r follows from Didimo et al. [DKLO22, Lemma 7, Lemma 8] together with Lemma 4.9.

Regarding the two step values s^l and s^r, we only show the equality for s^l, as s^r follows analogously, and start with the "$\geq$"-direction. We here have to show that s^l is greater than any of the three terms on the right-hand side.

As a start, consider Term (4.8). Unless both Iversion brackets in Term (4.8) result in a value of 1, the total term is 0 and $s^l \geq 0$ trivially holds. Therefore, suppose both $b_1^r > 0$ and $b_2^l > 0$, which implies $[b_1^r > 0] \cdot [b_2^l > 0] = 1$. Then there exist orthogonal representations $\mathcal{H}_1$ of G_1 with $\sigma(\mathcal{H}_1) = 1$ and $\mathcal{H}_2$ of G_2 with $\sigma(\mathcal{H}_2) = -1$. Using the rotation combination $[r_1^s, r_1^t, r_2^s, r_2^t] = [-1, 0, 0, 1]$ results in an orthogonal representation $\mathcal{H}$ of G as also seen in Figure 4.10a. It then follows that $\ell_s(e_1^s) = \ell_s(e_2^t) = -1$ and therefore $s^l \geq 1$.

Now consider Term (4.9). Again, unless both conditions in the Iversion brackets are true, $s^l \geq 0$ trivially holds. Therefore, suppose $s_2^l > 0$ and $b_1^r \geq 2$ and let $b = \min(b_1^r - 2, s_2^l - 1)$. Then there exists an orthogonal representation $\mathcal{H}_1$ of G_1 with $\sigma(\mathcal{H}_1) = b + 2$, and an orthogonal representation $\mathcal{H}_2$ of G_2 with $\sigma(\mathcal{H}_2) = b$ containing a negatively-labelled edge in every st-path of G_2. By connecting $\mathcal{H}_1$ and $\mathcal{H}_2$ using the rotation combination $[r_1^s, r_1^t, r_2^s, r_2^t] = [-1, 0, 0, 1]$ we get an orthogonal representation H of G, as the newly created face f has the rotation

$$\mathrm{rot}(f) = \mathrm{rot}(e_2^s, e_1^s) + \sigma(\mathcal{H}_1) - \sigma(\mathcal{H}_2) + \mathrm{rot}(e_1^t, e_2^t) = 1 + b + 2 - b + 1 = 4.$$

The case $s_2^l = 1$ and $b_1^r = 2$ is shown in Figure 4.10b. Every st-path has to either traverse G_1 or G_2. Traversing G_1, it contains the edge e_1^s with $\ell_s(e_1^s) = r_1^s = -1$. Traversing G_2 it contains with $\ell_s(e_2^s) = r_2^s = 0$ a negatively-labelled edge as by construction. The orthogonal representation $\mathcal{H}$ has spirality

$$\sigma(H) = \ell_s(e^t) = r_1^s + \sigma(\mathcal{H}_1) + r_1^t = -1 + b + 2 + 0 = b + 1 = \min(b_1^r - 1, s_2^l).$$

With Definition 4.10, this implies $s^l \geq \min(b_1^r, s_2^l + 1) \cdot [s_2^l > 0] \cdot [b_1^r \geq 2]$.

Now to the "$\leq$"-direction. We here have to show that for every orthogonal representation of G, s^l is smaller or equal to at least one term inside the maximum on the left-hand side. As every such term must be non-negative, the case $s^l = 0$ is trivial. Therefore, suppose $s^l = x > 0$. Then there exists an orthogonal representation $\mathcal{H}$ of G with $\sigma(\mathcal{H}) = \ell_s(e^t) = x - 1$ and with an edge having a negative relative label in every st-path. Let $\mathcal{H}_1$ be the induced

orthogonal representation of G_1 and $\mathcal{H}_2$ be the induced orthogonal representation of G_2. The fact $\ell_s(e^t) = x - 1$ implies the following.

$$\begin{aligned}\sigma(\mathcal{H}_1) &= \ell_{s_1}(e_1^t) \\ &= \underbrace{r_1^s + \ell_{s_1}(e_1^t) + r_1^t}_{=\ell_s(e^t)=x-1} \underbrace{-r_1^s - r_1^t}_{\in\{0,2\}} \in \{x-1, x+1\} \end{aligned} \tag{4.13}$$

$$\begin{aligned}\sigma(\mathcal{H}_2) &= \ell_{s_2}(e_2^t) \\ &= \underbrace{r_2^s + \ell_{s_2}(e_2^t) + r_2^t}_{=\ell_s(e^t)=x-1} \underbrace{-r_2^s - r_2^t}_{\in\{-2,0\}} \in \{x-3, x-1\} \end{aligned} \tag{4.14}$$

The fact $s^l = x > 0$ implies that in every st-path a negatively-labelled edge has to be present, and particularly in every st-path traversing G_2. The negatively-labelled edge can not be in the set $\{e^s, e^t, e_2^s, e_2^t\}$ because $\ell_s(e^s) = 0$, $\ell_s(e^t) = x - 1 \geq 0$, $\ell_s(e_2^s) = r_2^s \geq 0$, and

$$\ell_s(e_2^t) = \underbrace{\ell_s(e_2^t) + r_2^t}_{=\ell_s(e^t)=x-1>0} - r_2^t \geq 0. \tag{4.15}$$

Therefore, a negatively-labelled edge must be present in every path from s_2 to t_2 inside $\mathcal{H}_2$. We now make a case distinction.

Case 1: $s^l = x = 1$. Here we show that Term (4.8) must also be 1. For a proof by contradiction assume $b_1^r = 0$ or $b_2^l = 0$, which would result in the Term (4.8) being 0 and not 1. Having $b_2^l = 0$ implies $\sigma(\mathcal{H}_2) \geq 0$ and combining this with Equation (4.14), $\sigma(\mathcal{H}_2) = 0$ follows. And as $\mathcal{H}_2$ contains a negatively-labelled edge in every path from s_2 to t_2 inside $\mathcal{H}_2$ we know that $s_2^l > 0$. But with Lemma 4.12 this would imply $b_2^l > 0$ and a contradiction is formed. The same argumentation holds if $b_1^r = 0$ in combination with Equation (4.13).

Case 2: $s^l = x \geq 2$. Not both r_1^s and r_2^s can be 0 at the same time. This implies that either Equation (4.13) or Equation (4.14) has a stronger bound. More specifically, either $\sigma(\mathcal{H}_1) = x - 1 + 1 - r_1^t \geq x > 0$ or $\sigma(\mathcal{H}_2) = x - 1 - 1 - r_2^t \geq x - 2 \geq 0$ holds. Using both equations we can, with the knowledge that G_2 contains an edge with a negative relative label, show for Term (4.8) that

$$s^l = x \leq \min(\sigma(\mathcal{H}_1), \sigma(\mathcal{H}_2) + 2) \leq \min(b_1^r, s_2^l + 1).$$

We now have shown that for an arbitrary orthogonal representation $\mathcal{H}$ of G the left step value s^l is always smaller than either Term (4.8) or Term (4.9) and equality follows for s^l.

What is left is the equality proof for s^z. For the "$\geq$"-direction, suppose that $s_1^z = 1$ and $b_2^l \geq 2$. Then there exist an orthogonal representation $\mathcal{H}_1$ of G_1 with an st-path P_1 having only relative label 0 and an orthogonal representation $\mathcal{H}_2$ of G_2 with $\sigma(\mathcal{H}_2) = -2$. A rotation combination of $[r_1^s, r_1^t, r_2^s, r_2^t] = [0, 0, 1, 1]$ results in a combined orthogonal representation $\mathcal{H}$ of G as also seen in Figure 4.10c. The path $P = e_1^s + P_1 + e_1^t$ contains with $r_1^s = r_1^t = 0$ only edges with relative label 0 and $s^z = 1$ follows. The same holds true for the other case of Term (4.12) and the rotation combination $[r_1^s, r_1^t, r_2^s, r_2^t] = [-1, -1, 0, 0]$. For the "$\leq$"-direction suppose $s^z = 1$. Then there exists an orthogonal representation $\mathcal{H}$ of G containing an st-path with only zero-labelled edges. This path has to traverse either G_1 or G_2. Without loss of generality, let G_1 contain this path, which implies $s_1^z = 1$ as well as $r_1^s = r_1^t = 0$. Then $r_2^s = r_2^t = 1$ must hold and using the same argumentation as in Equation (4.14), $\sigma(\mathcal{H}_2) = -2$ and $b_2^l \geq 2$ follows, which then implies for Term (4.12) that

$$\max\{[b_1^r \geq 2] \cdot s_2^z, [b_2^l \geq 2] \cdot s_1^z\} \geq [b_2^l \geq 2] \cdot s_1^z = 1 = s^z.$$

□

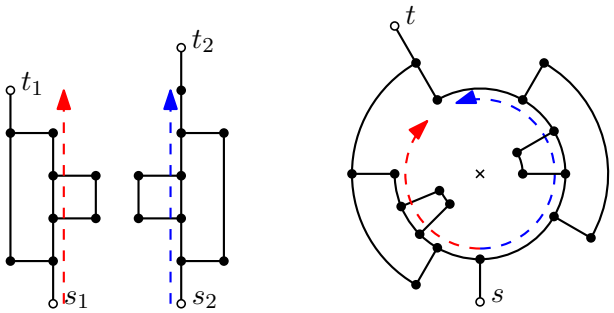

Figure 4.11: On the left, two 2-legged SP-graphs and on the right their parallel composition surrounding f_c. The arrows indicating the direction of st-paths in the orthogonal drawings point in different directions in the ortho-radial one.

Until now, we have only looked at tree nodes not containing the central face f_c, and tried to find ways to calculate step values. These step values are now used to create f_c at the marked parallel node in the decomposition tree. We start with restricting the possible combinations of step values for a 2-legged SP-graph.

Lemma 4.20. *There does not exist a 2-legged rectilinear-plane series-parallel 3-graph with*

$$[s^l, s^r, s^z] \in \{[0, x, 0], [x, 0, 0]\}$$

for any $x \in \mathbb{N}_0$.

Proof. Only the proof for $[s^l, s^r, s^z] \notin [x, 0, 0]$ is given, since the other case follows analogously. To form a contradiction, assume a 2-legged rectilinear-plane series-parallel 3-graph G exists with step values $[x, 0, 0]$, $x \in \mathbb{N}_0$. As both $\mathcal{Q}$- and $\mathcal{D}$-nodes have step values $[0, 0, 1]$, G has to be the result of some composition of two subgraphs G_1 and G_2. Let $[b_1^l, b_1^r, s_1^l, s_1^r, s_1^z]$ be the structure of G_1 and $[b_2^l, b_2^r, s_2^l, s_2^r, s_2^z]$ be the structure of G_2. We now show that for G to have the step values $[x, 0, 0]$, at least one of the subgraphs must have the step values $[y, 0, 0]$ or $[0, y, 0]$ for $y \in \mathbb{N}$. This implies that G would have to be the result of an infinite composition chain. Therefore, such a G does not exist.

Case 1: G is the result of a parallel composition of G_1 and G_2. As $s^r = 0$, both Term (4.8) and Term (4.9) in Lemma 4.19 have to be 0. With $b_2^l \geq s_2^l$ (Lemma 4.12) this implies either $b_1^r = 0$ or $b_2^l = 0$. But for G to be rectilinear-plane, Lemma 4.19 also states that $b_1^r + b_2^l \geq 2$. Therefore, one of the two bend values must be 0 and the other one greater or equal to 2. Without loss of generality, let $b_1^r \geq 2$ and $b_2^l = 0$. With the inequality $b_2^l \geq s_2^l$ we also get $s_2^l = 0$. Moreover, with $b_1^r \geq 2$ and $s^z = 0$, Equation (4.12) implies that $s_2^z = 0$ as well. Therefore, the step values of G_2 must be of the form $[0, y, 0]$ for some $y \in \mathbb{N}_0$.

Case 2: G is the result of a series composition of G_1 and G_2. Then Lemma 4.17 restricts the step values of the children such that

$$\begin{aligned} &(s_1^r = 0 \wedge s_2^r = 0) && \text{Terms (4.4) and (4.6)} \\ \wedge\ &(s_1^z = 0 \vee s_2^z = 0) && \text{Equation (4.7)} \end{aligned}$$

This implies that for at least one child the step values must be of the form $[y, 0, 0]$ for some $y \in \mathbb{N}_0$. □

The following lemma shows that for 2-legged series-parallel 3-graphs an edge always has the same label, no matter in which essential cycle, as long as we consider an orientation of the edge.

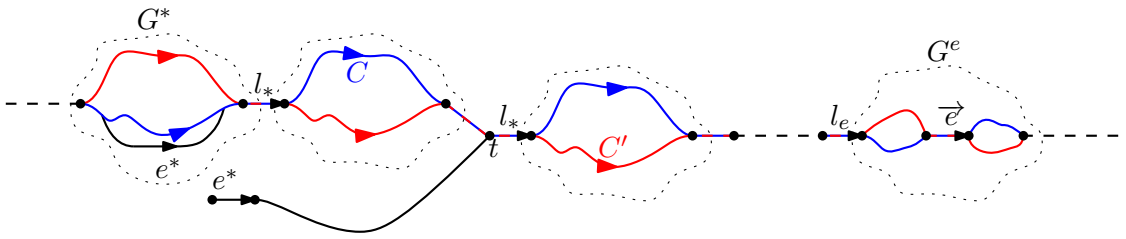

Figure 4.12: A representation of the cyclic chain of subgraphs including the cycles C and C' from Lemma 4.21. The cycles share a common edge e in the subgraph G^e and enter it via the common leg l_e. The two possible locations of e^* are both represented here. It may either be contained in the subgraph G^* contained in the cyclic chain or be outside the chain (and therefore closer to f_c) and connected to it at a terminal t.

Lemma 4.21. *Let $(G, \mathcal{E})$ be a 2-legged series-parallel plane 3-graph that admits a (possibly invalid) ortho-radial representation $\mathcal{T}$ with a reference edge e^* and let C and C' be two simple essential cycles sharing the same oriented edge $\vec{e}$. Then $\ell_C(\vec{e}) = \ell_{C'}(\vec{e})$.*

Proof. Let $\mathcal{G}$ be the set of inclusion-wise maximal 2-legged series-parallel subgraphs of G, where their induced representations are orthogonal. Both cycles C and C' can not be totally contained in a single subgraph of $\mathcal{G}$ since they are essential cycles and can therefore only be contained in an ortho-radial representation. As the union of the subgraphs in $\mathcal{G}$ is the whole graph G, both cycles must traverse a cyclic chain of subgraphs in $\mathcal{G}$ instead. And as both cycles must traverse the subgraph $G_e \in \mathcal{G}$ containing e, they must traverse the same cyclic chain we call $\mathcal{S}$. Otherwise, some subgraph in $\mathcal{G}$ is either not inclusion-wise maximal or its induced representation would be an ortho-radial one. For the cycles to be simple and both traverse the same oriented edge $\vec{e} \in G_e$, they must traverse G_e, and therefore every subgraph in $\mathcal{S}$, also in the same direction. See Figure 4.12 for an illustration.

There are two cases based on the location of e^*. If e^* is contained in a subgraph we call $G^* \in \mathcal{S}$, then let l^* be the leg of G^* over which both cycles leave this subgraph. There must exist a reference path from e^* to l^* such that this reference path respects both C and C'. This implies $\ell_C(l^*) = \ell'_C(l^*)$. If e^* is not contained in a subgraph in $\mathcal{S}$, there exists some leg l^* of a subgraph in $\mathcal{S}$ with a reference path from e^* to l^* only entering the cyclic chain at l^*. Then this reference path respects C and C', and again it follows that $\ell_C(l^*) = \ell_{C'}(l^*)$.

Knowing that a single leg in the cyclic chain has the same label, it follows with Lemma 4.5 that every leg of every subgraph in $\mathcal{S}$ has the same label. Let l_e be the leg of G_e over which C and C' enter G_e. Again Lemma 4.5 implies that $\mathrm{rot}(C[l_e, e]) = \mathrm{rot}(C'[l_e, e])$ and with $\ell_C(l_e) = \ell'_C(l_e)$ it follows that $\ell_C(e) = \ell_C(l_e) + \mathrm{rot}(C[l_e, e]) = \ell'_C(l_e) + \mathrm{rot}(C'[l_e, e]) = \ell'_C(e)$. □

With Lemma 4.21 we now write $\ell(\vec{e})$ instead of $\ell_C(e)$ if the oriented edge $\vec{e}$ is contained in C. We can even define a label for oriented edges that currently are not contained in any essential cycle, as once they are, the labels would be equal. To make it clear in which way an oriented edge is directed, we use the following notation. We use $\vec{e}$ to represent the orientation of e as it occurs in an st-path of G, and we use $\overleftarrow{e}$ to represent the reversed orientation of $\vec{e}$. We use the notation $\overline{G}$ for the reversed 2-legged SP-graph of G where the terminals s and t are flipped. If $\vec{e} \in G$, then $\overleftarrow{e} \in \overline{G}$.

We are now ready to create the central face at some $\mathcal{P}$-node in the recursion. To get a feeling for what this means, Figure 4.11 shows an example drawing of two children and their

parallel composition around the center. As the embedding is fixed, the left subgraph G_1 wraps clockwise while the right subgraph G_2 wraps counterclockwise around the circle. Therefore, a left bend in G_1 and a right bend in G_2 may both point radially outwards.

Definition 4.22. *Let $(G, \mathcal{E})$ be a 2-legged rectilinear-plane series-parallel 3-graph and let $\mathcal{T}$ be a valid ortho-radial representation of G. Then $\mathcal{T}$ is called* st-outwards *if the legs of G point radially outwards.*

Lemma 4.23. *Let ϕ be a marked $\mathcal{P}$-node at which the face f_0 should be created and where its children ϕ_1 and ϕ_2 both are rectilinear-plane. If $[b_1^l, b_1^r, s_1^l, s_1^r, s_1^z]$ is the structure of ϕ_1 and $[b_2^l, b_2^r, s_2^l, s_2^r, s_2^z]$ is the structure of ϕ_2, then there exists a valid ortho-radial representation of ϕ if and only if any of the following equations hold.*

$$s_1^z = s_2^z = 1 \tag{4.16}$$

$$b_1^l, s_2^r \geq 1 \vee b_2^r, s_1^l \geq 1 \tag{4.17}$$

$$b_1^l \geq 2 \vee b_2^r \geq 2 \tag{4.18}$$

Moreover, if G admits any valid ortho-radial representation, then it also admits an st-outwards one.

Proof. Let G be the induced graph of ϕ, G_1 be the induced subgraph of ϕ_1, and G_2 be the induced subgraph of ϕ_2. Also let s_1, t_1 be the terminals of G_1 and s_2, t_2 the terminals of G_2 as well as $e_1^s, e_2^s, e_1^t, e_2^t$ be the legs of G_1 and G_2.

First, we prove the equivalence for the existence of a valid ortho-radial representation and then that there always exists one that is st-outwards. For the " $\Longleftarrow$ "-direction we make a case distinction.

Case 1: Equation (4.16) holds. We then know that $s_1^z = s_2^z = 1$. Therefore, orthogonal representations $\mathcal{H}_1$ of G_1 and $\mathcal{H}_2$ of G_2 exist with $\sigma(\mathcal{H}_1) = \sigma(\mathcal{H}_2) = 0$ and both with an st-path having only relative label 0. Now let $\mathcal{T}$ be the representation of G obtained by combining $\mathcal{H}_1$ and $\mathcal{H}_2$ with rotation combination $[r_1^s, r_1^t, r_2^s, r_2^t] = [-1, -1, 1, 1]$. See Figure 4.13 for an example of how the complete ortho-radial representation gets connected. For the new central and outer face it follows that

$$\mathrm{rot}(f_c) = \mathrm{rot}(f_o) = \underbrace{\ell_{s_1}(e_1^t)}_{=\sigma(\mathcal{H}_1)=0} + \underbrace{\mathrm{rot}(e_1^t, e_2^t)}_{=0} - \underbrace{\ell_{s_2}(e_2^t)}_{=\sigma(\mathcal{H}_2)=0} + \underbrace{\mathrm{rot}(e_2^s, e_1^s)}_{=0} = 0,$$

and $\mathcal{T}$ is an ortho-radial representation. Now use $\vec{e_1^s}$ as the reference edge in $\mathcal{T}$. We then know that $\ell_C(e) = \ell(\vec{e}) = \ell_{s_1}(e)$ for an edge $e \in G_1$. For an edge $e \in G_2$, let P be a path from e_2^s to the starting vertex of $\vec{e}$. It then holds that

$$\ell_C(e) = \ell(\overleftarrow{e}) = \mathrm{dir}(\vec{e_1^s}, P, \overleftarrow{e}) = \mathrm{rot}(\overleftarrow{e_1^s} + P) = \underbrace{-\mathrm{rot}(e_2^s, e_1^s)}_{=0} + \ell_{s_2}(e) = \ell_{s_2}(e).$$

Let C be an arbitrary simple essential cycle in $\mathcal{T}$ and let P_1 be the traversed path in G_1 and P_2 the traversed path in G_2. Then P_2 is an st-path of the reverse graph $\overline{G_2}$. By Definition 4.10 and Lemma 4.16 both P_1 and P_2 contain either only zero-labelled edges relative to e_1^s and e_2^s or at least one path contains both a positively- and a negatively-labelled edge relative to their starting leg. As these relative labels directly translate to labels of C, it follows that C either only contains zero-labelled edges or at least one positively- and one negatively-labelled edge.

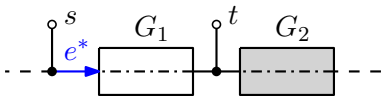

Figure 4.13: Two subgraphs G_1 and G_2, both with $s^z = 1$, forming a valid ortho-radial representation based only on step values. The highlighted edge e^* is the reference edge.Both subgraphs have $s^z = 1$.

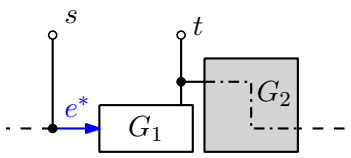

(a) Subgraph G_1 has $b_1^l > 0$ and G_2 has $s_2^r > 0$.

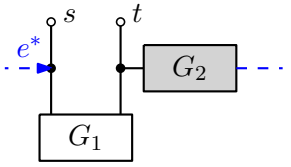

(b) Subgraph G_1 has $b_2^l \geq 2$.

Figure 4.14: Two subgraphs G_1 and G_2 forming a valid ortho-radial representation based both on bend and step values. The highlighted edge e^* is the reference edge.

Case 2: Equation (4.17) holds. Due to being analogous, we only discuss the first case where $b_1^l \geq 1$ and $s_2^r > 0$. There must exist an orthogonal representation $\mathcal{H}_1$ of G_1 with $\sigma(\mathcal{H}_1) = -1$ and an orthogonal representation $\mathcal{H}_2$ of G_2 with $\sigma(\mathcal{H}_2) = 0$ containing an edge in every st-path with a positive relative label. Let $\mathcal{T}$ be the combined representation of $\mathcal{H}_1$ and $\mathcal{H}_2$ with rotation combination $[r_1^s, r_1^t, r_2^s, r_2^t] = [-1, 0, 1, 1]$ as shown in Figure 4.14a. Then

$$\mathrm{rot}(f_c) = \mathrm{rot}(f_o) = \underbrace{\ell_{s_1}(e_1^t)}_{=\sigma(\mathcal{H}_1)=-1} + \underbrace{\mathrm{rot}(e_1^t, e_2^t)}_{=1} - \underbrace{\ell_{s_2}(e_2^t)}_{=\sigma(\mathcal{H}_2)=0} + \underbrace{\mathrm{rot}(e_2^s, e_1^s)}_{=0} = 0.$$

Therefore, $\mathcal{T}$ is an ortho-radial representation. We again use $\vec{e_1^s}$ as the reference edge in $\mathcal{T}$ and the same connection between relative and normal labels as in Case 1 holds. Let C be an arbitrary simple essential cycle in $\mathcal{T}$, P_1 the path through G_1, and P_2 the path through G_2. As e_1^t is a leg of G_1, we know that it must be part of P_1 and $\ell_C(e_1^t) = \ell_{s_1}(e_1^t) = \sigma(\mathcal{H}_1) = -1$. By the construction of $\mathcal{H}_2$ we also know that P_2 contains an edge e_2 with $\ell_C(e_2) = \ell_{s_2}(e_2) > 0$. So C is valid and therefore also $\mathcal{T}$ is valid.

Case 3: Equation (4.18) holds. We again only discuss the case $b_1^l \geq 2$. Then there exists an orthogonal representation $\mathcal{H}_1$ of G_1 with $\sigma(\mathcal{H}_1) = -2$ as well as some orthogonal representation $\mathcal{H}_2$ of G_2 with $\sigma(\mathcal{H}_2) = 0$. Let $\mathcal{T}$ be the representation of G when combining $\mathcal{H}_1$ and $\mathcal{H}_2$ with the rotation combination $[r_1^s, r_1^t, r_2^s, r_2^t] = [0, 0, 1, 1]$ as shown in Figure 4.14b. It follows that

$$\mathrm{rot}(f_c) = \mathrm{rot}(f_o) = \underbrace{\ell_{s_1}(e_1^t)}_{=\sigma(\mathcal{H}_1)=-2} + \underbrace{\mathrm{rot}(e_1^t, e_2^t)}_{=1} - \underbrace{\ell_{s_2}(e_2^t)}_{=\sigma(\mathcal{H}_2)=0} + \underbrace{\mathrm{rot}(e_2^s, e_1^s)}_{=1} = 0.$$

Use $\overleftarrow{e_2^s}$ as the reference edge. Let C be an arbitrary simple essential cycle in $\mathcal{T}$ and P_1 be the path taken through G_1. From the used rotation combination we know that $\mathrm{rot}(e_2^s, e_1^s) = 1$, and this implies $\ell_C(e_1^s) = \mathrm{rot}(e_2^s, e_1^s) = 1$ and $\ell_C(e_1^t) = \mathrm{rot}(e_2^s, e_1^s) + \underbrace{\ell_{s_1}(e_1^t)}_{=-2} = -1$. Therefore, C already contains a positively- and negatively-labelled edge in its path through G_1 and $\mathcal{T}$ must be valid.

Regarding the " $\Longrightarrow$ "-direction, we use a proof by contradiction. So assume all equations do not hold, but there exists a valid ortho-radial representation $\mathcal{H}$ of G with reference edge e^*. Let $\mathcal{H}_1$ be the induced orthogonal representation of G_1 and $\mathcal{H}_2$ the induced orthogonal representation of G_2. Due to Equation (4.16) not being fulfilled, we know that

$s^z = 0$ for at least one subgraph. With Equation (4.17) not being fulfilled and Lemma 4.13, the same holds for s^l and s^r. Using Lemma 4.20, there only exist two possible situations where this is given. Either $[s_1^l, s_1^r, s_1^z] = [0, 0, 1]$ and $[s_2^l, s_2^r, s_2^z] = [x, y, 0],\ x, y \in \mathbb{N}$ or the inverse assignment. We only prove the case where $[s_1^l, s_1^r, s_1^z] = [0, 0, 1]$, since the other case follows analogously. From $s_2^r > 0$ and Equation (4.17) not being fulfilled, it follows that $b_1^l = 0$ and therefore $\sigma(\mathcal{H}_1) \geq 0$. We can calculate the spirality of $\mathcal{H}_2$ based on the spirality of $\mathcal{H}_1$ and $\text{rot}(f_c) = 0$ to be

$$\begin{aligned}
&\sigma(\mathcal{H}_2)\\
=&\underbrace{\sigma(\mathcal{H}_2) + \text{rot}(e_2^t, e_1^t) - \sigma(\mathcal{H}_1) + \text{rot}(e_1^s, e_2^s)}_{= -\text{rot}(f_c) = 0} - \underbrace{\text{rot}(e_2^t, e_1^t)}_{\in \{-1,0\}} + \underbrace{\sigma(\mathcal{H}_1)}_{\geq 0} - \underbrace{\text{rot}(e_2^t, e_1^t)}_{\in \{-1,0\}}\\
\geq&\sigma(\mathcal{H}_1). \qquad (4.19)
\end{aligned}$$

To form a contradiction, we differentiate between the concrete value of $\sigma(\mathcal{H}_1)$ and show for each case that $b_2^r \geq 2$ in Equation (4.18) would hold.

Case 1: $\sigma(\mathcal{H}_1) \geq 2$. Then Equation (4.19) directly implies $\sigma(\mathcal{H}_2) \geq 2$.

Case 2: $\sigma(\mathcal{H}_1) = 0$. As $[s_1^l, s_1^r, s_1^z] = [0, 0, 1]$ we know that $\mathcal{H}_1 \notin \Omega_+(G_1, \mathcal{E}_1), \Omega_-(G_1, \mathcal{E}_1)$ with $\mathcal{E}_1$ being the induced embedding of G_1. Therefore, Lemma 4.15 implies that $\mathcal{H}_1 \in \Omega_z(G_1, \mathcal{E}_1)$. So there exists an st-path P_1 through G_1 with only zero labels relative to e_1^s. Therefore, in any simple essential cycle C containing P_1 we know that all edges of P_1 have the same, but maybe non-zero, normal label x. With $\text{rot}(e_1^t, e_2^t) \geq 0$ we know that $\ell_C(e_2^t) = x$ as well. No matter the value of x it follows with $s_2^z = 0$ that C must contain a positively- and negatively-labelled edge inside the path taken through $\mathcal{H}_2$ for C to be valid. As C was arbitrary, every st-path in $\mathcal{H}_2$ must contain a positive and negative label. Equation (4.19) implies $\sigma(\mathcal{H}_2) \geq 0$, and the same argumentation as in Lemma 4.14 (only swapping relative labels with normal labels) implies that $b_2^r \geq 2$.

Case 3: $\sigma(\mathcal{H}_1) = 1$. At first, we bound the relative labels in two special st-paths of G_1. As $s_1^l = 0$, there must exist an st-path through G_1 without a negative relative label. We call this special path S.

Now assume that in every st-path of G_1 an edge e exists with $\ell_s(e) \geq 2$. Then between s and every such e there must exist adjacent vertices u, v, w in the current st-path with $\text{rot}(uv, vw) = 1$. Lemma 4.11 then implies the existence of another orthogonal representation $\mathcal{H}_1'$ of G_1 with $\sigma(\mathcal{H}_1') = 1 - 1 = 0$. But as every st-path only contains one vertex with a different rotation in $\mathcal{H}_1'$, the relative label of the edge e in each st-path is only reduced by 1 and therefore still positive. By Definition 4.10, this would imply $s_1^r > 0$, which stands in contradiction to $[s_1^l, s_1^r, s_1^z] = [0, 0, 1]$. Therefore, there must exist an st-path in G_1, where every edge has at most a relative label of 1. We call this special st-path T. With $z \coloneqq \ell(\vec{e_1^s})$ it follows that

$$\begin{aligned}
\ell(\vec{e}) &\geq z,\ \forall e \in S\\
\ell(\vec{e}) &\leq z + 1,\ \forall e \in T
\end{aligned}$$

Now given an arbitrary value z, observe that either S or T can not contain negatively- as well as positively-labelled edges at the same time. Moreover, as $\sigma(\mathcal{H}_1) = 1$, both paths can also not contain only zero-labelled edges. Using this knowledge, we show that every st-path in the second graph G_2 must contain both a positively- and a negatively-labelled edge. With the same argumentation as in Lemma 4.14 (only swapping relative labels with normal labels) this implies that $b_2^r \geq 2$ and the " $\Longleftarrow$ "-direction will be shown. This is done separately for the following two cases.

Case 3a: $z \geq 0$. Then both S and T contain positively-labelled edges, but S does not contain a negatively-labelled edge. Let P_2 be an arbitrary st-path in G_2. Then $S + P_2$ forms

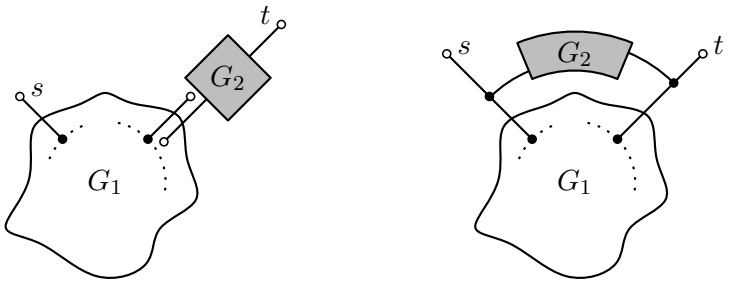

Figure 4.15: A series composition and a parallel composition of two subgraphs G_1 and G_2, where G_1 already contains the central face. G_1 is st-outwards and G_2 has no specific properties.

a simple essential cycle and for this cycle to be valid, P_2 must contain a negatively-labelled edge. For the edge $e_2^t \in P_2$, we also know that

$$\ell_C(e_2^t) = \ell_C(e_1^t) + \mathrm{rot}(e_1^t, e_2^t) \geq \ell_C(e_1^t) = \underbrace{\ell_C(e_1^s)}_{=z\geq 0} + \underbrace{\ell_{e_1^s}(e_1^t)}_{=1} \geq 1.$$

Therefore, P_2 also contains the positively-labelled edge e_2^t. As P_2 was arbitrary, every st-path of G_2 contains a positively- and a negatively-labelled edge.

Case 3b: $z < 0$. Then both S and T contain negatively-labelled edges, but T does not contain a positively-labelled edge. Let P_2 be an arbitrary st-path in G_2. Then $T + P_2$ forms a simple essential cycle and for this cycle to be valid, P_2 must contain a negatively-labelled edge. For the edge $e_2^s \in P_2$ we also know that

$$\ell_C(e_2^s) \leq \ell_C(e_1^s) = z < 0.$$

Therefore, P_2 also contains the negative edge e_2^s and as P_2 was arbitrary every st-path of G_2 must contain a negatively- and a positively-labelled edge.

Finally, we would have to show that if a valid ortho-radial representation exists, then there also exists one which is st-outwards. But if such a representation exists, the " $\Longrightarrow$ "-direction implies that one of Equations (4.16) to (4.18) holds. And due to the " $\Longleftarrow$ "-direction already constructing an st-outwards representation in any case, this fact is already proven. □

After creating the initial valid ortho-radial representation around the central face, extending the representation is trivial as the following lemma shows.

Lemma 4.24. *Let ϕ be an inner node where one of its children contains f_c and is ortho-linear plane while the other child-node is rectilinear-plane. Then a valid ortho-radial representation of ϕ exists that is also st-outwards.*

Proof. Let ϕ_1 and ϕ_2 be the child nodes of ϕ and without loss of generality let ϕ_1 be the node still containing f_c. We make a proof by induction over the depth n of the marked $\mathcal{P}$-node in the subtree rooted at the child ϕ_1. For the base case $n = 1$ we know that ϕ_1 is actually the marked $\mathcal{P}$-node. We make a case distinction over the type of the node ϕ.

Case 1: ϕ is an $\mathcal{S}$-node. From Lemma 4.23 we know that an st-outwards valid ortho-radial representation for ϕ_1 exists. As an orthogonal representation with spirality 0 exists for the other child node, the combination of these two representations still results in an st-outwards valid ortho-radial representation. Figure 4.15 shows this in an abstract view.

Case 2: ϕ is a $\mathcal{P}$-node. From Lemma 4.23 we know that ϕ_1 admits an st-outwards valid ortho-radial representation. We also know that an orthogonal representation $\mathcal{H}_2$ of ϕ_2 exists with $\sigma(\mathcal{H}_2) = 0$. By using a rotation combination of $[-1, -1, 0, 0]$ as shown in Figure 4.15, one can combine both representations into one ortho-radial representation $\mathcal{T}$ of G as the newly created face has rotation 4. Every newly created simple essential cycle C in $\mathcal{T}$ has to pass through the outwards directed edges of G_1, one of which has a positive label in C, while the other one has a negative label. Therefore, $\mathcal{T}$ is valid. As the legs of ϕ also point radially outwards, the representation is st-outwards.

The inductive case for $n > 1$ follows analogously to the base case, only here we use the induction hypothesis instead of Lemma 4.23 to imply an st-outwards valid ortho-radial representation of the child ϕ_1. □

Combining the individual results about constructing a valid ortho-radial representation for 2-legged SP-graphs yields the following result.

Theorem 4.25. *Given a 2-legged series-parallel plane 3-graph $(G, \mathcal{E})$, a fixed outer face f_o, and a fixed inner face f_c, a valid ortho-radial representation of G, if one exists, can be found in $\mathcal{O}(n)$ time.*

Proof. The creation of a decomposition tree of G is possible in linear time and let ϕ be the node where f_c is formed. Applying, based on the type of node, either Lemma 4.17 or Lemma 4.19 at each sub-node of ϕ results in either a structure for every sub-node or in one parallel-node not fulfilling the condition in Lemma 4.19. If this condition is not fulfilled, it is immediately clear that no ortho-radial representation for the graph G can exist. Conversely, if every parallel node fulfills the condition, Lemma 4.23 states the requirements for a valid ortho-radial representation of ϕ. If these are also met, then there exists a valid ortho-radial representation for ϕ and Lemma 4.24 implies that then also a valid ortho-radial representation for G exists. As the size of the decomposition tree is linear to the size of G and each node only takes constant time to compute the structure and check the conditions, the tree can be traversed in linear time.

The valid ortho-radial representation can then be computed via a second top-down recursion over the decomposition tree, where each aforementioned result states how an orthogonal or valid ortho-radial representation with the required properties can be constructed and, in turn, what properties the representations of their child-nodes require to do so. □

4.1.3 Finding Bend-Minimum Ortho-Radial Representations

Theorem 4.25 states that a valid ortho-radial representation for a given 2-legged SP-graph G can be computed in linear time, provided one exists. In the case that no valid ortho-radial representation exists, we now find the minimum number of bends that have to be added to G to allow a valid ortho-radial representation. Bends are added by adding special *bend-vertices* to edges in G. These allow an edge to artificially bend, while the results of the previous section can still be used. Figure 4.16 shows an example of a graph that only admits a valid ortho-radial representation if a bend-vertex is added. The modified decomposition tree includes the bend-vertex via a new $\mathcal{S}$-node.

Lemma 4.26. *Let $(G, \mathcal{E})$ be a 2-legged series-parallel plane 3-graph, let $\mathcal{T}$ be a decomposition tree of G, and let H be a graph obtained by adding a single bend-vertex at an arbitrary edge e in G. Then there exists a decomposition tree $\mathcal{T}_\mathcal{H}$ of H obtained by adding a series-connection with a new $\mathcal{D}$-node at a specific point in the decomposition tree $\mathcal{T}$.*

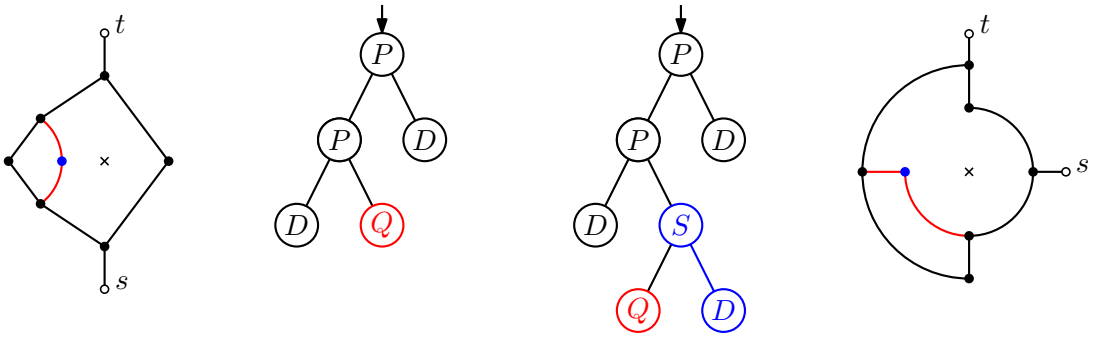

Figure 4.16: On the left, a 2-legged SP-graph without a valid ortho-radial representation, as the left-most face is a triangle, and the decomposition tree of the graph. Adding the blue bend-vertex to the red edge makes the graph admit the valid representation shown on the right. The second decomposition tree includes an $\mathcal{S}$-node and a $\mathcal{D}$-node representing the bend-vertex.

Figure 4.17: On the left, a 2-legged SP-graph where the conditions in Lemma 4.23 are not fulfilled. When adding the blue bend-vertex to the red edge, the graph admits the valid ortho-radial representation shown on the right.

Proof. Let ϕ be the node furthest down in $\mathcal{T}$ that still contains the edge e in its induced subgraph G_ϕ. Then e must be a leg of G_ϕ. The additional bend vertex in H can be represented by a series-composition of ϕ with a new $\mathcal{D}$-node. The order of this series composition depends on whether e is incident to the starting or end terminal. Let ψ be a $\mathcal{S}$-node representing this series-composition. By replacing ϕ with ψ the resulting tree is a decomposition tree of H. □

There are two places in the construction where extra bend-vertices may be required. First in Lemma 4.19, where the condition for a $\mathcal{P}$-node forming an orthogonal representation may not be met (see Figure 4.16), and second in Lemma 4.23, where the central face is formed and a condition ensures that created essential cycles are valid.

Regarding Lemma 4.23, Figure 4.17 shows an example of a graph not fulfilling the condition of the lemma and how the addition of a bend-vertex makes the graph admit a valid ortho-radial representation. The following lemma states that in this case a single bend-vertex is always enough so that the node admits a valid ortho-radial representation.

Lemma 4.27. *Let ϕ be a $\mathcal{P}$-node at which the face f_c should be created and where its children ϕ_1 and ϕ_2 both are rectilinear-plane. If all the conditions in Lemma 4.23 do not hold and therefore no valid ortho-radial representation exists, the addition of a single bend-vertex is enough so that ϕ admits a valid ortho-radial representation.*

Proof. Let G_1 and G_2 be the induced subgraphs of ϕ_1 and ϕ_2, respectively. Due to the conditions in Lemma 4.23 not being met, we know that one subgraph has the step values $[s_a^l, s_a^r, s_a^z] = [0, 0, 1]$ and the other subgraph has the values $[s_b^l, s_b^r, s_b^z] = [x, y, 0],\ x, y \in \mathbb{N}$.

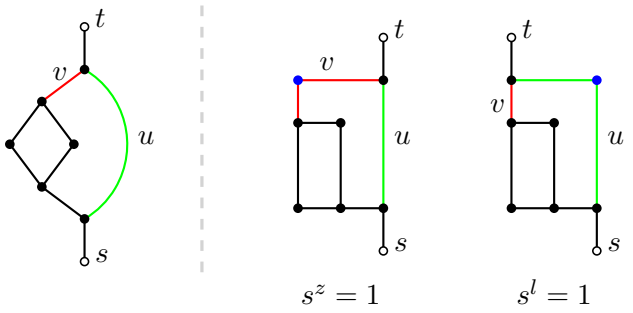

Figure 4.18: On the left, a 2-legged SP-graph where the condition in Lemma 4.19 is not fulfilled and a bend-vertex must be added. On the right, two orthogonal representations with a bend-vertex on the edges v or u. The zero and left step values depends on where the bend-vertex is placed.

Without loss of generality, let $a = 1$ and $b = 2$. As ϕ admits no valid ortho-radial representation, we also know with Equation (4.17) that $b_1^l = 0$. The addition of a bend-vertex at one of the legs of ϕ_1 increases b_1^l to 1. This is enough to fulfill the condition $b_1^l \geq 0 \wedge s_2^r > 0$ in Equation (4.17) and the existence of a valid ortho-radial representation follows. □

Regarding Lemma 4.19, assume we encounter a $\mathcal{P}$-node ϕ not containing f_c for which the condition $b_1^r + b_2^l \geq 2$ does not hold. Then the addition of $2 - b_1^r - b_2^l$ bend vertices along some edges would be the minimum required amount such that an orthogonal representation for ϕ exists. But one has to decide where to put these bend vertices. In general, meaning series-parallel 4-graphs, this is not trivial to decide [DKLO22]. As both children are 2-legged though, there always exist the legs of each child, which can be selected for bending. The problem however is that the distribution of bend-vertices could influence the step values of ϕ, which at a later recursion step may be important. For example, the optimal left step value may only be achievable if the bend-vertex is added at one specific edge, possibly somewhere inside the graph. In general, these placements also differ per value and one would have to move the bend-vertices to the optimal place according to the desired properties of the representation. Figure 4.18 shows a situation where a zero step value of 1 is only achievable when placing the bend-vertex on the edge v while a left step value of 1 is only achievable when placing the bend-vertex on the edge u. We now show that one does not have to check every edge in the graph when adding bend-vertices. Rather, it is enough to only consider the four legs of the children of ϕ.

First up, we show that placing bend-vertices on the legs of a graph results in the highest possible bend and step values. Afterwards, we use this knowledge to calculate the *structure* of a $\mathcal{P}$-node including bend-vertices.

Lemma 4.28. *Let $(G, \mathcal{E})$ be a 2-legged rectilinear-plane series-parallel 3-graph and let H be the graph obtained by adding a single bend-vertex at an arbitrary edge e in G. Then there exists a graph F which is obtained by instead adding the bend-vertex at a leg of G so that the bend values as well as the left and right step values of H are smaller or equal to those of F.*

Proof. Let $\mathcal{T}$ be the decomposition tree of G and let $\mathcal{T}_\mathcal{H}$ be the decomposition tree of H from Lemma 4.26. The newly added $\mathcal{D}$-node has the structure $[b^l, b^r, s^l, s^r, s^z] = [1, 1, 0, 0, 1]$ where its bend values are both 1 and the left and right step values are both 0. The linearity of the equations in Lemma 4.17 and Lemma 4.19 imply that the bend and step values of the root of $\mathcal{T}_\mathcal{H}$, and therefore of H, are at most by 1 greater than the ones of G.

What is left to show is that the addition of a bend-vertex at one of the legs of G increases these values by at least 1. We again represent this bend-vertex by a series-composition of G with a $\mathcal{D}$-node. No matter on which leg the bend-vertex is placed, we know due to Lemma 4.17 that the bend values of this new graph always increase by 1. To get the same result for the left and right step values, one has to pick a specific leg for bending. Let s^l_G, b^r_G, and b^l_G be the left step as well as the bend values of G. We distinguish between two cases.

Case 1: $b^l_G > 0$. Then Equation (4.3) in Lemma 4.17 implies that the addition of a bend vertex at the leg e^t results in a graph F with left step value $s^l_F \geq s^l_G + 1$.

Case 2: $b^r_G \geq 0$. We can assume that $b^l_G = 0$ and due to Lemma 4.13, $s^l_G = 0$ follows. Then Equation (4.2) in Lemma 4.17 implies that the addition of a bend vertex at the leg e^s results in a graph F with left step value $s^l_F \geq b^r_G \geq s^l_G + 1$.

Proving the same fact for the right step value of F works analogous. □

Lemma 4.29. *Let ϕ be an inner $\mathcal{P}$-node not containing f_c for which*

$$b^r_1 + b^l_2 < 2.$$

Then $2 - b^r_1 - b^l_2$ bend-vertices have to be added to realize an orthogonal representation for ϕ. To calculate the structure for ϕ including these bend-vertices, it is enough to look at all distributions of the bend-vertices on $e^s_1, e^t_1, e^s_2, e^t_2$ and take per bend and step value the highest one over all distributions.

Proof. According to Lemma 4.28, the addition of a bend-vertex on one of the leg of a child-graph always increases its bend values by one. Then $2 - b^r_1 - b^l_2$ bend-vertices are enough to fulfill the condition $b^r_1 + b^l_2 \geq 2$.

Regarding the calculation of the structure of ϕ, Lemma 4.28 shows that for the child nodes all values in the structure except s^z assume their highest value if the bend-vertices are placed at their legs. Therefore, only the distribution of bend-vertices to $e^s_1, e^t_1, e^s_2, e^t_2$ have to be considered. Note that the exclusion of s^z in Lemma 4.28 is not a problem as even if a bend-vertex would increase the zero step value of a child, then only an orthogonal representation of the child with spirality 0 would benefit from this increase. But these bend-vertices are explicitly added to increase the spirality of the child nodes representation so that an orthogonal representation of the parallel composition exists in the first place. Therefore, an orthogonal representation of the child with spirality 0 can never be used in the construction. □

We know that the number of edges to add is at most two, and so there are at most 16 different distributions to check. Per distribution, the step values can be computed via Lemma 4.17 by combining each child serially with a $\mathcal{D}$-node per bend-vertex. In total, we form the following result.

Theorem 4.30. *Given a 2-legged series-parallel plane 3-graph $(G, \mathcal{E})$, a fixed outer face f_o, and a fixed inner face f_c, a bend-minimum valid ortho-radial representation of G if one exists, can be found in $\mathcal{O}(n)$ time.*

Proof. The same approach as described in Theorem 4.25 can be used. The difference is that if a node in the recursion does not fulfill the conditions, one has to add bend-vertices as described in Lemma 4.29 and Lemma 4.27. In both situations, the addition of bend-vertices and the calculation of the structure of these nodes only take constant time.

What is left to prove is that the resulting ortho-radial representation is actually bend-minimum. For this, we define for a given node ϕ in the decomposition tree $\mathcal{B}(\phi)$ to be the number of bend-vertices added by Lemmas 4.27 and 4.29 in the recursion up to ϕ. Moreover, for an arbitrary valid ortho-radial representation $\mathcal{T}$ with bend-vertices we define $b(\mathcal{T})$ to be the number of bend-vertices specifically added in $\mathcal{T}$. Let ϕ be a node in the decomposition tree of G. We now prove by induction over the depth of the subtree n rooted at ϕ that $\mathcal{B}(\phi) = b(\mathcal{T}_\phi^{\min})$, where $\mathcal{T}_\phi^{\min}$ is a bend-minimum valid ortho-radial representation of the induced subgraph of ϕ. This implies that once the recursion has reached the root τ, the budget $\mathcal{B}(\tau)$ equals the minimum number of bends required for a valid ortho-radial representation of the whole graph G.

Base case: If $n = 1$, then ϕ is a leaf node and $\mathcal{B}(\phi) = 0 = b(\mathcal{T}_\phi^{\min})$, so the statement is trivial.

Inductive case: Let $n > 1$ and assume that the statement holds for all $k < n$. Then ϕ is a node of $\mathcal{T}$ that is not a leaf and denote by ϕ_1 and ϕ_2 the children of ϕ. The subtrees of the two children have depth at most $n - 1$, so the induction hypothesis implies that both $\mathcal{B}(\phi_1) = b(\mathcal{T}_{\phi_1}^{\min})$ and $\mathcal{B}(\phi_2) = b(\mathcal{T}_{\phi_2}^{\min})$. We also know that $\mathcal{B}(\phi) = \mathcal{B}(\phi_1) + \mathcal{B}(\phi_2) + b_\phi$ where b_ϕ are the number of bends in the construction that are used at the node ϕ to realize a valid ortho-radial representation. Let $\mathcal{T}_\phi^{\min}$ be a bend-minimum valid ortho-radial representation of ϕ and let $\mathcal{T}_1$ as well as $\mathcal{T}_2$ be the induced valid ortho-radial representation of ϕ_1 and ϕ_2.

From the inductive hypothesis we know that $b(\mathcal{T}_1) \geq \mathcal{B}(\phi_1)$ and $b(\mathcal{T}_2) \geq \mathcal{B}(\phi_2)$. In actuality, as $\mathcal{T}_1$ and $\mathcal{T}_2$ are the induced representations of the whole representation $\mathcal{T}$, they may have more bend-vertices than would be necessary for each subgraph on its own. So let $0 \leq m_1 = b(\mathcal{T}_1) - \mathcal{B}(\phi_1)$ and $0 \leq m_2 = b(\mathcal{T}_2) - \mathcal{B}(\phi_2)$. We now show $b_\phi \leq m_1 + m_2$ since this then implies that

$$\mathcal{B}(\phi) = \mathcal{B}(\phi_1) + \mathcal{B}(\phi_2) + b_\phi \leq b(\mathcal{T}_1) + b(\mathcal{T}_2) = b(\mathcal{T}_\phi^{\min}).$$

If, according to the construction, no bend-vertices have to be added at ϕ, we have $b_\phi = 0$ and the inequality trivially holds. In the case where $b_\phi > 0$, Lemma 4.27 and Lemma 4.29 show that if fewer than b_ϕ bend-vertices are added to the already existing bend-vertices in ϕ_1 and ϕ_2, no valid ortho-radial representation of ϕ exists. This would be a contradiction to the existence of $\mathcal{T}_\phi^{\min}$. This proves $\mathcal{B}(\phi) \leq b(\mathcal{T}_\phi^{\min})$, and as $\mathcal{B}(\phi) \geq b(\mathcal{T}_\phi^{\min})$ holds by definition, equality follows. □

4.2 Non-st-Outwards Ortho-Radial Representations

In Section 4.3 it will be necessary to also find ortho-radial representations for 2-legged series-parallel 3-graphs that are not st-outwards, but have their legs pointing in other directions. To create such representations, Lemmas 4.23 and 4.24 have to be adapted. The first step is to generalize the notion of step values for orthogonal representations, because in non-st-outwards ortho-radial representations more properties are required of their subgraphs.

4.2.1 General Step Values

Section 4.1 introduces the notion of step values, which are used to ensure the existence of edges with desired labels. For this, the left and right step value s^l and s^r measures how much a representation of the graph can bend in one direction, while having at least one edge per st-path that is bent into the opposite direction. The zero step value s^z indicates if an orthogonal representation exists with an st-path that only has relative label 0. We

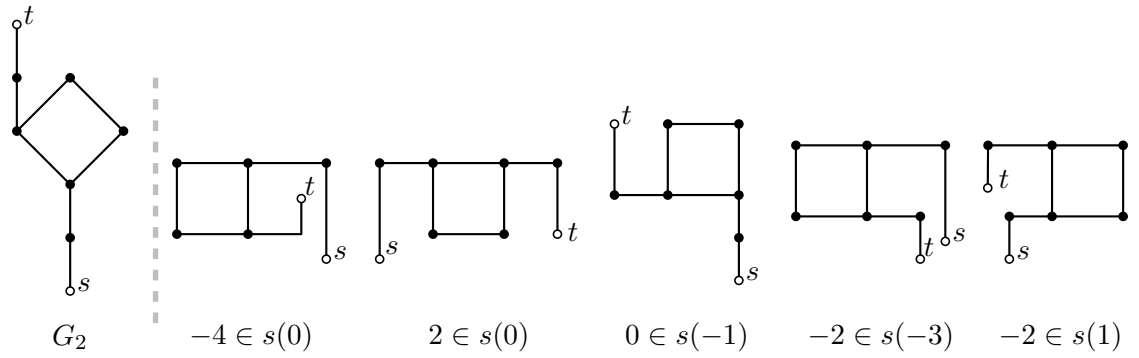

G_2 $\quad -4 \in s(0)$ $\quad 2 \in s(0)$ $\quad 0 \in s(-1)$ $\quad -2 \in s(-3)$ $\quad -2 \in s(1)$

Figure 4.19: A 2-legged SP-graph and examples of orthogonal representations implying the step value expressions below each representation.

now generalize the left and right step values into a combined step value s, and also add a new step value s^{lr}.

The step values s^l and s^r only ensure that an edge e in every st-path exists with relative label $\ell_s(e) < 0$ or $\ell_s(e) > 0$, but gives no indication of what the actual relative label of e may be. The new step value includes a parameter indicating the required relative label for e.

Definition 4.31. *Let $(G, \mathcal{E})$ be a 2-legged rectilinear-plane series-parallel 3-graph. We define the* bend step value $s : \mathbb{Z} \to 2^{\mathbb{Z}}$ *as a function for which the following holds.*

$$x \in s(y) \iff \exists\ \mathcal{H} \in \Omega(G, \mathcal{E}) : \sigma(\mathcal{H}) = x,\ \forall\ P \in \mathcal{P}_{st}(G) : \exists\ e \in P : \ell_s(e) = y$$

The expression $x \in s(y)$ is called a step value expression.

If $x \in s(y)$ for some $x, y \in \mathbb{Z}$ then there exists an orthogonal representation, where every st-path first contains an edge with relative label y before resulting in a total spirality of x. See Figure 4.19 for some examples of step value expressions and matching representations. The following lemma shows how some step value expressions imply others. For better clarity, we use the definition of signed intervals $[x, y]_s$.

Lemma 4.32. *Let $(G, \mathcal{E})$ be a 2-legged rectilinear-plane series-parallel 3-graph with bend step value s. Then the following statements hold.*

$$x \in s(y) \implies x \in s(y') \qquad \forall\ y' \in [0, y]_s \tag{4.20}$$
$$x \in s(y) \implies x \in s(y') \qquad \forall\ y' \in [0, x]_s \tag{4.21}$$
$$x \in s(y) \implies x' \in s(y) \qquad \forall\ x' \in [x, y]_s \tag{4.22}$$
$$x \in s(y) \implies x - z \in s(y - z) \qquad \forall\ z \in [0, y]_s \tag{4.23}$$

Proof. For Equation (4.20), the step value expression $x \in s(y)$ implies the existence of an orthogonal representation $\mathcal{H}$ with $\ell_s(e) = y$ for some edge in every st-path. Along such an st-path there must exist edges between e^s and e having any relative label between 0 and y. This directly implies $x \in s(y')$ for $y' \in [0, y]_s$.

Regarding Equation (4.21), the step value expression $x \in s(y)$ implies an orthogonal representation $\mathcal{H}$ with $\ell_s(e^t) = \sigma(\mathcal{H}) = x$. Along every st-path there must exist edges with all values between 0 and x. This directly implies $x \in s(y')$ for $y' \in [0, x]_s$.

For Equation (4.22), let, without loss of generality, $x < y$. We show this fact for $x' = x + 1$ and the statement follows from iteration. Because $x \in s(y)$ holds, there exists an orthogonal

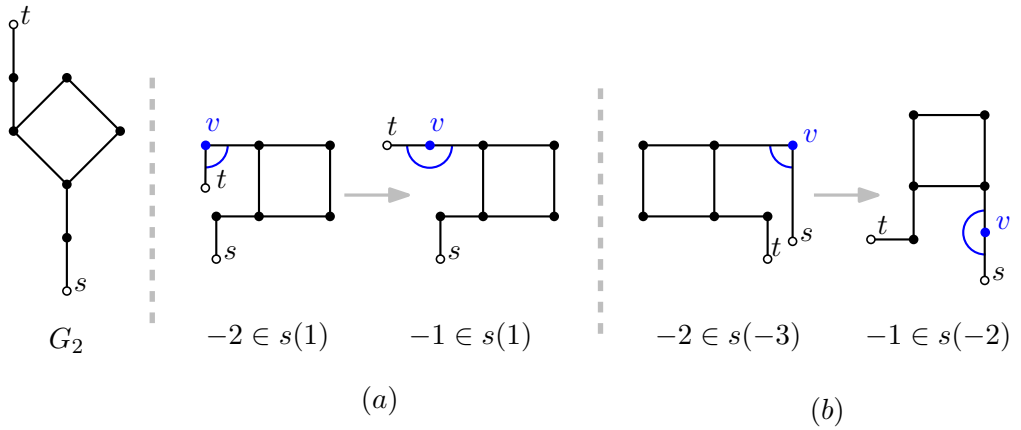

Figure 4.20: A graph with two pairs of orthogonal representations. The existence of the left representation in each pair implies the existence of the right. The blue vertex v changes its rotation in the path between the representations.

representation $\mathcal{H}$ of G with $\sigma(\mathcal{H}) = x$ such that every st-path contains an edge e with $\ell_s(e) = y > x$. So there must exist vertices u, v, w along every st-path between every such edge e and e^t with $\text{rot}(uv, vw) = -1$. See Figure 4.20a for an example. Lemma 4.11 then implies the existence of another orthogonal representation $\mathcal{H}'$ with $\sigma(\mathcal{H}') = \sigma(\mathcal{H}) + 1 = x + 1 = x'$. Moreover, $\mathcal{H}'$ and $\mathcal{H}$ only differ in its rotation at each vertex v and for every edge e it still holds that $\ell_s(e) = y$. The existence of $\mathcal{H}'$ then implies $z \in s(y)$.

For Equation (4.23), let, without loss of generality, $y < 0$. We show this fact for $z = -1$ and the statement follows from iteration. Because $x \in s(y)$ holds, there exists an orthogonal representation $\mathcal{H}$ of G with $\sigma(\mathcal{H}) = x$ such that every st-path contains an edge e with $\ell_s(e) = y < 0$. So there must exist vertices u, v, w along every st-path between e^s and e with $\text{rot}(uv, vw) = -1$. See Figure 4.20b for an example. Lemma 4.11 then implies the existence of another orthogonal representation $\mathcal{H}'$ with $\sigma(\mathcal{H}') = \sigma(\mathcal{H}) + 1 = x + 1 = x - z$. Moreover, $\mathcal{H}'$ and $\mathcal{H}$ only differ in its rotation at each vertex v, and for every edge e it holds that $\ell_s(e) = \ell_s(e) + 1 = y + 1 = y - z$. The existence of $\mathcal{H}'$ then implies $x - z \in s(y - z)$. □

Lemma 4.32 directly implies that $s(y)$ is an interval for every $y \in \mathbb{Z}$ as well as $x \leq s^l \; \forall \; x \in s(-1)$ and $x \geq -s^r \; \forall \; x \in s(1)$. It also holds that $s(0) = [-b^l, b^r]$. The bend step value therefore also represents the old bend values b^l, b^r. We will from now on use $x \in s(0)$ instead of $x \leq b^r, b^l$.

The old step values s^l and s^r as well as the new bend step value s only imply the existence of one edge with a given relative label. The condition for a valid ortho-radial representation requires an edge with a positive and with a negative relative label, though. Oftentimes, the spirality x implied by the step value expression $x \in s(y)$ is enough to also imply an edge of the opposite sign, but if $x = 0$, this may not always work. We therefore introduce a new step value which indicates that both a positive and a negative relative label is present, while the representation has spirality 0.

Definition 4.33. *Let $(G, \mathcal{E})$ be a 2-legged rectilinear-plane series-parallel 3-graph. We define the* left-right step value s^{lr} *as*

$$s^{lr} = \begin{cases} 1 & \text{if } \exists\ \mathcal{H} \in \Omega(G, \mathcal{E}) : \sigma(\mathcal{H}) = 0, \forall P \in \mathcal{P}_{st}(G) : \exists\ e, e' \in P : \ell_s(e) < 0,\ \ell_s(e') > 0 \\ 0 & \text{otherwise.} \end{cases}$$

The following lemma shows how a left-right step value $s^{lr} = 1$ implies other step value expressions.

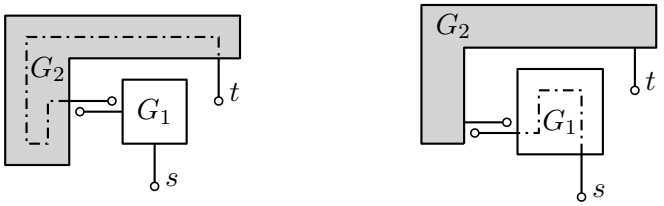

Figure 4.21: Two series-compositions resulting in the step value expression $2 \in s(-2)$, but with different properties of the subgraphs G_1 and G_2.

Lemma 4.34. *Let $(G, \mathcal{E})$ be a 2-legged rectilinear-plane series-parallel 3-graph with $s^{lr} = 1$. Then $0 \in s(1)$, $0 \in s(-1)$, as well as $2, -2 \in s(0)$ follows.*

Proof. If $s^{lr} = 1$, then there exists an orthogonal representation $\mathcal{H}$ of G with $\sigma(\mathcal{H}) = 0$ and edges with a positive as well as a negative relative label in every st-path. These edges have at least relative label 1 and -1, respectively. $0 \in s(-1)$ and $0 \in s(1)$ then follows directly from Definition 4.31. $2, -2 \in s(0)$ follows from Lemma 4.14. □

Having both new step values defined, we now adapt the structure of an orthogonal representation to be simply $[s, s^z, s^{lr}]$ instead of $[b^l, b^r, s^l, s^r, s^z]$. Each $\mathcal{Q}$-node has the structure $[s_\mathcal{Q}, 1, 0]$ with $s_\mathcal{Q}(0) = \{0\}$ and each $\mathcal{D}$-node has the structure $[s_\mathcal{D}, 1, 0]$ with $s_\mathcal{D}(0) = \{0, 1\}$. We now show analogous to Section 4.1 how the bend step value and left-right step value of inner nodes are dependent on the ones of their child nodes. To more easily describe this correlation, we use the $+$ operator between sets to mean $A+B \coloneqq \{a+b \mid a \in A, b \in B\}$.

Lemma 4.35. *Let ϕ be an $\mathcal{S}$-node not containing f_c where its children ϕ_1 and ϕ_2 both are rectilinear-plane. Also, let $[s_1, s_1^z, s_1^{lr}]$ be the structure of ϕ_1 and $[s_2, s_2^z, s_2^{lr}]$ be the structure of ϕ_2. Then the bend step value s and the left-right step value s^{lr} of ϕ satisfy the following.*

$$s(y) = \Big(\bigcup_{i \in [0,y)_s} (s_1(0) \cap \{i\}) + s_2(y-i) \Big) \cup s_1(y) + s_2(0) \tag{4.24}$$

$$s^{lr} = 1 \iff \bigvee \begin{cases} s_1^{lr} = 1, s_2^{lr} = 1, \\ 0 \in s_1(-i) \wedge 0 \in s_2(i) \text{ for } i \in \{-1, 1\}, \\ i \in s_1(0) \wedge -i \in s_2(-2i) \text{ for } i \in \{-1, 1\}, \\ i \in s_1(-i) \wedge -i \in s_2(0) \text{ for } i \in \{-1, 1\} \end{cases} \tag{4.25}$$

Proof. Let G be the induced graph of ϕ, G_1 be the induced subgraph of ϕ_1, and G_2 the induced subgraph of ϕ_2. Also let s_1, t_1 be the terminals of G_1, s_2, t_2 be the terminals of G_2, and $e_1^s, e_2^s, e_1^t, e_2^t$ be the legs of G_1 and G_2.

We start with Equation (4.24) and first show the "$\supseteq$"-direction. Let $y \in \mathbb{Z}$ and first let $i \in [0, y)_s$ such that $z \in (s_1(0) \cap \{i\}) + s_2(y-i)$. For $s_1(0) \cap \{i\}$ to not be the empty set, $i \in s_1(0)$ must hold and for z to be in the whole set it follows that $z - i \in s_2(y-i)$. Then there exists an orthogonal representation $\mathcal{H}_1$ of G_1 with $\sigma(\mathcal{H}_1) = i$ and an orthogonal representation $\mathcal{H}_2$ of G_2 with $\sigma(\mathcal{H}_1) = z - i$ where in every st-path an edge e exists with $\ell_{s_2}(e) = y - i$. Let $\mathcal{H}$ be the orthogonal representation of G obtained by combining $\mathcal{H}_1$ and $\mathcal{H}_2$. Figure 4.21a shows this for $i = -1$ and $3 \in s_2(-1)$ resulting in the step value expression $2 \in s(-2)$. Then every edge e from above now has relative label $\ell_s(e) = \sigma(\mathcal{H}_1) + \ell_{s_2}(e) = i + y - i = y$ and $\mathcal{H}$ has spirality $\sigma(\mathcal{H}) = i + z - i = z$. This implies $z \in s(y)$. Second, assume $z \in s_1(y) + s_2(0)$. Then there exists an orthogonal

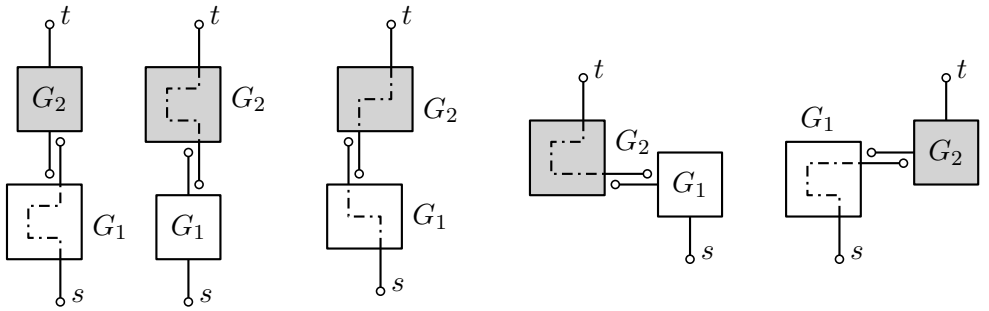

Figure 4.22: Ways of creating a left-right step value $s^{lr} = 1$ in a series composition of two subgraphs G_1 and G_2.

representation $\mathcal{H}_1$ of G_1 with $\sigma(\mathcal{H}_1) = x$ and an edge e in every st-path with $\ell_{s_1}(e) = y$, as well as an orthogonal representation $\mathcal{H}_2$ of G_2 with $\sigma(\mathcal{H}_2) = z - x$. The combined representation has spirality z, and the relative labels of edges e from above stay the same. This also implies $z \in s(y)$. This situation is depicted in Figure 4.21b, where $-1 \in s_1(-2)$ and $3 \in s_2(0)$ results in $2 \in s(-2)$.

Now to the "$\subseteq$"-direction of Equation (4.24). Without loss of generality, let $y \leq 0$ and let $z \in s(y)$. Then there exists an orthogonal representation $\mathcal{H}$ of G with $\sigma(\mathcal{H}) = z$ and an edge e in every st-path with $\ell_s(e) = y$. Let $\mathcal{H}_1$ and $\mathcal{H}_2$ be the induced orthogonal representations of G_1 and G_2, and let $i \coloneqq \sigma(\mathcal{H}_1)$ and therefore $\sigma(\mathcal{H}_2) = z - i$. There are two possible cases.

Case 1: Every st-path in G_1 already contains an edge with $y = \ell_s(e) = \ell_{s_1}(e)$. This implies $i \in s_1(y)$. The existence of $\mathcal{H}_2$ also implies $z - i \in s_2(0)$ and therefore $z \in s_1(y) + s_2(0)$ follows.

Case 2: There exists an st-path P_1 in G_1, such that $y < \ell_s(e) = \ell_{s_1}(e)$ for all $e \in P_1$. This also implies $i \in [0, y)_s$. Now assume that $z - i \notin s_2(y - i)$ would hold. Then there exists a path P_2 through G_2 such that $y - i < \ell_{s_2}(e)$ for all $e \in P_2$. The path $P = P_1 + P_2$ then is an st-path of G, and it holds for all $e \in P$ that

$$\ell_s(e) = \begin{cases} \ell_{s_1}(e) > y & \text{if } e \in G_1, \\ \sigma(\mathcal{H}_1) + \ell_{s_2}(e) > i + y - i = y & \text{otherwise.} \end{cases}$$

This is a contradiction to $z \in s(y)$. So $z - i \in s_2(y - i)$ must hold. As $\sigma(\mathcal{H}_1) = i$, it follows that $z \in (s_1(0) \cap \{i\}) + s_2(y - i)$.

Now to Equation (4.25) where we start with the "$\Longleftarrow$"-direction. If $s_1^{lr} = 1$ or $s_2^{lr} = 1$, it is obvious that also $s^{lr} = 1$ since there always exists an orthogonal representation of the other subgraph with spirality 0 as for example in Figure 4.22a. Without loss of generality, let $i = 1$ and let $\mathcal{H}_1$ and $\mathcal{H}_2$ be such that one of the other conditions hold, and let $\mathcal{H}$ be the combined orthogonal representation of G.

If $0 \in s_1(i)$ and $0 \in s_2(-i)$, then there exist edges e in every st-path of G_1 with $\ell_s(e) = \ell_{s_1}(e) = i$ and there exist edges e' in every st-path of G_2 with $\ell_s(e') = \sigma(\mathcal{H}_1) + \ell_{s_2}(e') = -i$. So in $\mathcal{H}$ every st-path has a positive relative label in G_1 and a negative relative label in G_2 as seen in Figure 4.22b. Finally, $\sigma(\mathcal{H}) = 0 + 0 = 0$ implies $s^{lr} = 1$.

If $i \in s_1(0)$, then $\ell_s(e^t) = \sigma(\mathcal{H}_1) = i$ and with $-i \in s_2(-2i)$ there exists an edge in every st-path of G_2 with $\ell_s(e) = \sigma(\mathcal{H}_1) + \ell_{s_2}(e) = i - 2i = -1$. See Figure 4.22c for an example. Due to $\sigma(\mathcal{H}) = i - i = 0$, $s^{lr} = 1$ follows.

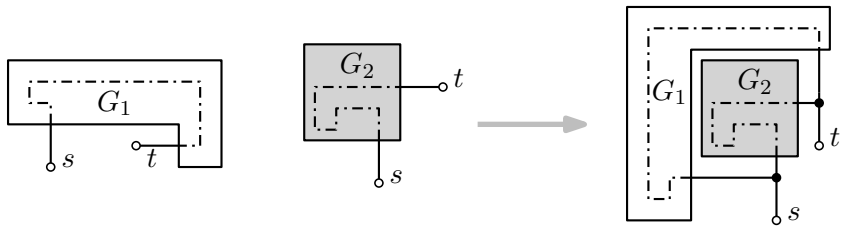

Figure 4.23: On the left, two orthogonal representations of the graphs G_1 and G_2 representing the shown step value expressions. On the right, an orthogonal representation of the parallel-composition of G_1 and G_2 and its implying step value expression using the representations on the left.

Finally, if $i \in s_1(-i)$ holds (see Figure 4.22d), then $\ell_s(e^t) = \sigma(\mathcal{H}_1) = 1$ and there exists an edge e every st-path of G_1 with $\ell_s(e) = \ell_{s_1}(e) = -1$. With $-i \in s_2(0)$, also $\sigma(\mathcal{H}) = i - i = 0$ holds and $s^{lr} = 1$ follows.

For the " $\Longrightarrow$ "-direction, assume $s^{lr} = 1$. Then there exists an orthogonal representation of G having spirality 0 with a positive and a negative relative label in every path. When looking at which of these labels are contained in which subgraph, the situation never arises where two st-paths P and P' exist, such that P only has negative relative labels in G_1 and P' only has negative relative labels in G_2. Because then there exists a third st-path created by the parts of P and P' not containing a negative relative label, which now in total would not contain a negative relative label as well. This is a contradiction to $s^{lr} = 1$ and the same argumentation holds for positive instead of negative relative labels. Due to this, at least G_1 or G_2 must have a positive or negative relative label in every of its st-paths and depending on which subgraph contains which relative label, we deduce one of the four conditions. We now make a case distinction.

Case 1: $\sigma(\mathcal{H}_1) = 0$. Then $\sigma(\mathcal{H}_2) = 0$ so that $\mathcal{H}$ has the spirality 0. If now G_1 also contains both a positive and negative relative label in every st-path, $s_1^{lr} = 1$ follows, while if G_2 contains both a positive and a negative relative label in every st-path, $s_2^{lr} = 1$.

If G_1 contains relative labels of one sign in every st-path but not of the other, then $0 \in s_1(i)$ holds with $i \in \{1, -1\}$, depending on which sign is present. To still have $s^{lr} = 1$, G_2 must contain relative labels of the opposite sign in every st-path, which implies $0 \in s_2(-i)$.

Case 2: $\sigma(\mathcal{H}_1) = x < 0$. Then $\sigma(\mathcal{H}_2) = -x$ for $\mathcal{H}$ to have spirality 0. If now G_1 also contains a positive relative label in every st-path, then $x \in s_1(1)$, which with Lemma 4.32 also implies $-1 \in s_1(1)$. Due to $\sigma(\mathcal{H}_2) = -x$, we also know from Lemma 4.32 that at least $1 \in s_2(0)$. With $i = -1$ we now have $i \in s_1(-i)$ and $-i \in s_2(0)$.

If G_2 contains a positive relative label in every st-path then for every edge e in G_2 with $\ell_s(e) = 1$ we know $\ell_{s_2}(e) = -\sigma(\mathcal{H}_1) + \ell_s(e) = -x + 1$. This implies $-x \in s_2(-x + 1)$ and $1 \in s_2(2)$ follows from Equation (4.23) with $z = -x - 1$. Due to $\sigma(\mathcal{H}_1) = x$, we also know from Lemma 4.32 that at least $-1 \in s_1(0)$ and with $i = -1$ we now have $i \in s_1(0)$ and $-i \in s_2(-2i)$.

Case 3: $\sigma(\mathcal{H}_1) > 0$, the same argumentation as in Case 2 implies with $i = 1$ that $i \in s_1(-i)$ and $-i \in s_2(0)$, as well as $i \in s_1(0)$ and $-i \in s_2(-2i)$. □

Lemma 4.36. *Let ϕ be a rectilinear-plane $\mathcal{P}$-node not containing f_c with its two children ϕ_1 and ϕ_2 having structures $[s_1, s_1^z, s_1^{lr}]$ and $[s_2, s_2^z, s_2^{lr}]$, respectively. Then the bend step value s and the left-right step value s^{lr} of ϕ satisfy the following.*

$$s(0) = \Big[\min\big((s_1(0) - 2) \cap s_2(0)\big), \max\big(s_1(0) \cap (s_2(0) + 2)\big)\Big]$$

$$x \in (y) \iff \begin{cases} x \in s(0) & \text{if } \ y \in [0, x]_s, \quad (4.26) \\ x \in (s_1(y+1) - 1) \cap (s_2(y) + 1) & \text{if } y \notin [0, x]_s \wedge y < 0, \quad (4.27) \\ x \in (s_1(y) - 1) \cap (s_2(y-1) + 1) & \text{if } y \notin [0, x]_s \wedge y > 0 \quad (4.28) \end{cases}$$

$$s^{lr} = 1 \iff 2 \in s_1(0) \wedge -2 \in s_2(0)$$

Proof. Let G be the induced graph of ϕ, G_1 be the induced subgraph of ϕ_1, and G_2 the induced subgraph of ϕ_2. Also let s_1, t_1 be the terminals of G_1 and s_2, t_2 the terminals of G_2 as well as $e_1^s, e_2^s, e_1^t, e_2^t$ be the legs of G_1 and G_2.

We start with the bend step value s and let $y \in \mathbb{Z}$. Equality for $y = 0$ is a direct implication of Lemma 4.19 and Term (4.26) follows from Equation (4.21). We show both directions for Term (4.27) separately, and we start with the "$\supseteq$"-direction. So let $y < 0$ and let $x \in (s_1(y+1)-1) \cap (s_2(y)+1)$. Then there exists an orthogonal representation $\mathcal{H}_1$ of G_1 with $\sigma(\mathcal{H}_1) = x + 1$ and an edge in every st-path with $\ell_{s_1}(e) = y + 1$, as well as an orthogonal representation $\mathcal{H}_2$ of G_2 with $\sigma(\mathcal{H}_2) = x - 1$ and an edge e in every st-path with $\ell_{s_2}(e) = y$. Figure 4.23 depicts the orthogonal representations of G_1 and G_2 for the case $2 \in s(-2)$. Using a rotation combination of $[r_1^s, r_2^s, r_1^t, r_2^t] = [-1, 0, 0, 1]$ results in a combined orthogonal representation $\mathcal{H}$ of G, as the rotation of the newly created face f between G_1 and G_2 is

$$\mathrm{rot}(f) = \underbrace{\mathrm{rot}(e_2^s, e_1^s)}_{=1} + \sigma(\mathcal{H}_1) - \sigma(\mathcal{H}_2) + \underbrace{\mathrm{rot}(e_1^t, e_2^t)}_{=1} = 1 + x + 1 - (x - 1) + 1 = 4.$$

The spirality of $\mathcal{H}$ is then $\sigma(\mathcal{H}) = r_1^s + \sigma(\mathcal{H}_1) + r_1^t = -1 + x + 1 + 0 = x$. Moreover, for every edge e in G_1 with $\ell_{s_1}(e) = y + 1$ it now follows that $\ell_s(e) = r_1^s + \ell_{s_1}(e) = -1 + y + 1 = y$ and for every edge e in G_2 with $\ell_{s_2}(e) = y$ it follows that $\ell_s(e) = r_2^s + \ell_{s_2}(e) = y$. In total, this implies $x \in s(y)$. The proof of the "$\supseteq$"-direction for Term (4.28) follows analogously, only here the rotation combination $[r_1^s, r_2^s, r_1^t, r_2^t] = [0, 1, -1, 0]$ is used.

For the "$\subseteq$"-direction of Term (4.27), let $x \in s(y)$ and again let $y < 0$. Then there exists an orthogonal representation $\mathcal{H}$ of G with $\sigma(\mathcal{H}) = x$ and an edge e in every st-path having $\ell_s(e) = y$ with $y \notin [0, x]_s$. This implies $x > y$. As $\ell_s(e^s) = 0$ and $\ell_s(e^t) = x$, the edges with relative label y must be present in G_1 and G_2. Relative to e_1^s and e_2^s these edges have the labels $\ell_{s_1}(e) = \ell_s(e) - r_1^s = y - r_1^s$ and $\ell_{s_2}(e) = \ell_s(e) - r_2^s = y - r_2^s$. With $\mathcal{H}_1$ and $\mathcal{H}_2$ being the induced orthogonal representations of G_1 and G_2, we know $x - r_1^s - r_1^t = \sigma(\mathcal{H}_1) \in s_1(y - r_1^s)$. Equations (4.20) and (4.23) with $r_1^s, r_1^t \in \{-1, 0\}$ first imply $x - r_1^t + 1 \in s_1(y+1)$ and finally $x + 1 \in s_1(y+1)$. Similarly, $x - r_2^s - r_2^t \in s_2(y - r_2^s)$ implies with Equations (4.22) and (4.23) as well as $r_2^s, r_2^t \in \{0, 1\}$ that $x - 1 \in s_2(y)$. In total, $x \in (s_1(y+1)-1) \cap (s_2(y)+1)$ follows. The proof for Term (4.28) follows analogously.

Now on to the equivalence proof for $s^{lr} = 1$. For the "$\Longleftarrow$"-direction, let $\mathcal{H}_1$ be an orthogonal representation of G_1 with $\sigma(\mathcal{H}_1) = 2$ and let $\mathcal{H}_2$ be an orthogonal representation of G_2 with $\sigma(\mathcal{H}_2) = -2$. Using rotation combination $r_1^s = r_1^t = -1$ and $r_2^s = r_2^t = 1$ results in an orthogonal representation $\mathcal{H}$ of G, as the rotation of the new face f is $\mathrm{rot}(f) = \sigma(\mathcal{H}_1) - \sigma(\mathcal{H}_2) + 0 = 2 - 2 = 4$. Moreover, $\sigma(\mathcal{H}) = -1 + \sigma(\mathcal{H}_1) - 1 = 0$ and every st-path in G has to either traverse e_1^s and e_1^t or e_2^s and e_2^t for which $\ell_s(e_1^s) = r_1^s = -1$, $\ell_s(e_1^t) = -r_1^t = 1$, $\ell_s(e_2^s) = r_2^s = 1$, and $\ell_s(e_2^t) = -r_2^t = -1$ hold. The existence of $\mathcal{H}$ implies $s^{lr} = 1$.

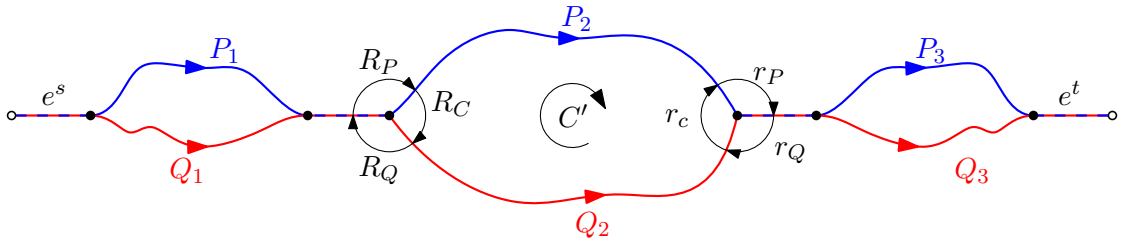

Figure 4.24: A series-parallel 3-graph with two st-paths P and Q surrounding the central face. The simple cycle C' is formed by the subpaths P_2 and $\overleftarrow{Q}_2$. The three rotations R_P, R_Q, R_C as well as r_P, r_Q, r_C form a total rotation of -2.

For the " $\Longrightarrow$ "-direction, let $s^{lr} = 1$ and let $\mathcal{H}$ be an orthogonal representation of G with spirality 0 containing both a positive and a negative relative label in every st-path. As $\ell_s(e_1^s) = 0$ and $\ell_s(e_1^t) = \sigma(\mathcal{H}) = 0$, these labels must be present in G_1 and G_2. If r_1^s is 0, then these edges also have the same labels relative to e_1^s, and Lemma 4.14 implies $b_1^r \geq 2$ and therefore $2 \in s_1(0)$. If r_1^s is -1, then $\sigma(\mathcal{H}_1) \geq 1$ and every edge e with $\ell_s(e) \geq 1$ now has $\ell_{s_1}(e) = \ell_s(e) - r_1^s \geq 2$. So $1 \in s_1(2)$, which implies $2 \in s_1(0)$. With the same argumentation using G_2, also $-2 \in s_2(0)$ follows. □

Different to Section 4.1, the structure of a graph now not only contains simple bounds, but the more complex bend step value s. This changes the runtime of computing a structure.

Lemma 4.37. *Given a 2-legged series-parallel rectilinear-plane 3-graph G, a structure $[s, s^z, s^{lr}]$ of G can be computed in $\mathcal{O}(n^2)$ time.*

Proof. A decomposition tree of G can be computed in linear time with $\mathcal{O}(n)$ nodes. Per inner node ϕ, the calculation of $[s_\phi, s_\phi^z, s_\phi^{lr}]$ takes constant time for the zero step value s^z and the left-right step value s^{lr}. The time taken for calculating the bend step value s can be bounded by the number of sets in the codomain of s not being the empty set. As the in absolute terms highest relative label is proportional to the number of vertices n at which the label may change, s can be represented by at most $2n$ sets that according to Lemma 4.32 are intervals. By only calculating the bounds of each interval in Lemmas 4.35 and 4.36, the bend step value s can be calculated in $\mathcal{O}(n)$ time. In total, the structure of G can then be computed in $\mathcal{O}(n^2)$ time. □

4.2.2 Creating Ortho-Radial Representations

Based on the generalized step values from Section 4.2.1, we now create and extend non-st-outwards ortho-radial representations. This requires a structure also for nodes containing f_c. The definition of step values for orthogonal representation can be simply used for ortho-radial representations though. As a start, the notions of relative labels and spirality are no longer well-defined for ortho-radial representations since different st-paths may have different rotational values. For example, the ortho-radial representation in Figure 4.11 has a rotation of -2 for all st-paths traversing G_1 but a rotation of 2 for st-paths traversing G_2. The following lemma shows an important connection between the rotations of such two paths.

Lemma 4.38. *Let $(G, \mathcal{E})$ be a 2-legged series-parallel plane 3-graph that admits a (not necessarily valid) ortho-radial representation $\mathcal{T}$ of G. If there exist two st-paths P and Q*

with $\mathrm{rot}(P) \neq \mathrm{rot}(Q)$*, then* $P + \overline{Q}$ *forms an essential cycle* C*, which is not necessarily oriented clockwise, and*

$$\mathrm{rot}(P) - \mathrm{rot}(Q) = \begin{cases} -4 & \text{if } C \text{ goes clockwise around } f_c, \\ 4 & \text{otherwise.} \end{cases}$$

Proof. Assume C is not an essential cycle. Then $P \cup Q$ forms a 2-legged subgraph G' of G. The induced ortho-radial representation $\mathcal{T}'$ of G' is simply an orthogonal representation, as it does not contain essential cycles. Then P and Q would be two st-paths with different rotations in an orthogonal representation, which stands in contradiction to Lemma 4.5. Therefore, C must be an essential cycle. The cycle C is not simple since it contains at least the two legs e^s, e^t twice; once in P and once, in the other direction, in Q. We split up P and Q into six sections P_1, P_2, P_3 as well as Q_1, Q_2, Q_3 such that $C = P_1 + P_2 + P_3 + Q_1 + Q_2 + Q_3$ and $C' \coloneqq P_2 + Q_2$ forms a simple essential sub-cycle of C. See Figure 4.24 for an illustration. As G is a 3-graph and C' is simple, we know that P_1 and Q_1 share their last edge and P_3 and Q_3 share their first edge. To calculate the rotation of paths correctly, we also have to take into account the rotations at the two join points. We call R_P the rotation from P_1 to P_2, R_Q the rotation from $\overleftarrow{Q}_2$ to $\overleftarrow{Q}_1$, and R_C the rotation from $\overleftarrow{P}_2$ to Q_2. Similarly, we call r_P the rotation from P_2 to P_3, r_Q the rotation from $\overleftarrow{Q}_3$ to $\overleftarrow{Q}_2$, and r_C the rotation from Q_2 to $\overleftarrow{P}_2$. See again Figure 4.24 for an illustration. From the definition of ortho-radial representations we know $R_P + R_Q + R_C = -2 = r_P + r_q + r_C$ as well as $0 = \mathrm{rot}(C')$. The subgraph $P_1 \cup Q_1$ is a 2-legged series-parallel 3-graph, which does not include the central face, and therefore $\mathrm{rot}(P_1) = \mathrm{rot}(Q_2)$ and similarly $\mathrm{rot}(P_3) = \mathrm{rot}(Q_3)$. Now suppose that C, and therefore also C', goes clockwise around f_c. It then follows that

$$\begin{aligned}
&\mathrm{rot}(P) - \mathrm{rot}(Q) \\
&= \mathrm{rot}(P_1) + R_P + \mathrm{rot}(P_2) + r_P + \mathrm{rot}(P_3) - (\mathrm{rot}(Q_1) - R_Q + \mathrm{rot}(Q_2) - r_Q + \mathrm{rot}(Q_3)) \\
&= \underbrace{\mathrm{rot}(P_1) - \mathrm{rot}(Q_1)}_{=0} + \underbrace{\mathrm{rot}(P_3) - \mathrm{rot}(Q_3)}_{=0} + \mathrm{rot}(P_2) - \mathrm{rot}(Q_2) + R_P + R_Q + r_P + r_Q \\
&= \mathrm{rot}(P_2) - \mathrm{rot}(Q_2) + R_P + R_Q + R_C - R_C + r_P + r_Q + r_C - r_C \\
&= \underbrace{\mathrm{rot}(P_2) - r_C - \mathrm{rot}(Q_2) - R_C}_{=\mathrm{rot}(C')=0} + \underbrace{R_P + R_Q + R_C}_{=-2} + \underbrace{r_P + r_Q + r_C}_{=-2} \\
&= -4.
\end{aligned}$$

On the other hand, if C goes anticlockwise around f_c, the signs of the rotational values at the connection points switch, and we get $\mathrm{rot}(P) - \mathrm{rot}(Q) = 4$. □

Definition 4.39. *Let* $(G, \mathcal{E})$ *be a 2-legged series-parallel plane 3-graph. We call an st-path* P *a* clockwise st-path *if for all other st-paths* $Q \in \mathcal{P}_{st}(G)$ *where* $P + \overline{Q}$ *forms an essential cycle, this cycle goes clockwise around* f_c*. If these cycles go anticlockwise around* f_c*, then we call* P *an* anticlockwise st-path*.*

With P being a clockwise st-path and Q being an anticlockwise st-path, Lemma 4.38 imply that $\mathrm{rot}(P) - \mathrm{rot}(Q) = 4$. Using clockwise and anticlockwise st-paths, we again define a notion of spirality.

Definition 4.40. *Let* $(G, \mathcal{E})$ *be a 2-legged series-parallel plane 3-graph that admits a (not necessarily valid) ortho-radial representation* $\mathcal{T}$ *of* G*. Given a clockwise st-path* P*, the* spirality of $\mathcal{T}$ $\sigma : \Theta(G, \mathcal{E}) \to \mathbb{Z}$ *is defined as*

$$\sigma(\mathcal{T}) = \mathrm{rot}(P).$$

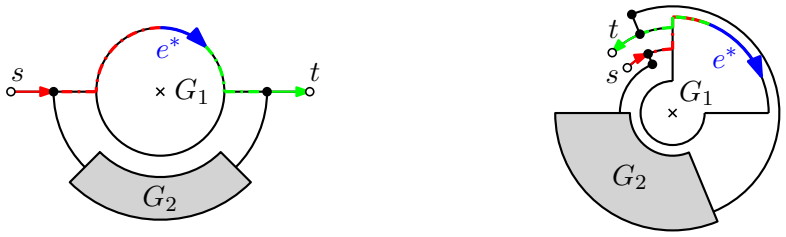

Figure 4.25: Two parallel connections both with $\sigma(G_1) = -2$. On the left, the leg vertices of G_1 point radially outwards and on the right they both point anticlockwise. Using the dashed reference paths, the oriented spiralities are $(1, -1)$ for the left graph and $(0, -2)$ for the right graph.

The well-definedness of Definition 4.40 is a direct implication of Lemma 4.38. Also, the above definition of spirality is a natural extension to the one for orthogonal representations. If a given ortho-radial representation would be simply an orthogonal one, meaning $f_c = f_o$, then every st-path is clockwise (as well as anticlockwise), and the spirality as defined in Definition 4.40 is again simply the rotation of any st-path in the graph. In an ortho-radial representation $\mathcal{T}$, Lemma 4.38 implies for an anticlockwise st-path Q that $\sigma(\mathcal{T}) = \text{rot}(Q) - 4$.

The definition of spirality alone is not descriptive enough. See for example Figure 4.25. In both case the spirality of G_1 is -2. But the left ortho-radial representation has its legs pointing radially outwards, while the right ortho-radial representation has legs pointing anticlockwise. This difference has a direct effect on the conditions to form the ortho-radial representation of G_1 as well as on the parallel connection with G_2. We formally define the difference between the two representations via the label of the edges $\vec{e^s}$ and $\vec{e^t}$.

Definition 4.41. *Let $(G, \mathcal{E})$ be a 2-legged series-parallel plane 3-graph that admits a (possibly invalid) ortho-radial representation $\mathcal{T}$ of G with reference edge e^*. We define the* oriented spirality $(\sigma^s, \sigma^t) \in \mathbb{Z} \times \mathbb{Z}$ *to be*

$$(\sigma^s, \sigma^t) = (\ell(\vec{e^s}), \ell(\vec{e^t})).$$

The oriented spirality represents the label of e^s when entering G as well as the label of e^t when exiting G. So if P_s is a reference path from e^* to e^s and if P_t is a reference path from e^* to e^t, then $(\sigma^s, \sigma^t) = (\text{dir}(e^*, P_s, \vec{e^s}), \text{dir}(e^*, P_t, \vec{e^t}))$. See again Figure 4.25, where the left graph has an oriented spirality of $(1, -1)$. The red path makes one right turn and with the fourth case in the definition of combinatorial directions we know $\sigma^s = 1$. Similarly, the green path makes one left turn and with the first case in the definition of combinatorial directions $\sigma^t = -1$ follows. In the right graph the oriented spirality is $(0, -2)$ because the red path to e^s has rotation 0 and again the fourth case implies $\ell(\vec{e^s}) = 0$. The green path has also rotation 0, but here the third case in the definition of combinatorial embeddings applies, and we get $\ell(\vec{e^t}) = -2$.

The same reference paths for defining the oriented spirality can be used to calculate the label for $\overleftarrow{e^s}$ and $\overleftarrow{e^t}$, and it follows that $\ell(\overleftarrow{e^s}) = \sigma^s - 2$ and $\ell(\overleftarrow{e^t}) = \sigma^t + 2$. Oriented spirality and normal spirality stand in close connection to each other as the following lemma shows.

Lemma 4.42. *Let $(G, \mathcal{E})$ be a 2-legged series-parallel plane 3-graph that admits a (not necessarily valid) ortho-radial representation $\mathcal{T}$ of G with reference edge e^* and oriented spirality (σ^s, σ^t). Then $\sigma(\mathcal{T}) = \sigma^t - \sigma^s$.*

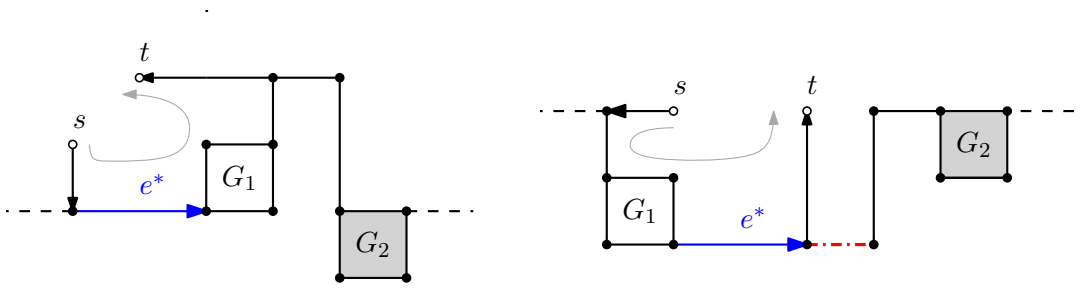

Figure 4.26: On the left, an ortho-radial representation with oriented spirality $(-1, 2)$ consisting of two subgraphs G_1 and G_2 and on the right a depiction of an incomplete ortho-radial representation of the same graph with oriented spirality $(2, -1)$, with a missing red edge. Both representations have spirality -3 indicates by the gray arrow.

Proof. Let P be an st-path of G traversing e^*. If P is a clockwise st-path, then

$$\begin{aligned}\sigma(\mathcal{T}) = \operatorname{rot}(P) &= \operatorname{rot}(P[e^s, e^*]) + \operatorname{rot}(P[e^*, e^t]) \\ &= -\operatorname{dir}(\vec{e^*}, \overline{P(e^s, e^*)}, \vec{e^s}) + \operatorname{dir}(\vec{e^*}, P(e^*, e^t), \vec{e^t}) = \sigma^t - \sigma^s,\end{aligned}$$

and if P is an anticlockwise st-path, then

$$\begin{aligned}\sigma(\mathcal{T}) = \operatorname{rot}(P) - 4 &= \operatorname{rot}(P[e^s, e^*]) + \operatorname{rot}(P[e^*, e^t]) - 4 \\ &= -\operatorname{dir}(\overleftarrow{e^*}, \overline{P(e^s, e^*)}, \vec{e^s}) - 2 + \operatorname{dir}(\overleftarrow{e^*}, P(e^*, e^t), \vec{e^t}) - 2 = \sigma^t - \sigma^s.\end{aligned}$$

□

Figure 4.26 depicts another example to further see the importance of oriented spirality and its connection to normal spirality. On the left is a valid ortho-radial representation with spirality -3 and oriented spirality $(-1, 2)$. At least for this graph, every clockwise st-path traverses G_1 and every anticlockwise st-path traverses G_2. A clockwise st-path has rotation -3, while an anticlockwise st-path has rotation 1. On the right, the same graph with the same spirality of -3 is shown, but with oriented spirality $(-2, 1)$. The representation is not an ortho-radial representation indicated by the red gap, where the two subgraphs are not joined together. In fact, there is no valid ortho-radial representation of this graph having oriented spirality $(-2, 1)$. This further confirms that the notion of oriented spirality conveys information that is required to form a correct recursive algorithm. Next, we connect relative labels to normal labels depending on the oriented spirality of the representation.

Lemma 4.43. *Let ϕ be a $\mathcal{P}$-node containing f_c, let G be its induced graph, G_1,G_2 be the induced graphs of the children of ϕ such that G admits a (not necessarily valid) ortho-radial representation $\mathcal{T}$ with oriented spirality (σ^s, σ^t) and reference edge e^*. If G_1 does not contain f_c, then it follows for every edge $\vec{e}$ of G_1 that*

$$\ell_{s_1}(e) = \ell(\vec{e}) - \sigma^s - r_1^s.$$

If G_2 does not contain f_c, then it follows for every edge $\overleftarrow{e}$ in G_2 that

$$\ell_{s_2}(e) = \ell(\overleftarrow{e}) - \sigma^s + 2 - r_2^s.$$

Proof. First, suppose that G_1 does not contain f_c and let $\vec{e}$ be an edge in G_1. Then $\ell_{s_1}(e) = \mathrm{dir}(\vec{e_1^s}, P, \vec{e})$ for a reference path P in G_1 and

$$\mathrm{dir}(\vec{e_1^s}, P, \vec{e}) = \underbrace{r_1^s + \mathrm{dir}(\vec{e_1^s}, P, \vec{e})}_{= \mathrm{dir}(\vec{e^s}, e_1^s + P, \vec{e}) = \ell(\vec{e}) - \sigma^s} - r_1^s = \ell(\vec{e}) - \sigma^s - r_1^s.$$

Now suppose that the induced representation of G_2 is an orthogonal representation and let $\vec{e}$ be an edge in an st-path of G_2. Then $\ell_{s_2}(e) = \mathrm{dir}(\vec{e_2^s}, P, \overleftarrow{e}) + 2$ for a reference path P in G_2 and

$$\mathrm{dir}(\vec{e_2^s}, P, \overleftarrow{e}) = \underbrace{r_2^s + \mathrm{dir}(\vec{e_2^s}, P, \overleftarrow{e})}_{= \mathrm{dir}(\vec{e^s}, e_2^s + P, \overleftarrow{e}) = \ell(\overleftarrow{e}) - \sigma^s} - r_2^s = \ell(\overleftarrow{e}) - \sigma^s - r_2^s.$$

□

We now start with the marked $\mathcal{P}$-node where f_c is created and describe which structures the child nodes require to form a valid ortho-radial representation.

Lemma 4.44. *Let ϕ be a marked $\mathcal{P}$-node where f_c is created and let G be its induced subgraph such that G admits a (not necessarily valid) ortho-radial representation $\mathcal{T}$ of G with oriented spirality (σ^s, σ^t) and spirality $\sigma(\mathcal{T})$. Let $\mathcal{H}_1$ and $\mathcal{H}_2$ be the induced orthogonal representations of the child nodes of ϕ. Then the following holds.*

$$\sigma(\mathcal{H}_1) = \sigma(\mathcal{T}) - r_1^s - r_1^t$$
$$\sigma(\mathcal{H}_2) = 4 + \sigma(\mathcal{T}) - r_2^s - r_2^t$$

Proof. Let P be an st-path of G traversing G_1. Then $P[e_1^s, e_1^t]$ is an st-path of G_1. It then holds that

$$\sigma(\mathcal{H}_1) = \mathrm{rot}(P[e_1^s, e_1^t]) = \underbrace{\mathrm{rot}(P[e_1^s, e_1^t]) + r_1^s + r_1^t}_{= \mathrm{rot}(P) = \sigma(\mathcal{T})} - r_1^t - r_1^s = \sigma(\mathcal{T}) - r_1^s - r_1^t.$$

Now let Q be an st-path of G traversing G_2. Then $Q[e_2^s, e_2^t]$ is an st-path of G_2 and Lemma 4.38 implies $\mathrm{rot}(Q) = 4 + \sigma(\mathcal{H})$. It now holds that

$$\sigma(\mathcal{H}_2) = \mathrm{rot}(P[e_2^s, e_2^t]) = \underbrace{\mathrm{rot}(P[e_2^s, e_2^t]) + r_2^s + r_2^t}_{= \mathrm{rot}(Q) = 4 + \sigma(\mathcal{H})} - r_2^s - r_2^t.$$

□

Definition 4.45. *Let $(G, \mathcal{E})$ be a 2-legged series-parallel plane 3-graph with terminals s and t admitting a (possibly invalid) ortho-radial representation. We define the* clockwise subgraphs $\overrightarrow{G}$ *to be the subgraph described by the union of all clockwise st-paths having terminals s and t.*

$$\overrightarrow{G} = \bigcup \{P \in \mathcal{P}_{st}(G) \mid P \text{ clockwise}\}$$

We define the anticlockwise subgraphs $\overleftarrow{G}$ *to be the reverse of the subgraph described by the union of all anticlockwise st-paths having flipped terminals t and s.*

$$\overleftarrow{G} = \overline{(\bigcup \{P \in \mathcal{P}_{st}(G) \mid P \text{ anticlockwise}\})}$$

Moreover, we define the strict clockwise and strict anticlockwise subgraphs $\overrightarrow{G}^-$ and $\overleftarrow{G}^-$ *to be their non-strict counterparts excluding the two legs e^s and e^t of G.*

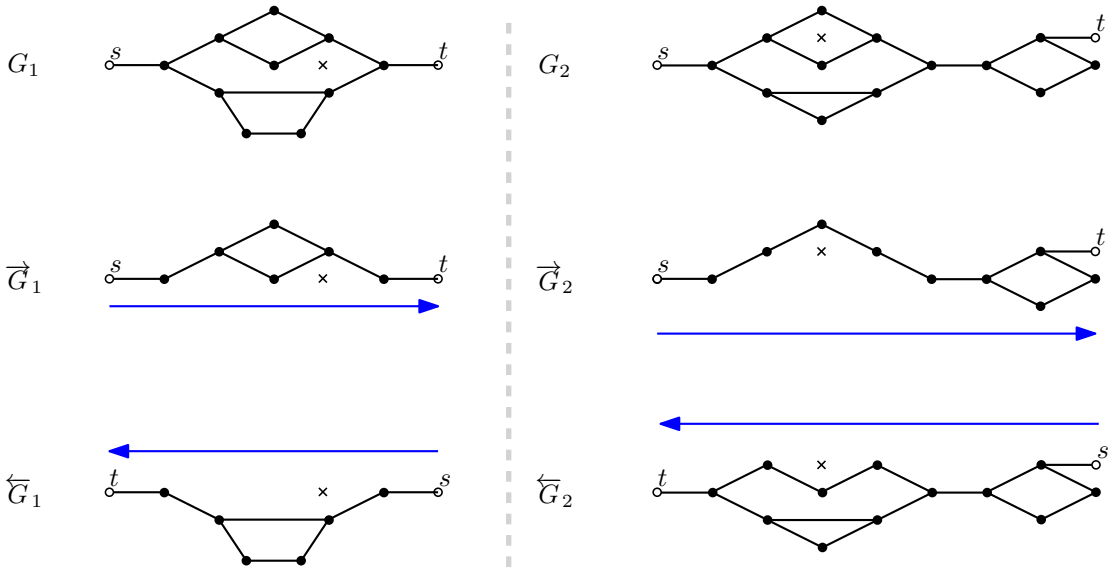

Figure 4.27: Two 2-legged series-parallel plane 3-graphs together with their clockwise subgraphs $\overrightarrow{G}$ and their anticlockwise subgraphs $\overleftarrow{G}$.

See Figure 4.27 for an example of a graph and its clockwise and anticlockwise subgraphs. It is clear to see that $\overrightarrow{G}$ and $\overleftarrow{G}$ are both 2-legged series-parallel plane 3-graph and that $\overrightarrow{G}^-$ and $\overleftarrow{G}^-$ are in general only series-parallel plane 3-graphs. As both $\overrightarrow{G}$ and $\overleftarrow{G}$ do not contain the central face, their induced representations are always simple orthogonal representations. If G is a parallel composition, then $\overrightarrow{G}^-$ and $\overleftarrow{G}^-$ are both 2-legged and disjoint. If G is the induced graph of a marked $\mathcal{P}$-node with subgraphs G_1 and G_2, then $\overrightarrow{G}^- = G_1$ and $\overleftarrow{G}^- = \overleftarrow{G_2}$, and a simple essential cycle always traverses $\overrightarrow{G}^-$ and $\overleftarrow{G}^-$ in their correct orientation.

Lemma 4.46. *Let ϕ be a $\mathcal{P}$-node containing f_c and let G be its induced subgraph such that it admits a (not necessarily valid) ortho-radial representation $\mathcal{T}$ of G with oriented spirality (σ^s, σ^t), spirality $\sigma(\mathcal{T})$, and reference edge e^*. Let G_1 and G_2 be the induced subgraphs of the children of ϕ.*

If G_1 does not contain f_c and has the structure $[s_1, s_1^z, s_1^{lr}]$, then every st-path of $\overrightarrow{G}^- = G_1$ contains a positively-labelled edge / a negatively-labelled edge if and only if one of the matching conditions hold.

a positive label	a negative label
$\sigma^s + r_1^s > 0$,	$\sigma^s + r_1^s < 0$,
$\sigma^t - r_1^t > 0$,	$\sigma^t - r_1^t < 0$,
$\sigma(\mathcal{H}_1) \in s_1(-(\sigma^s + r_1^s) + 1)$	$\sigma(\mathcal{H}_1) \in s_1(-(\sigma^s + r_1^s) - 1)$

Moreover, every st-path of $\overrightarrow{G}^-$ contains both a positively- and a negatively-labelled edge if and only if one of the following conditions hold.

$$\sigma^s + r_1^s > 0 \wedge (\sigma^t - r_1^t < 0 \vee \sigma(\mathcal{H}_1) \in s_1(-(\sigma^s + r_1^s) - 1))$$

$$\sigma^s + r_1^s < 0 \wedge (\sigma^t - r_1^t > 0 \vee \sigma(\mathcal{H}_1) \in s_1(-(\sigma^s + r_1^s) + 1))$$

$$(\sigma^s + r_1^s = \sigma^t - r_1^t = 0) \wedge s_1^{lr} = 1$$

If G_2 does not contain f_c and has the structure $[s_2, s_2^z, s_2^{lr}]$, then every st-path of $\overleftarrow{G}^- = \overline{G_2}$ contains a positively-labelled edge / a negatively-labelled edge if and only if one of the matching conditions hold.

a positive label	a negative label
$\sigma^s - 2 + r_2^s > 0$,	$\sigma^s - 2 + r_2^s < 0$,
$\sigma^t + 2 - r_2^t > 0$,	$\sigma^t + 2 - r_1^t < 0$,
$\sigma(\mathcal{H}_2) \in s_2(-(\sigma^s - 2 + r_2^s) + 1)$	$\sigma(\mathcal{H}_2) \in s_2(-(\sigma^s - 2 + r_2^s) - 1)$

Moreover, every st-path of $\overleftarrow{G}^-$ contains both a positively- and a negatively-labelled edge if and only if one of the following conditions hold.

$$\sigma^s - 2 + r_2^s > 0 \wedge (\sigma^t + 2 - r_2^t < 0 \vee \sigma(\mathcal{H}_2) \in s_2(-(\sigma^s - 2 + r_2^s) - 1))$$

$$\sigma^s - 2 + r_2^s < 0 \wedge (\sigma^t + 2 - r_2^t > 0 \vee \sigma(\mathcal{H}_2) \in s_2(-(\sigma^s - 2 + r_2^s) + 1))$$

$$(\sigma^s - 2 + r_2^s = \sigma^t + 2 - r_2^t = 0) \wedge s_2^{lr} = 1$$

Proof. First, suppose G_1 does not contain f_c and let P be an arbitrary st-path of $\overrightarrow{G}^- = G_1$. Then P must traverse the two oriented legs $\vec{e}_1^{\,s}$ and $\vec{e}_1^{\,t}$. The label of $\vec{e}_1^{\,s}$ and $\vec{e}_1^{\,t}$ computed relative to the label of $\vec{e}^{\,s}$ and $\vec{e}^{\,t}$ are

$$\ell(\vec{e}_1^{\,s}) = \ell(\vec{e}^{\,s}) + r_1^s = \sigma^s + r_1^s \qquad\qquad \ell(\vec{e}_1^{\,t}) = \ell(\vec{e}^{\,t}) - r_1^t = \sigma^t - r_1^t.$$

On the one hand, suppose that P contains at least one positively-labelled edge. If either $\ell(\vec{e}_1^{\,s})$ or $\ell(\vec{e}_1^{\,t})$ is positive, then the respective inequality in the condition holds. If neither of these edges have a positive label, then there must exist another edge $\vec{e}$ inside G_1 having a positive label. Lemma 4.43 implies that $\ell_{s_1}(e) = \ell(\vec{e}) - \sigma^s - r_1^s \geq -(\sigma^s + r_1^s) + 1$. As P was arbitrary, it follows that $\sigma(\mathcal{H}_1) \in s_1(-(\sigma^s + r_1^s) - 1)$ and the third condition holds. On the other hand, suppose that a condition for a positive label is fulfilled. It is easy to see that either $\ell(\vec{e}_1^{\,s}) > 0$ or $\ell(\vec{e}_1^{\,t}) > 0$, or due to $\sigma(\mathcal{H}_1) \in s_1(-(\sigma^s + r_1^s) - 1)$ there exists an edge $\vec{e}$ in P with a positive label.

The equality proof for having a negative label in the path through G_1 follows analogously, only here the inequality signs flip and for an edge $\vec{e}$ in P with a negative label we instead have $\ell_{s_1}(e) = \ell(\vec{e}) - \sigma^s - r_1^s \leq -(\sigma^s + r_1^s) - 1$. The proof for paths taken through $\overleftarrow{G}^-$ also follows analogously with $\overleftarrow{G}^- = \overline{G_2}$ when using the labels for $\overleftarrow{e}_2^{\,s}$ and $\overleftarrow{e}_2^{\,t}$ as well as the connection between relative and normal labels of edges inside G_2 from Lemma 4.43.

Now to the proof for having both a negatively- and a positively-labelled edge in the path through G_1 or G_2. We only consider the case where the edges are present in G_1 since the other case again follows analogously. We make a case distinction.

Case 1: $\ell(\vec{e}_1^{\,s}) = \ell(\vec{e}_1^{\,t}) = 0$. This is equivalent to $\sigma^s + r_1^s = \sigma^t - r_1^t = 0$. Lemma 4.43 also implies $\ell_{s_1}(e_1^t) = 0$ and therefore $\sigma(\mathcal{H}_1) = 0$. Having both a positively-labelled and a negatively-labelled edge is then equivalent to $s_1^{lr} = 1$, again using Lemma 4.43.

Case 2: $\ell(\vec{e}_1^{\,s}) \neq 0$ or $\ell(\vec{e}_1^{\,t}) \neq 0$. Without loss of generality, let $\ell(\vec{e}_1^{\,s}) > 0$. Then every traversed path already has a positively-labelled edge as shown above. If now $\ell(\vec{e}_1^{\,s}) < 0$, then G_1 already has both a positively- and a negatively-labelled edge. Otherwise, the step value condition has to hold as shown above. □

Lemma 4.47. *Let ϕ be a marked $\mathcal{P}$-node creating the central face where its two child nodes ϕ_1, ϕ_2 are both rectilinear-plane and have the structures $[s_1, s_1^z, s_1^{lr}]$ and $[s_2, s_2^z, s_2^{lr}]$, respectively. Then the induced graph G of ϕ has a valid ortho-radial representation $\mathcal{T}$ with oriented spirality (σ^s, σ^t) and normal spirality $\sigma(\mathcal{T}) = x$ if and only if the matching conditions hold.*

$\sigma^s \backslash \sigma^t$	≤ -3	-2	-1	0	≥ 1
≥ 3	$x+2 \in s_1(0)$, $x+4 \in s_2(0)$	$-\sigma^s \in s_1(0)$, $-\sigma^s+2 \in s_2(0)$	$-\sigma^s \in s_1(0)$, $-\sigma^s+2 \in s_2(0)$ or $-\sigma^s+1 \in s_1(-\sigma^s)$, $-\sigma^s+3 \in s_2(0)$ or $-\sigma^s+1 \in s_1(0)$, $-\sigma^s+2 \in s_2(-\sigma^s+1)$	*See Table 4.1*	*See Table 4.1*
2	$\sigma^t \in s_1(0)$, $\sigma^t+2 \in s_2(0)$	$-2 \in s_1(0)$	$-1 \in s_1(0)$, $0 \in s_2(-1)$ or $-2 \in s_1(0)$	$-1 \in s_1(-2)$ or $1 \in s_2(-1)$	*See Table 4.1*
1	$\sigma^t \in s_1(0)$, $\sigma^t+2 \in s_2(0)$ or $\sigma^t+1 \in s_1(1)$, $\sigma^t+3 \in s_2(0)$ or $\sigma^t+1 \in s_1(0)$, $\sigma^t+2 \in s_2(1)$	$-1 \in s_1(0)$, $0 ins_1(1)$ or $-2 \in s_1(0)$	*Lemma 4.23*	$1 \in s_2(0)$, $0 \in s_1(-1)$ or $2 \in s_2(0)$	$\sigma^t+2 \in s_2(0)$, $\sigma^t \in s_1(0)$ or $\sigma^t+1 \in s_2(-1)$, $\sigma^t-1 \in s_1(0)$ or $\sigma^t+1 \in s_2(0)$, $\sigma^t \in s_1(-1)$
0	*See Table 4.2*	$1 \in s_2(2)$ or $-1 \in s_1(1)$	$1 \in s_2(0)$, $0 \in s_1(1)$ or $2 \in s_2(0)$	$2 \in s_2(0)$	$\sigma^t+2 \in s_2(0)$, $\sigma^t \in s_1(0)$
≤ -1	*See Table 4.2*	*See Table 4.2*	$-\sigma^s+2 \in s_2(0)$, $-\sigma^s \in s_1(0)$ or $-\sigma^s+1 \in s_2(-\sigma^s+2)$, $-\sigma^s-1 \in s_1(0)$ or $-\sigma^s+1 \in s_2(0)$, $-\sigma^s \in s_1(-\sigma^s+1)$	$-\sigma^s+2 \in s_2(0)$, $-\sigma^s \in s_1(0)$	$x+2 \in s_2(0)$, $x \in s_1(0)$

Table 4.1: Conditions for the case $\sigma^s \geq 2$ and $\sigma^t \geq 0$.

x	Condition
$x \leq -4$	$x+1 \in s_1(-\sigma^s), x+3 \in s_2(0)$ or $x+2 \in s_1(-\sigma^s), x+4 \in s_2(0)$ or $x+2 \in s_1(0), x+3 \in s_2(-\sigma^s+1)$
$x = -3$	$-2 \in s_1(-\sigma^s)$ or $0 \in s_2(-\sigma^s+1), -1 \in s_1(0)$
$x = -2$	$-1 \in s_1(-\sigma^s)$ or $1 \in s_2(-\sigma^s+1)$
$x = -1$	$2 \in s_2(-\sigma^s+1)$ or $0 \in s_1(-\sigma^s), 1 \in s_2(0)$
$x \geq 0$	$x+1 \in s_1(-\sigma^s), x+2 \in s_2(0)$ or $x+1 \in s_1(0), x+3 \in s_2(-\sigma^s+1)$ or $x \in s_1(0), x+2 \in s_2(-\sigma^s)$

Proof. We will use Lemmas 4.44 and 4.46 with the set of all possible rotation combinations $[r_1^s, r_1^t, r_2^s, r_2^t]$ to proof each condition. Again, some rotation combinations never result in an ortho-radial representation. It is impossible to have $r_1^s = r_2^s = 0$, as this will create an illegal angle assignment around the leg-vertex of s. The same is true for the leg-vertex of t, where $r_1^t = r_2^t = 0$ is invalid. So values where r_1^s and r_1^t are -1 give total freedom to the choice of r_2^s and r_2^t. Any other value restricts this choice.

Table 4.2: Conditions for the case $\sigma^s \leq 0$ and $\sigma^t \leq -2$.

x	Condition
$x \geq 0$	$x+3 \in s_2(-\sigma^s+2), x+1 \in s_1(0)$ or $x+2 \in s_2(-\sigma^s+2), x \in s_1(0)$ or $x+2 \in s_2(0), x+1 \in s_1(-\sigma^s+1)$
$x=-1$	$2 \in s_2(-\sigma^s+2)$ or $0 \in s_1(-\sigma^s+1), 1 \in s_2(0)$
$x=-2$	$1 \in s_2(-\sigma^s+2)$ or $-1 \in s_1(-\sigma^s+1)$
$x=-3$	$-2 \in s_1(-\sigma^s+1)$ or $0 \in s_2(-\sigma^s+2), -1 \in s_1(0)$
$x \leq -4$	$x+3 \in s_2(-\sigma^s+2), x+2 \in s_1(0)$ or $x+3 \in s_2(0), x+1 \in s_1(-\sigma^s+1)$ or $x+4 \in s_2(0), x+2 \in s_1(-\sigma^s+2)$

Lemma 4.44 connects the spirality of the ortho-radial representation to the spiralities of $\mathcal{H}_1$ and $\mathcal{H}_2$ and therefore imply the necessary spirality of G_1 and G_2. To ensure the validity of the ortho-radial representation we use Lemma 4.46. Here we can exclude the case where one simple essential cycle only contains zero-labelled edges. The oriented spirality must have the value $(1,-1)$ for this to happen and this case is already covered in Lemma 4.23. So from now on we assume $(\sigma^s, \sigma^t) \neq (1,-1)$. For a formed representation to be valid, every simple essential cycle must now always contain a positively- as well as a negatively-labelled edge. Due to ϕ being the marked node, we know $\overrightarrow{G}^- = G_1$ and $\overleftarrow{G}^- = \overline{G_2}$, and Lemma 4.46 applies for both subgraphs. If the correct conditions hold such that Lemma 4.46 implies that every simple essential cycle contains in one subgraph a positively-labelled edge and in either the same or the other subgraph a negatively-labelled edge, then the representation is valid. The inverse of this statement is not obviously true. There may exist a simple essential cycle C having only non-negative edges in G_1 and only non-positive edges in G_2 as well as a simple essential cycle C' having only non-positive edges in G_1 and only non-negative edges in G_2. This case is not covered by Lemma 4.46. But would these two simple essential cycles exist, then there would also exist two other simple essential cycles, obtained by combining the parts of C and C' that only have non-negative or non-positive labels. These new cycles are then invalid and would be a contradiction to the validity of the representation. Therefore, Lemma 4.46 also implies the conditions given a valid ortho-radial representation.

The proof will now work as follows. Given a fixed oriented spirality (σ^s, σ^t), the process of finding conditions for G_1 and G_2 that are equivalent to G admitting a valid ortho-radial representation is now to test all possible and valid rotation combinations. Per combination, one in general also has to check all possible distributions of positive and negative labels over the two subgraphs as explained above. Lemmas 4.44 and 4.46 then give the required conditions. Over all these, one has to pick the set of the least strict conditions for G_1 and G_2. These conditions combined are then equivalent to G admitting a valid ortho-radial representation with a specific oriented spirality. To find these least strict conditions, we have to minimize per subgraph either the spirality conditions $|\sigma(\mathcal{H}_1)|$ and $|\sigma(\mathcal{H}_2)|$ from Lemma 4.44 or, if in a specific circumstance one of the step value conditions in Lemma 4.46 have to be used, we have to minimize this step value expression instead of the spirality condition. According to Lemma 4.32, a step value expression $z \in s(y)$ is least strict if $|y|$ as well as $|y-z|$ assume their minimum values. We deliberately ignore the case in Lemma 4.46 where a subgraph has both a positive and a negative label in every st-path if the left-right step value s^{lr} is non-zero for this subgraph. As we will see later, this possibility always results in a stricter condition compared to the ones not using s^{lr}. In summary, the terms that may have to be minimized are the following.

1. The spirality condition for G_1:

$$|\sigma(\mathcal{H}_1)| = \sigma(\mathcal{T}) - r_1^s - r_1^t| = |x - r_1^s - r_1^t| \tag{4.29}$$

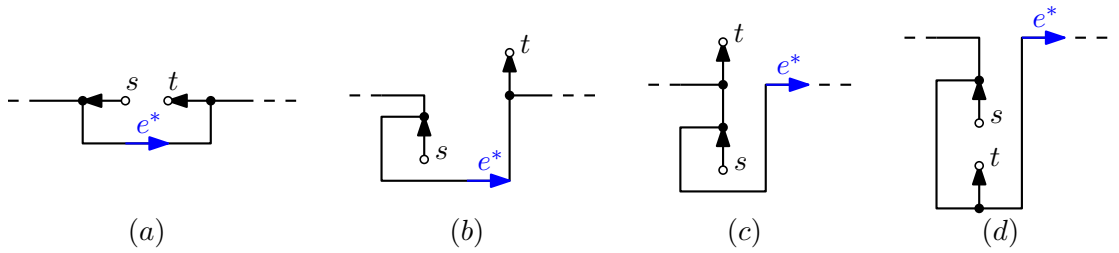

Figure 4.28: Parallel connections around f_c with different oriented spiralities, where the subgraphs are implied by the bent lines between the leg vertices. The oriented spiralities are $(2,-2)$ for (a) and $(3,-1)$ for (b), (c), and (d).

2. The step value condition $\sigma(\mathcal{H}_1) \in s_1(-(\sigma^s + r_1^s) + 1)$ for a positive label in G_1:

$$|-(\sigma^s + r_1^s) + 1| = |1 - \sigma^s - r_1^s| \tag{4.30}$$
$$|-(\sigma^s + r_1^s) + 1 - (\sigma^t - \sigma^s - r_1^s - r_1^t)| = |1 - \sigma^t + r_1^t| \tag{4.31}$$

3. The step value condition $\sigma(\mathcal{H}_1) \in s_1(-(\sigma^s + r_1^s) - 1)$ for a negative label in G_1:

$$|-(\sigma^s + r_1^s) - 1| = |1 + \sigma^s + r_1^s| \tag{4.32}$$
$$|-(\sigma^s + r_1^s) - 1 - (\sigma^t - \sigma^s - r_1^s - r_1^t)| = |1 + \sigma^t - r_1^t| \tag{4.33}$$

4. The spirality condition for G_2:

$$|\sigma(\mathcal{H}_2)| = |4 + \sigma(\mathcal{T}) - r_2^s - r_2^t| = |4 + x - r_2^s - r_2^t| \tag{4.34}$$

5. The step value condition $\sigma(\mathcal{H}_2) \in s_2(-(\sigma^s - 2 + r_2^s) + 1)$ for a positive label in G_2:

$$|-(\sigma^s - 2 + r_2^s) + 1| = |3 - \sigma^s - r_2^s| \tag{4.35}$$
$$|-(\sigma^s - 2 + r_2^s) + 1 - (4 + \sigma^t - \sigma^s - r_2^s - r_2^t)| = |1 + \sigma^t - r_2^t| \tag{4.36}$$

6. The step value condition $\sigma(\mathcal{H}_2) \in s_2(-(\sigma^s - 2 + r_2^s) - 1)$ for a negative label in G_2:

$$|-(\sigma^s - 2 + r_2^s) - 1| = |1 - \sigma^s - r_2^s| \tag{4.37}$$
$$|-(\sigma^s - 2 + r_2^s) - 1 - (4 + \sigma^t - \sigma^s - r_2^s - r_2^t)| = |3 + \sigma^t - r_2^t| \tag{4.38}$$

If no single rotation combination minimizes all the terms for a given oriented spirality, then there exist multiple independent optimal conditions (for example the ones for the case $(3,-2)$). We will now reduce the number of oriented spiralities that have to be checked manually to a finite amount via a case distinction based on the oriented spiralities.

Case 1: $\sigma^s \geq 2$ and $\sigma^t \leq -2$. See Figure 4.28a for an example with $\sigma^s = 2$ and $\sigma^t = -2$. Then no matter which rotation combination is chosen, the inequalities $\sigma^s + r_1^s > 0$ and $\sigma^t - r_1^t < 0$ hold. Lemma 4.46 then implies that G_1 always contains both a positive and a negative label in every st-path no matter the rotation combination and the only conditions to minimize are the spirality conditions. The values $r_1^s = r_1^t = -1$ and $r_2^s = r_2^t = 0$ minimize these in Equations (4.29) and (4.34) to $|\sigma(\mathcal{H}_1)| = |x + 2|$ and $|\sigma(\mathcal{H}_2)| = |x + 4|$. The existence of a valid ortho-radial representation is therefore equivalent to $x + 2 \in s_1(0)$ and $x + 4 \in s_2(0)$.

Case 2: $\sigma^s \geq 3$ and $\sigma^t = -1$. Then no matter which rotation combination is chosen, $\sigma^s + r_1^s > 0$ and Lemma 4.46 implies that G_1 always contains a positive label in every st-path.

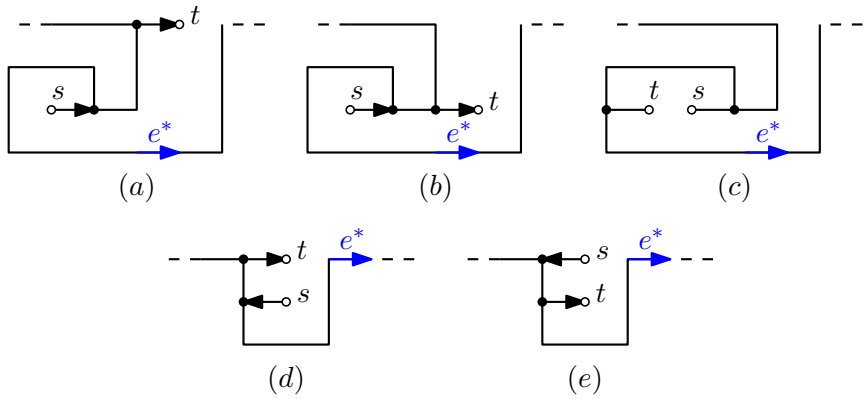

Figure 4.29: Parallel connections around f_c with different oriented spiralities, where the subgraphs are implied by the bent lines between the leg vertices. The spiralities are $(4, 0)$ for $(a), (b)$, and (c) as well as $(2, 0)$ for (d) and (e).

Using $r_1^s = -1$ minimizes Equations (4.29) and (4.32) while leaving a choice for the value of r_2^s. Negative labels may now occur in G_1 or G_2.

Suppose the negative labels also occur in G_1. Then there are two possibilities for this to happen. First, $r_1^t = 0$ (see Figure 4.28b), which implies $\sigma^t - r_1^t = -1 < 0$ in Lemma 4.46. Here, the spirality for G_1 is $\sigma(\mathcal{H}_1) = -1 - \sigma^s - r_1^s - r_1^t = -\sigma^s$, which implies $-\sigma^s \in s_1(0)$. Regarding the spirality condition for G_2, $r_2^t = 0$ would be invalid and the values $r_2^s = 0, r_2^t = 1$ now minimize Equation (4.34) to $4 + \sigma^t - \sigma^s - 1 = 2 - \sigma^s$. Second, $r_1^t = -1$ (see Figure 4.28c), which implies $\sigma^t - r_1^t = 0$ and according to Lemma 4.46 the step value condition for negative labels in G_1 must hold. This implies $-\sigma^s + 1 = \sigma(\mathcal{H}_1) \in s_1(-(\sigma^s + r_1^s) - 1) = s_1(-\sigma^s)$. Regarding the spirality conditions for G_2, the optimal values $r_2^s = r_2^t = 0$ minimize the required spirality of G_2 to $4 + \sigma^t - \sigma^s = 3 - \sigma^s$. In total, we get the conditions $-\sigma^s \in s_1(0), 2 - \sigma^s \in s_2(0)$ or $-\sigma^s + 1 \in s_1(-\sigma^s), -\sigma^s + 3 \in s_2(0)$.

Now suppose the negative labels occur in G_2 as seen in Figure 4.28d. As the conditions for this case do not depend on r_1^t, the value of $r_1^t = -1$ can be chosen to minimize Equation (4.29) and $-\sigma^s + 1 \in s_1(0)$ follows. Because $\sigma^s - 2 + r_2^s \geq 1 + r_2^s \geq 0$ and $\sigma^t + 2 - r_2^t = 1 - r_2^t \geq 0$, Lemma 4.46 implies that the only possibility for G_2 to have negative labels is the step value condition. Choosing $r_2^s = 0$ and $r_2^t = 1$ minimizes Equations (4.37) and (4.38) to $\sigma^s - 1$ and 1, respectively. In total, we get the conditions $-\sigma^s + 1 \in s_1(0)$ and $2 - \sigma^s \in s_2(-\sigma^s + 1)$.

Case 3: $\sigma^s \geq 2$ and $\sigma^t \geq 0$. Again, no matter which rotation combination is chosen, $\sigma^s + r_1^s > 0$ and Lemma 4.46 implies that G_1 always contains a positive label in every st-path. But due to $\sigma^t - r_1^t \geq 0$, $\sigma^s - 2 + r_2^s = r_2^s \geq 0$, and $\sigma^t + 2 - r_2^t \geq 1$, Lemma 4.46 implies that a negative label in every st-path is only achievable with a step value condition. If the condition for G_1 is used, then values $r_1^s = -1$ and $r_1^t = 0$ minimize Equations (4.32) and (4.33). If the condition for G_2 is used, then values $r_2^s = 0$ and $r_2^t = 1$ minimize Equations (4.37) and (4.38). To find optimal values for the spirality condition, we have to make a further case distinction.

Case 3a: $x = \sigma^t - \sigma^s \leq -4$. Then Equations (4.29) and (4.34) assume their minimum values with $r_1^s = r_1^t = -1$ and $r_2^s = r_2^t = 0$, respectively. The optimal rotation values for the spirality conditions are now partly incompatible with the optimal values for the step value conditions. Based on which step value condition is used and based on the theoretically optimal rotation values for each separate condition we get the following minimal conditions.

1. G_1 contains the negative edges. Then the combination $r_1^s = -1, r_1^t = 0, r_2^s = 0, r_2^t = 1$ implies the conditions $x + 1 \in s_1(-\sigma^s)$ and $x + 3 \in s_2(0)$ (see Figure 4.29a

with $\sigma^s = 3, \sigma^t = 0$) while the combination $r_1^s = r_1^t = -1, r_2^s = r_2^t = 0$ implies the conditions $x + 2 \in s_1(-\sigma^s)$ and $x + 4 \in s_2(0)$ (see Figure 4.29b).

2. G_2 contains the negative edges (see Figure 4.29c). Then the combination $r_1^s = r_1^t = -1, r_2^s = 0, r_2^t = 1$ implies the optimal conditions $x+2 \in s_1(0)$ and $x+3 \in s_2(-\sigma^s + 1)$.

Case 3b: $x = \sigma^t - \sigma^s \geq 0$. Then Equations (4.29) and (4.34) assume their minimum values with $r_1^s = r_1^t = 0$ and $r_2^s = r_2^t = 1$. The optimal rotations for the spirality conditions are again partly incompatible with the optimal values for the step value conditions. Based on which step value condition is used and based on the theoretically optimal rotation values for each separate condition we get the following minimal conditions.

1. G_1 contains the negative edges. The combination $r_1^s = -1, r_1^t = 0, r_2^s = r_2^t = 1$ implies the optimal condition $x + 1 \in s_1(-\sigma^s)$ and $x + 2 \in s_2(0)$

2. G_2 contains the negative edges. The combination $r_1^s = -1, r_1^t = 0, r_2^s = 0, r_2^t = 1$ implies the condition $x+1 \in s_1(0)$ and $x+3 \in s_2(-\sigma^s + 1)$ while the combination $r_1^s = r_1^t = 0, r_2^s = r_2^t = 1$ implies the condition $x \in s_1(0)$ and $x + 2 \in s_2(-\sigma^s)$.

Case 3c: $x = \sigma^t - \sigma^s \in [-3, -1]$. Based on the actual value of x, different rotational values may be more optimal. If $x = -3$, then Equation (4.29) becomes $|-3 - r_1^s - r_1^t|$ and is minimal with $r_1^s = r_1^t = -1$ while Equation (4.34) becomes $|4 - 3 - r_2^s - r_2^t|$ and is minimal with $r_2^s = 0, r_2^t = 1$ or $r_2^s = 1, r_2^t = 0$. If $x = -2$, then Equation (4.29) becomes $|-2 - r_1^s - r_1^t|$ and is minimal with $r_1^s = r_1^t = -1$ while Equation (4.34) becomes $|4 - 2 - r_2^s - r_2^t|$ and is minimal with $r_2^s = r_2^t = 1$. Finally, if $x = -1$, then Equation (4.29) becomes $|-1-r_1^s-r_1^t|$ and is minimal with $r_1^s = -1, r_1^t = 0$ or $r_1^s = 0, r_1^t = -1$ while Equation (4.34) becomes $|4 - 1 - r_2^s - r_2^t|$ and is minimal with $r_2^s = r_2^t = 1$. The following shows the optimal conditions based on x and where the negative labels are contained. Figures 4.29d and 4.29e shows the case $x = -2$ with $\sigma^t = 2$ and $\sigma^s = 0$.

- If $x = -3$ and G_1 contains the negative labels, then the combination $(r_1^s, r_1^t, r_2^s, r_2^t) = (-1, 0, 0, 1)$ implies the optimal condition $-2 \in s_1(-\sigma^s)$ (and $\sigma(\mathcal{H}_2) = 0$).
- If $x = -3$ and G_2 contains the negative labels, then the combination $(r_1^s, r_1^t, r_2^s, r_2^t) = (-1, -1, 0, 1)$ implies the optimal condition $-1 \in s_1(0)$ and $0 \in s_2(-\sigma^s + 1)$.
- If $x = -2$ and G_1 contains the negative labels, then the combination $(r_1^s, r_1^t, r_2^s, r_2^t) = (-1, 0, 1, 1)$ implies the optimal condition $-1 \in s_1(-\sigma^s)$ (and $\sigma(\mathcal{H}_2) = 0$).
- If $x = -2$ and G_2 contains the negative labels, then the combination $(r_1^s, r_1^t, r_2^s, r_2^t) = (-1, -1, 0, 1)$ implies the optimal condition $1 \in s_2(-\sigma^s + 1)$ (and $\sigma(\mathcal{H}_1) = 0$).
- If $x = -1$ and G_1 contains the negative labels, then the combination $(r_1^s, r_1^t, r_2^s, r_2^t) = (-1, 0, 1, 1)$ implies the optimal condition $0 \in s_1(-\sigma^s)$ and $1 \in s_2(0)$.
- If $x = -1$ and G_2 contains the negative labels, then the combination $(r_1^s, r_1^t, r_2^s, r_2^t) = (-1, 0, 0, 1)$ implies the optimal condition $2 \in s_2(-\sigma^s + 1)$ (and $\sigma(\mathcal{H}_1) = 0$).

Case 4: $\sigma^s = 1$ and $\sigma^t \leq -3$. Then no matter which rotation combination is used, $\sigma^t - r_1^t < 0$ and Lemma 4.46 implies that G_1 contains a negative label in every st-path.

If also the positively-labelled edges are present in G_1, then there are two possible optimal rotation combinations to check. The first case is $r_1^s = 0$, which implies $\sigma^s + r_1^s > 0$ in Lemma 4.46. The minimal conditions for G_1 and G_2, namely Equations (4.29) and (4.34), are then met with $r_1^s = 0, r_1^t = -1, r_2^s = 1, r_2^t = 0$, and it follows that $\sigma^t \in s_1(0)$ and $\sigma^t + 2 \in s_2(0)$. The second case is $r_1^s = -1$ (see Figure 4.30a), which implies $\sigma^s + r_1^s \leq 0$ and the step value condition must hold for G_1. Then the equations Equations (4.30), (4.31) and (4.34) are minimized with the combination $r_1^s = r_1^t = -1, r_2^s = r_2^t = 0$, and it follows that $\sigma^t + 1 \in s_1(1)$ as well as $\sigma^t + 3 \in s_2(0)$.

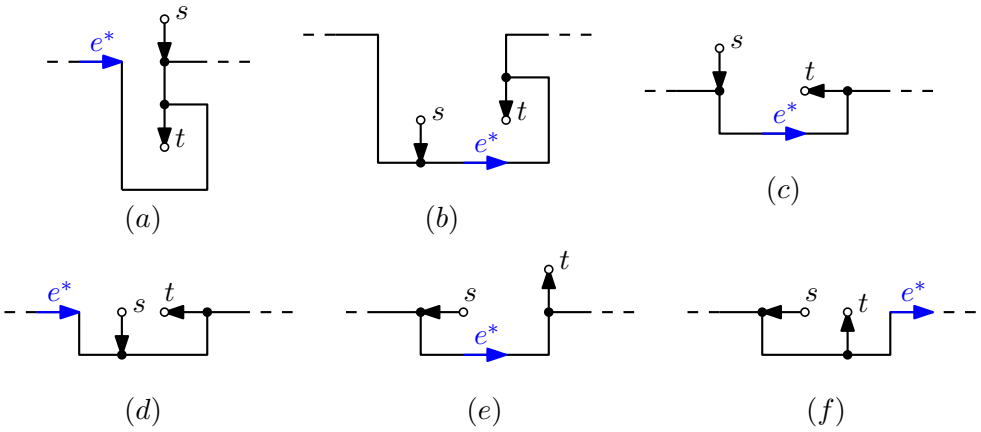

Figure 4.30: Parallel connections around f_c with different oriented spiralities. The subgraphs are implied by the bent lines between the leg vertices. The oriented spiralities are $(1,-3)$ for (a) and (b), $(1,-2)$ for (c) and (d), as well as $(2,-1)$ for (e) and (f).

If the positively-labelled edges are present in G_2, then due to $\sigma^s - 2 + r_2^s = r_2^s - 1 \leq 0$ and $\sigma^t + 2 - r_2^t \leq -1 - r_2^t < 0$, Lemma 4.46 implies that the step value condition must hold. Equations (4.29), (4.37) and (4.38) are minimized by $r_1^s = r_1^t = -1, r_2^s = 1, r_2^t = 0$, and it follows that $x+2 \in s_1(0)$ and $x+3 \in s_2(1)$. Figure 4.30b shows this case for $\sigma^s = 1, \sigma^t = -3$.

Case 5: $(\sigma^s, \sigma^t) \in \{(2,-1),(1,-2)\}$. By simple minimization over all possible rotation combinations, the optimal conditions

- for $(\sigma^s, \sigma^t) = (2,-1)$ are $-1 \in s_1(0)$ and $0 \in s_2(-1)$ with $r_1^s = r_1^t = -1, r_2^s = 0, r_2^t = 1$ as well as $-2 \in s_2(0)$ (and $\sigma(\mathcal{H}_2) = 0$) with $r_1^s = -1, r_1^t = 0, r_2^s = 0, r_2^t = 1$ (see Figures 4.30e and 4.30f).
- for $(\sigma^s, \sigma^t) = (1,-2)$ are $-1 \in s_1(0)$ and $0 \in s_2(1)$ with $r_1^s = r_1^t = -1, r_2^s = 1, r_2^t = 0$ as well as $-2 \in s_2(0)$ (and $\sigma(\mathcal{H}_2) = 0$) with $r_1^s = 0, r_1^t = -1, r_2^s = -1, r_2^t = 0$ (see Figures 4.30c and 4.30d).

Case 6: All other oriented spirality values are simply the mirrored results of some oriented spirality covered in a previous case. This is due to the conditions in Lemmas 4.44 and 4.46 being point symmetric around the oriented spirality $(1,-1)$. The mirroring swaps the conditions for G_1 and G_2, changes the sign of constants, and transforms σ^t into $\sigma^t + 2$ as well as σ^s into $\sigma^s - 2$.

The last open point is to show that choosing the s^{lr} condition in Lemma 4.46 always results in a stricter condition compared to every other option. The total condition for G_1 having both a positive and a negative label in every st-path using the s^{lr} step value is

$$(\sigma^s + r_1^s = \sigma^t - r_1^t = 0) \wedge s_1^{lr} = 1.$$

There are only the oriented spiralities $(\sigma^s, \sigma^t) \in \{(1,0),(0,-1),(0,0)\}$, where G_1 may satisfy this condition. The oriented spirality $(1,-1)$ would also fall under this case, but again this case is already covered in Lemma 4.23. Lemma 4.34 shows that s_1^{lr} implies $0 \in s_1(-1)$ and $0 \in s_1(1)$ as well as $-2 \in s_1(0)$ and $2 \in s_1(0)$. These inequalities can be used in every of the three cases above to reduce the condition back to an already covered one and the same applies for G_2. □

Lemma 4.47 states the required properties to form a valid ortho-radial representation around f_c with a desired oriented spirality. In Section 4.1 all further recursion steps

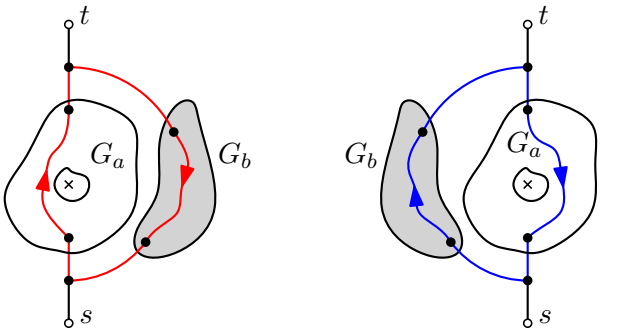

Figure 4.31: A parallel-connection where the child G_a still contains f_c and G_a is either the left child (a) or the right child (b). The blue and red cycles indicate new essential cycles at the parallel composition. The red cycle traverses $\overrightarrow{G_a}$ and the blue cycle traverses $\overleftarrow{G_a}$.

after this point where trivial according to Lemma 4.24. This fact relies on the ortho-radial representation being st-upwards, but since this is no longer the case in the current situation, handling later $\mathcal{P}$-nodes in the recursion is more complicated. If an ortho-radial representation is extended at a $\mathcal{P}$-node with subgraphs G_a and G_b such that the subgraph G_a still contains f_c, then G_a either is the right or the left child as shown in Figure 4.31. If G_a is the left child, then new essential cycles are formed with an st-path of $\overrightarrow{G_a}$ and an st-path of $\overleftarrow{G_b}$. Conversely, if G_a is the right child, new essential cycles are formed with an st-path of $\overleftarrow{G_a}$ and an st-path of G_b. To ensure that every essential cycle is valid we have to know which labels are present in these paths. Different to orthogonal representations, we now define step values over a specific ortho-radial representation instead of over the general graph. Moreover, as the reference edge e^* already exists, the step values are simply markings indicating the existence of edges with positive, negative, or 0 labels. For this, we define the *step set* $\mathbb{S} = \{0, -, +, \pm\}$ and the following definition shows how a step value gets assigned.

Definition 4.48. *Let $\mathcal{T}$ be a (not necessarily valid) ortho-radial representation of a 2-legged series-parallel plane 3-graph G and let H be an oriented (not necessarily 2-legged) series-parallel subgraph of G not containing f_c. We then define the* step value $\int(H)$ *of the subgraph H as*

$$\int(H) = \begin{cases} 0 & \text{if } \exists P \in \mathcal{P}_{st}(H) : \forall e \in P : \ell(\vec{e}) = 0, \\ - & \text{if } \forall P \in \mathcal{P}_{st}(H) : \exists e \in P : \ell(\vec{e}) < 0 \wedge \exists P \in \mathcal{P}_{st}(H) : \ \forall e \in P : \ell(\vec{e}) \leq 0, \\ + & \text{if } \forall P \in \mathcal{P}_{st}(H) : \exists e \in P : \ell(\vec{e}) > 0 \wedge \exists P \in \mathcal{P}_{st}(H) : \ \forall e \in P : \ell(\vec{e}) \geq 0, \\ \pm & \text{if } \forall P \in \mathcal{P}_{st}(H) : \exists e, e' \in P : \ell(\vec{e}) < 0, \ell(\vec{e'}) > 0 \end{cases}$$

The ortho-radial representation $\mathcal{T}$ then has the clockwise step value $s^c = \int(\overrightarrow{G})$ *and the* anticlockwise step value $s^a = \int(\overleftarrow{G})$. *The pair (s^c, s^a) is called the* step value pair *of $\mathcal{T}$.*

The $\int(\cdot)$ function is well-defined because on the one hand, at most one case may apply at a time and on the other hand, if neither the $-$,$+$, nor $\pm$-case applies, the 0-case must hold.

Considering the situation in Figure 4.31b, if G_c has a step value $s^a = -$, every simple essential cycle needs a positively-labelled edge in its path taken through G_b for the cycle to be valid. The following lemma shows that either s^c or s^a must have the $\pm$ step value and that therefore only one side may create invalid essential cycles.

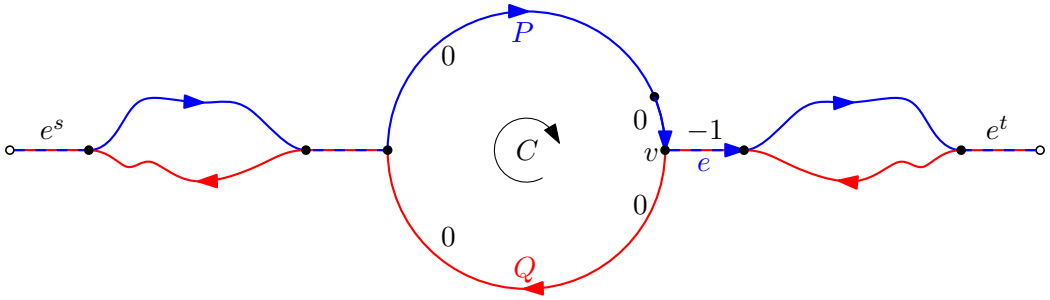

Figure 4.32: An st-path P of $\overrightarrow{G}$ and an st-path Q of $\overleftarrow{G}$. The essential cycle C only has label 0 and the edge e in P therefore has label -1.

Lemma 4.49. *Let $(G, \mathcal{E})$ be a 2-legged orthoradial-plane series-parallel 3-graph and let $\mathcal{T}$ be a valid ortho-radial representation of G with step value pair (s^c, s^a). Then either $s^c = \pm$ or $s^a = \pm$.*

Proof. For s^c and s^a to both not be $\pm$ there are a few cases to check. Assume $s^c = +$ and $s^a = -$. Due to $s^c = +$ and $\vec{e^t}$ being contained in every st-path of $\overrightarrow{G}$, Definition 4.48 implies $\ell(\vec{e^t}) \geq 0$. Similarly, $s^a = -$ and $\overleftarrow{e^t}$ being contained in every st-path of $\overleftarrow{G}$ implies $\ell(\vec{e^t}) + 2 = \ell(\overleftarrow{e^t}) \leq 0$. This forms the contradiction $0 \leq \ell(\vec{e^t}) \leq -2$. If $s^c = -$ and $s^a = +$ is assumed, then a similar contradiction can be formed with $\vec{e^s}$. Now Assume $s^c = s^a = +$. Then $\overrightarrow{G}$ as well as $\overleftarrow{G}$ do not contain edges with a negative label. Let C be a simple essential cycle in G. Then C consists of a subpath of an st-path P of $\overrightarrow{G}$ and a subpath of an st-path Q of $\overleftarrow{G}$ and as both do not contain negative labels, C also does not contain negative labels. The only option for C to still be valid is to only contain edge with label 0. Let v be the vertex in C connected with a path to e^t and let e be the first edge of this path. See Figure 4.32 for an illustration. Both P and Q must traverse e lying outside C. As all edges have label 0 in C, the only option for the label of $\vec{e}$ is $\ell(\vec{e}) = -1$, which is a contradiction to $s^c = +$. A similar contradiction, only at the meeting vertex close to e^s and with flipped signs, follows if $s^c = s^a = -$ is assumed. Finally, if $s^c = 0$, then $\ell(\vec{e^s}) = \ell(\vec{e^t}) = 0$. This implies $\ell(\overleftarrow{e^s}) = -2$ and $\ell(\overleftarrow{e^t}) = 2$ and $s^a = \pm$ follows. Similarly, if $s^a = 0$, $s^c = \pm$ follows. □

When expanding an ortho-radial representations at a $\mathcal{S}$ and $\mathcal{P}$-nodes, the step value pairs of the new representation are dependent on the step value pairs of the representations of the child nodes. For this, we consider the step value set $\mathbb{S}$ to be a *lattice* with the partial order $\{0 < -, 0 < +, + < \pm, - < \pm\}$ as shown in Figure 4.33. A lattice has two operations. The join operation $(s \sqcup s')$, representing the least upper bound of two elements and the meet operation $(s \sqcap s')$, representing the greatest lower bound of two elements. The next definition provides tables exactly showing what each operator does and specifically limits the domain of the meet operator. This is done to better represent what these operators mean in the context of step values, which then the lemma afterwards will explain in detail. It turns out that the join operator indicates the step value of a non-2-legged series-composition in relation to the step values of its children, and the meet operator indicates the same for a non-2-legged parallel-composition. For such a parallel composition, the excluded step value combinations never occur.

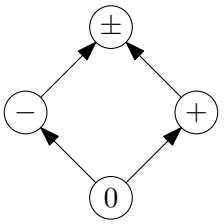

Figure 4.33: The lattice structure of the step value set $\mathbb{S}$.

Definition 4.50. *The operators* $\sqcap : \mathbb{S}^2 \backslash \{(+,-),(-,+),(0,+),(0,-),(-,0),(+,0)\} \to \mathbb{S}$ *and* $\sqcup : \mathbb{S}^2 \to \mathbb{S}$ *are defined as*

$\sqcap$	0	−	+	±
0	0			0
−		−		−
+			+	+
±	0	−	+	±

$\sqcup$	0	−	+	±
0	0	−	+	±
−	−	−	±	±
+	+	±	+	±
±	±	±	±	±

Lemma 4.51. *Let $\mathcal{T}$ be a (not necessarily valid) ortho-radial representation of a 2-legged series-parallel plane 3-graph G with reference edge e^*. Let H be an oriented (not necessarily 2-legged) series-parallel subgraph of G not containing f_c. If H is a non-2-legged series connection of subgraphs H_1 and H_2, then*

$$\int(H) = \int(H_1) \sqcup \int(H_2).$$

If H is a non-2-legged parallel connection of subgraphs H_1 and H_2, then

$$\int(H) = \int(H_1) \sqcap \int(H_2).$$

Proof. Let P be an st-path of H. If H is a series connection, then $P = P_1 + P_2$, where P_1 and P_2 are st-paths of H_1 and H_2. Definition 4.48 then implies the equality. If H is a parallel connection, then H_1 and H_2 are even 2-legged series-parallel plane 3-graphs, as H is a subgraph of G. One first has to proof that the usage of the $\sqcap$-operator is justified, as its definition range does not include every step value combination. Let $e_1^s, e_1^t, e_2^s, e_2^t$ be the legs of H_1 and H_2. We show this by contradiction and first assume that $\int(H_1) = -$ and $\int(H_2) = +$. This implies $\ell(\vec{e_2^t}) \geq 0$ and $\ell(\vec{e_1^t}) \leq 0$. The label of $\vec{e_1^t}$ can also be calculated relative to $\ell(\vec{e_2^t})$ to be

$$\ell(\vec{e_1^t}) = \ell(\vec{e_2^t}) + \mathrm{dir}(\vec{e_2^t}, \emptyset, \vec{e_1^t}) = \underbrace{\ell(\vec{e_2^t})}_{\geq 0} + \underbrace{\mathrm{rot}(e_2^t, e_1^t)}_{\in \{0,-1\}} + 2 > 0.$$

This forms the contradiction $0 < \ell(\vec{e_1^t}) \leq 0$. If $\int(H_1) = +$ and $\int(H_2) = -$ is assumed, then a contradiction can be similarly formed with the labels of e_1^s and e_2^s. Now assume that $\int(H_1) = 0$. Then $\ell(\vec{e_1^s}) = \ell(\vec{e_1^t}) = 0$. With the same argumentation over combinatorial directions above, we can follow for the labels $\vec{e_2^s}$ and $\vec{e_2^t}$ that $\ell(\vec{e_2^s}) > 0$ and $\ell(\vec{e_2^t}) < 0$. This implies $\int(H_2) = \pm$. Similarly, if $\int(H_2) = 0$, then $\int(H_1) = \pm$ follows. Therefore, $\int(H_1) \sqcap \int(H_2)$ is well-defined. Equality is then implied with $\mathcal{P}_{st}(H) = \mathcal{P}_{st}(H_1) \cup \mathcal{P}_{st}(H_2)$ and Definition 4.48. □

See Figure 4.34a for an example of how Lemma 4.51 can be applied. Here, the parallel composition of the two components with step values 0 and ± have in total a step value of $0 \sqcap \pm = 0$. The following series-composition with the edge having step value − results

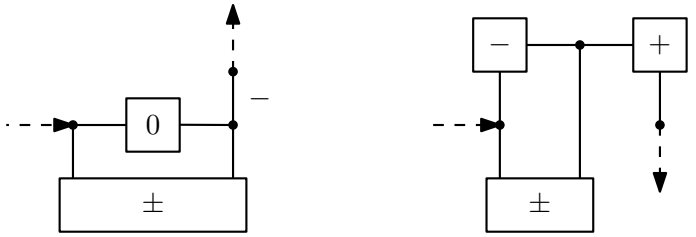

(a) (b)

Figure 4.34: Two 2-legged subgraphs of a bigger ortho-radial representation. The step value of a component of a subgraph is indicated inside the component.

in a total step value of $0 \sqcup - = -$ for the whole subgraph. Similarly, in the example of Figure 4.34b, the parallel composition with step values $-$ and $\pm$ has a step value of $- \sqcap \pm = -$ and in combination with the serially-composed third component the total step value is $- \sqcup + = \pm$.

Similar to orthogonal representations, we keep track of the oriented spiralities and the step values possible for a given tree node ϕ. We define the *structure of a tree node ϕ containing f_c* as a set $\mathcal{S}$ with $((\sigma^s, \sigma^t), (s^c, s^a)) \in \mathcal{S}$ if and only if G admits a valid ortho-radial representation with oriented spirality (σ^s, σ^t) and step value pair (s^c, s^a). Some step value pairs in combination with an oriented spirality make no sense. If for example $\sigma^s > 0$, then $\overrightarrow{G}$ always contains the positively-labelled edge $\vec{e^s}$. For this, we say that $x \in \mathbb{S}$ *allows* $y \in \mathbb{S}$, if there exists a $z \in \mathbb{S}$ with $x \sqcup z = y$. In other words either $x = y$, $x = 0$, or $y = \pm$ holds. We then call a theoretical structure-entry $((\sigma^s, \sigma^t), (s^c, s^a))$ *feasible* if $(\int(\vec{e^s}) \sqcup \int(\vec{e^t}))$ allows s^c and $(\int(\overleftarrow{e^s}) \sqcup \int(\overleftarrow{e^t}))$ allows s^a. The following lemma shows which structure is possible at the marked node creating f_c.

Lemma 4.52. *Let ϕ be a marked orthoradial-plane $\mathcal{P}$-node creating the central face with structure $\mathcal{S}$ where its two child nodes ϕ_1, ϕ_2 have the structure $[s_1, s_1^z, s_1^{lr}]$ and $[s_2, s_2^z, s_2^{lr}]$, respectively. If the induced graph G of ϕ admits a valid ortho-radial representation with oriented spirality (σ^s, σ^t) and normal spirality x, then $((\sigma^s, \sigma^t), (s^c, s^a)) \in \mathcal{S}$ if and only if the matching condition holds.*

(σ^s, σ^t)	(s^c, s^a)	Condition
$(\geq 3, \leq -3)$	$(\pm, \pm)$	Always
$(\geq 3, -2)$	$(\pm, +)$	If the $(\pm, \pm)$ condition does not hold
	$(\pm, \pm)$	$-\sigma^s + 2 \in s_2(-\sigma^s + 1)$ or $-\sigma^s - 1 \in s_1(0),\ -\sigma^s + 1 \in s_2(0)$
$(2, \leq -3)$	$(\pm, -)$	If the $(\pm, \pm)$ condition does not hold
	$(\pm, \pm)$	$\sigma^t + 2 \in s_2(1)$ or $\sigma^t - 1 \in s_1(0),\ \sigma^t + 1 \in s_2(0)$
$(\geq 3, -1)$	$(\pm, +)$	If the $(\pm, \pm)$ condition does not hold
	$(\pm, \pm)$	$-\sigma^s + 1 \in s_1(0),\ -\sigma^s + 2 \in s_2(-\sigma^s + 1)$
$(1, \leq -3)$	$(\pm, -)$	If the $(\pm, \pm)$ condition does not hold
	$(\pm, \pm)$	$\sigma^t + 1 \in s_1(0),\ \sigma^t + 2 \in s_2(1)$
$(\geq 2, \geq 0)$	$(\pm, +)$ $(+, \pm)$	See Table 4.4 and if $(\pm, \pm)$ condition does not hold

	$(\pm,\pm)$	$x+1 \in s_1(-\sigma^s)$, $x+3 \in s_2(-\sigma^s+1)$
$(2,-2)$	$(\pm,+)$	$-1 \in s_2(0)$
	$(\pm,-)$	$-1 \in s_2(0)$
	$(\pm,\pm)$	$-2 \in s_2(0)$
	$(\pm,0)$	$s_2^z = 1$
$(2,-1)$	$(\pm,-)$	If the $(\pm,\pm)$ condition does not hold
	$(\pm,\pm)$	$0 \in s_2(-1)$
$(1,-2)$	$(\pm,-)$	If the $(\pm,\pm)$ condition does not hold
	$(\pm,\pm)$	$0 \in s_2(1)$
$(-1,-1)$	$(\pm,\pm)$	*Always*
$(1,0)$	$(+,\pm)$	If the $(\pm,\pm)$ condition does not hold
	$(\pm,\pm)$	$0 \in s_1(-1)$
$(0,-1)$	$(+,\pm)$	If the $(\pm,\pm)$ condition does not hold
	$(\pm,\pm)$	$0 \in s_1(1)$
$(0,0)$	$(\pm,+)$	$1 \in s_1(0)$
	$(\pm,-)$	$1 \in s_1(0)$
	$(\pm,\pm)$	$2 \in s_1(0)$
	$(\pm,0)$	$s_1^z = 1$
$(\leq 0,\leq -2)$	$(-,\pm)$ $(\pm,-)$	See Table 4.5 and if $(\pm,\pm)$ condition does not hold
	$(\pm,\pm)$	$x+3 \in s_2(-\sigma^s+2)$, $x+1 \in s_1(-\sigma^s+1)$
$(1,\geq 1)$	$(+,\pm)$	If the $(\pm,\pm)$ condition does not hold
	$(\pm,\pm)$	$\sigma^t+1 \in s_2(0)$, $\sigma^t \in s_1(-1)$
$(\leq -1,-1)$	$(-,\pm)$	If the $(\pm,\pm)$ condition does not hold
	$(\pm,\pm)$	$-\sigma^s+1 \in s_2(0)$, $-\sigma^s \in s_1(-\sigma^s+1)$
$(0,\geq 1)$	$(+,\pm)$	If the $(\pm,\pm)$ condition does not hold
	$(\pm,\pm)$	$\sigma^t \in s_1(-1)$ or $\sigma^t+3 \in s_2(0)$, $\sigma^t+1 \in s_1(0)$
$(\leq -1,0)$	$(-,\pm)$	If the $(\pm,\pm)$ condition does not hold
	$(\pm,\pm)$	$-\sigma^s \in s_1(-\sigma^s+1)$ or $-\sigma^s+3 \in s_2(0)$, $-\sigma^s+1 \in s_1(0)$
$(\leq -1,\geq 1)$	$(\pm,\pm)$	Always

Proof. As G admits a valid ortho-radial representation with oriented spirality (σ^s,σ^t), the corresponding conditions in Lemma 4.47 hold. The proof is now to again go over every oriented spirality value and either show that a subcondition of Lemma 4.47 implies the given step value or show which additional optimal conditions are required. The approach is similar to Lemma 4.47, where the optimal conditions are the least strict conditions over all possible rotation combinations. We again make a case distinction over only half of the oriented spirality and use the symmetry of ortho-radial representations to imply the other half.

Table 4.4: Conditions for the case $(\geq 2, \geq 0)$.

x	Step value pair $(+, \pm)$	Step value pair $(\pm, +)$
$x \leq -4$	$x+2 \in s_1(0), x+3 \in s_2(-\sigma^s+1)$	$x+1 \in s_1(-\sigma^s), x+3 \in s_2(0)$ or $x+2 \in s_1(-\sigma^s), x+4 \in s_2(0)$
$x = -3$	$-1 \in s_1(0), 0 \in s_2(-\sigma^s+1)$	$-2 \in s_1(-\sigma^s)$
$x = -2$	$1 \in s_2(-\sigma^s+1)$	$-1 \in s_1(-\sigma^s)$
$x = -1$	$2 \in s_2(-\sigma^s+1)$	$0 \in s_1(-\sigma^s), 1 \in s_2(0)$
$x \geq 0$	$x+1 \in s_1(0), x+3 \in s_2(-\sigma+1)$ or $x \in s_1(0), x+2 \in s_2(-\sigma^s)$	$x+1 \in s_1(-\sigma^s), x+2 \in s_2(0)$

Table 4.5: Conditions for the case $(\leq 0, \leq -2)$.

x	Step value pair $(\pm, -)$	Step value pair $(-, \pm)$
$x \geq 0$	$x+2 \in s_2(0), x+1 \in s_1(-\sigma^s+1)$	$x+3 \in s_2(-\sigma^s+2), x+1 \in s_1(0)$ or $x+2 \in s_2(-\sigma^s+2), x \in s_1(0)$
$x = -1$	$1 \in s_2(0), 0 \in s_1(-\sigma^s+1)$	$2 \in s_2(-\sigma^s+2)$
$x = -2$	$-1 \in s_1(-\sigma^s+1)$	$1 \in s_2(-\sigma^s+2)$
$x = -3$	$-2 \in s_1(-\sigma^s+1)$	$0 \in s_2(-\sigma^s+2), -1 \in s_1(0)$
$x =\leq -4$	$x+3 \in s_2(0), x+1 \in s_1(-\sigma+1)$ or $x+4 \in s_2(0), x+2 \in s_1(-\sigma^s+2)$	$x+3 \in s_2(-\sigma^s-2), x+2 \in s_1(0)$

Case 1: $(1, -1)$. Then $\ell(\vec{e^s}) = 1,\ \ell(\overleftarrow{e^s}) = -1,\ \ell(\vec{e^t}) = -1$, and $\ell(\overleftarrow{e^t}) = 1$. So $\overrightarrow{G}$ as well as $\overleftarrow{G}$ always contain both a positive and a negative label in every of their st-paths.

Case 2: $(\geq 3, \leq -3)$. Then $\ell(\vec{e^s}) \geq 3,\ \ell(\overleftarrow{e^s}) \geq 1,\ \ell(\vec{e^t}) \leq -3$, and $\ell(\overleftarrow{e^t}) \leq -1$. So $\overrightarrow{G}$ as well as $\overleftarrow{G}$ always contain both a positive and a negative label in every of their st-paths.

Case 3: $(\geq 3, -2)$. Then $\ell(\vec{e^s}) \geq 3,\ \ell(\overleftarrow{e^s}) \geq 1$, and $\ell(\vec{e^t}) = -2$, but $\ell(\overleftarrow{e^t}) = 0$. So $\overrightarrow{G}$ always has both a positive and negative label, while $\overleftarrow{G}$ always has a positive label. If none of the conditions for other step value pairs hold, the step value pair $(\pm, +)$ applies. For $\overleftarrow{G}$ to also have a negative label and in turn G having the step value pair $(\pm, \pm)$, there are now two optimal conditions. Either using a rotation combination of $(-1, -1, 0, 0)$ as in Lemma 4.47 and a step value condition for a negative label in $\overleftarrow{G}$. This results in the extra condition $-\sigma^s+2 \in s_2(-\sigma^s+1)$. Or using $r_2^t = 1$, which implies $\sigma^t+2-r_2^t = \sigma^t+2-1 = -1$ and $\overleftarrow{G}$ contains the negatively-labelled edge $\overleftarrow{e_2^t}$ in every st-path. Equations (4.29) and (4.34) are then minimal with a rotation combination of $(-1, 0, 0, 1)$, and the optimal conditions are $-\sigma^s - 1 \in s_1(0)$ and $-\sigma^s + 1 \in s_2(0)$.

Case 4: $(2, \leq -3)$. Then $\ell(\vec{e^s}) = 2,\ \ell(\overleftarrow{e^s}) = 0$, and $\ell(\vec{e^t}) \leq -3$, but $\ell(\overleftarrow{e^t}) \leq -1$. So $\overrightarrow{G}$ always has both a positive and negative label while $\overleftarrow{G}$ always has a negative label. If none of the conditions for other step value pairs hold, the step value pair $(\pm, -)$ applies. For $\overleftarrow{G}$ to also have a positive label and in turn G having the step value pair $(\pm, \pm)$, there are now two optimal conditions. Using a rotation combination of $(-1, -1, 0, 0)$ as in Lemma 4.47 and a step value condition for a positive label in $\overleftarrow{G}$ results in the extra condition $\sigma^t + 2 \in s_2(1)$. Using $r_2^s = 1$ implies $\sigma^s - 2 + r_2^s = 1$. So $\overleftarrow{G}$ contains the positively-labelled edge $\overleftarrow{e^s}$ in every st-path. Equations (4.29) and (4.34) are then minimal with a rotation combination of $(-1, 0, 0, 1)$ and the optimal conditions are $\sigma^t - 1 \in s_1(0)$ and $\sigma^t + 1 \in s_2(0)$.

Case 5: $(\geq 3, -1)$. Then $\ell(\vec{e^s}) \geq 3,\ \ell(\overleftarrow{e^s}) \geq 1$, $\ell(\vec{e^t}) = -1$, and $\ell(\overleftarrow{e^t}) = 1$. Similar to Case 3, $\overrightarrow{G}$ always has both a positive and negative label and $\overleftarrow{G}$ always has a positive label. If none of the conditions for other step value pairs hold, the step value pair $(\pm, +)$ applies.

For $\overleftarrow{G}$ to also have a negative label and in turn G having the step value pair $(\pm,\pm)$, there is now only the step value condition left, as $\sigma^s - 2 + r_2^s \geq 1 + r_2^s \geq 1$ and $\sigma^t + 2 - r_2^t = 1 - r_2^t \geq 0$. Lemma 4.47 implies that the optimal condition for $\overleftarrow{G}$ having a negative label is $-\sigma^s + 1 \in s_1(0) \wedge -\sigma^s + 2 \in s_2(-\sigma^s + 1)$.

Case 6: $(1, \leq -3)$. Then $\ell(\vec{e^s}) = 1,\ \ell(\overleftarrow{e^s}) - 1,\ \ell(\vec{e^t}) \leq -3$, and $\ell(\overleftarrow{e^t}) \leq -1$. Then $\overrightarrow{G}$ always has both a positive and negative label and $\overleftarrow{G}$ always has a negative label. If none of the conditions for other step value pairs hold, the step value pair $(\pm,-)$ applies. For $\overleftarrow{G}$ to also have a positive label and in turn G having the step value pair $(\pm,\pm)$, there is only the step value condition left, as $\sigma^s - 2 + r_2^s = -1 + r_2^s \leq 0$ and $\sigma^t + 2 - r_2^t \leq -1 - r_2^t \leq -1$. Lemma 4.47 implies that the optimal condition for $\overleftarrow{G}$ having a positive label is $\sigma^t + 1 \in s_1(0) \wedge \sigma^t + 2 \in s_2(1)$.

Case 7: $(\geq 2, \geq 0)$. Then $\ell(\vec{e^s}) \geq 2,\ \ell(\overleftarrow{e^s}) \geq 0$, but $\ell(\vec{e^t}) \geq 0$ and $\ell(\overleftarrow{e^t}) \geq 2$. So $\overrightarrow{G}$ and $\overleftarrow{G}$ always have a positive label. As Lemma 4.49 implies that at least one part of the step value pair must be $\pm$, there are now the three possible step value pairs $(\pm,+),(+,\pm)$ and $(\pm,\pm)$ to check. For any step value pair one of the subgraphs must have a negative label as shown in Lemma 4.47 and a step value condition has to hold for this. We now make a case distinction over the concrete step values.

Case 7a: $(\pm,+)$ or $(+,\pm)$. Lemma 4.47 give the optimal conditions where either $\overrightarrow{G}$ or $\overleftarrow{G}$ contains a negatively-labelled edge. Given that the case $(\pm,\pm)$ does not apply, then exactly these special conditions must hold for the given step value pair.

Case 7b: $(\pm,\pm)$. Here, both $\overrightarrow{G}$ and $\overleftarrow{G}$ must use the step value condition. As shown in Lemma 4.47, the separate optimal rotations are $r_1^s = -1$ and $r_1^t = 0$ for a negative label in $\overrightarrow{G}$ and $r_2^s = 0$ and $r_2^t = 1$ for a negative label in $\overleftarrow{G}$. As these values are also compatible, the single optimal rotation combination is $[r_1^s, r_1^t, r_2^s, r_2^t] = [-1, 0, 0, 1]$, which results in the conditions $x + 1 \in s_1(-\sigma^s)$ and $x + 3 \in s_2(-\sigma^s + 1)$.

Case 8: $(2,-2)$. Then $\ell(\vec{e^s}) = 2,\ \ell(\overleftarrow{e^s}) = 0,\ \ell(\vec{e^t}) = -2$, and $\ell(\overleftarrow{e^t}) = 0$, so $\overrightarrow{G}$ always contains both a positive and a negative label, but the labels in $\overleftarrow{G}$ are totally dependent on the labels in $\overleftarrow{G}^-$. Trying for every step value pair all rotation combinations and computing the required conditions, we get the optimal condition $-1 \in s_2(0)$ for the step value pairs $(\pm,+)$ and $(\pm,-)$, and the condition $-2 \in s_2(0)$ for the step value pair $(\pm,\pm)$. Note again that with $r_2^s = r_2^t = 0$ and $s_2^{lr} = 1$, the step value pair $(\pm,\pm)$ is also achievable (see Lemma 4.47), but again $s_2^{lr} = 1$ implies $-2 \in s_2(0)$ due to Lemma 4.34.

Case 9: $(1,-2)$. Then $\ell(\vec{e^s}) = 1,\ \ell(\overleftarrow{e^s}) = -1,\ \ell(\vec{e^t}) = -2$, and $\ell(\overleftarrow{e^t}) = 0$, so $\overrightarrow{G}$ always contains both a positive and a negative label and $\overleftarrow{G}$ always contains a negative label. The last step value pair $(\pm,\pm)$ now also requires a positive label in $\overleftarrow{G}$. Trying, for every step value pair, all rotation combinations and computing the required conditions we get the optimal condition $0 \in s_2(1)$.

Case 10: $(2,-1)$. Similar to Case 7, $\overrightarrow{G}$ contains both a positive and a negative label, while $\overleftarrow{G}$ always contains a positive label. The condition for the step value pair $(\pm,\pm)$, which requires a negative label also in $\overleftarrow{G}$, can be computed to be $0 \in s_2(-1)$. □

The next lemma discusses an $\mathcal{S}$-node ϕ containing f_c with induced graph G and the connection between the structure of G and the structures of its children G_a and G_b. Intuitively, if G_a is the subgraph still containing f_c, then an ortho-radial representation of G_a is extended by the representation of G_b at one of the legs of G_a. Therefore, G_b can either change σ^s or σ^t of G_a. But as $\overleftarrow{G}$ as well as $\overrightarrow{G}$ traverses G_b, both step values may

be changed no matter at which leg G_b is connected. In any case, each step value of an ortho-radial representation of G must be allowed by the corresponding step value of the representation of its induced subgraph G_a.

Lemma 4.53. *Let ϕ be an $\mathcal{S}$-node containing f_c where the child ϕ_a still contains f_c and is ortholinear-plane while the other child ϕ_b is rectilinear-plane. Also, let $\mathcal{S}_a$ be the structure of ϕ_a and let $[s_b, s_b^z, s_b^{lr}]$ be the structure of ϕ_b. Then ϕ is ortholinear-plane with structure $\mathcal{S}$, and a feasible $((\sigma^s, \sigma^t), (s^c, s^a)) \in \mathcal{S}$ if and only if $((\sigma_a^s, \sigma_a^t), (s_a^c, s_a^a)) \in \mathcal{S}_a$ and with*

$$(d, i) = \begin{cases} (a, -1) & \text{if } s_a^c = \pm, \\ (c, 1) & \text{if } s_a^a = \pm, \end{cases}$$

1. *either $a = 1$, $\sigma^s = \sigma_a^s$, (s_a^c, s_a^a) allows (s^c, s^a), and with $y \coloneqq \sigma^t - \sigma_a^t$ the matching condition holds*
   - *If $(s_a^d, s^d) \in \{(+, \pm), (0, -)\}$, then $y \in s_b(-\sigma_a^t - 2 + i)$.*
   - *If $(s_a^d, s^d) \in \{(-, \pm), (0, +)\}$, then $y \in s_b(-\sigma_a^t + i)$.*
   - *If $(s_a^d, s^d) = (0, 0)$, then $\sigma^t = \sigma_a^t$ and $s_b^z = 1$.*
   - *If $(s_a^d, s^d) = (0, \pm)$, then either $\sigma^t = \sigma_a^t$ and $s_b^{lr} = 1$ or $y \in s_b(-\operatorname{sign}(y))$.*
   - *In any other case $y \in s_b(0)$.*
2. *or $a = 2$ as well as $\sigma^t = \sigma_a^t$, (s_a^c, s_a^a) allows (s^c, s^a), and with $y \coloneqq \sigma_a^s - \sigma^s$ the matching condition holds.*
   - *If $(s_a^d, s^d) \in \{(+, \pm), (0, -)\}$, then $y \in s_b(-\sigma^s - i)$.*
   - *If $(s_a^d, s^d) \in \{(-, \pm), (0, +)\}$, then $y \in s_b(-\sigma^s + 2 - i)$.*
   - *If $(s_a^d, s^d) = (0, 0)$, then $\sigma^s = \sigma_a^s$ and $s_b^z = 1$.*
   - *If $(s_a^d, s^d) = (0, \pm)$, then either $\sigma^t = \sigma_a^s$ and $s_b^{lr} = 1$ or $y \in s_b(y + \operatorname{sign}(y))$.*
   - *If in any other case $y \in s_b(0)$.*

Proof. Let $\mathcal{T}$ be a valid ortho-radial representation of G and let $\mathcal{T}_a$ be the induced valid ortho-radial representation of G_a. Then $\overrightarrow{G_a}$ and $\overleftarrow{G_a}$ are 2-legged series-parallel subgraphs of $\overrightarrow{G}$ and $\overleftarrow{G}$, respectively. Moreover, we know that $\overrightarrow{G}$ is the series composition of $\overrightarrow{G_a}$ and G_b, while $\overleftarrow{G}$ is the series composition of $\overleftarrow{G_a}$ and $\overleftarrow{G_b}$.

We start with the case $a = 1$ and show the " $\Longleftarrow$ "-direction. Let $((\sigma^s, \sigma^t), (s^c, s^a))$ be a feasible structure entry such that $((\sigma_a^s, \sigma_a^t), (s_a^c, s_a^a)) \in \mathcal{S}_a$ with $\sigma^s = \sigma_a^s$ and (s_a^c, s_a^a) allows (s^c, s^a). Let moreover $y = \sigma^t - \sigma_a^t$. Then there exists a valid ortho-radial representation $\mathcal{T}_a$ of G_a with oriented spirality (σ^s, σ_a^t) and step value pair (s_a^c, s_a^a). Combining $\mathcal{T}_a$ with an arbitrary orthogonal representation $\mathcal{H}_b$ of G_b results in a valid ortho-radial representation $\mathcal{T}$ of G, because no new faces or simple essential cycles are formed. Let $P \in \mathcal{P}_{st}(\overrightarrow{G})$ be a clockwise st-path of $\mathcal{T}$. Then $P = P_a + P_b$ with $P_a \in \mathcal{P}_{st}(\overrightarrow{G_a})$ and P_b being an st-path of G_b. If $\mathcal{H}_b$ has the spirality $y = \sigma^t - \sigma_a^t$, then it is clear to see that

$$\sigma(\mathcal{T}) = \operatorname{rot}(P) = \operatorname{rot}(P_a) + \operatorname{rot}(P_b) = \sigma_a^t - \sigma^s + \sigma^t - \sigma_a^t = \sigma^t - \sigma^s.$$

As $\sigma^s = \sigma_a^s$, we know that $\mathcal{T}$ must have the oriented spirality (σ^s, σ^t). The existence of an orthogonal representation of G_b having the spirality y is equivalent to $y \in s_b(0)$. We now make a case distinction over the step value pair (s_a^c, s_a^a) and (s^c, s^a) and change this condition based on the further properties required by the step value pair. Lemma 4.49 implies that

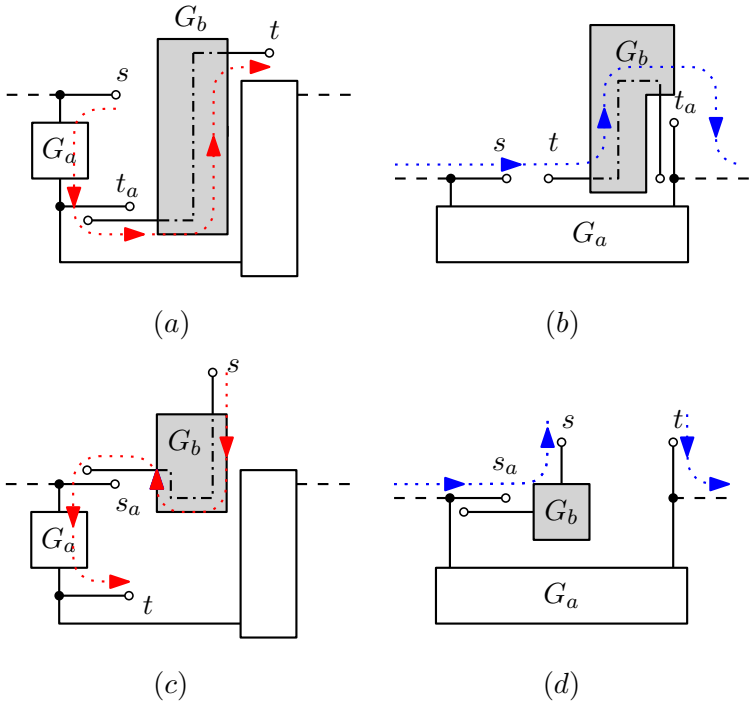

Figure 4.35: Four examples of a series-connection containing f_c, where G_b is either connected at t_a (a, b) or connected at s^a (c, d). The representation of G_b is always chosen such that either s^c, in case of the red paths, or s^a, in case of the blue paths, is improved to $\pm$.

one of the values in each step value pair must be $\pm$. Because (s_a^c, s_a^a) allows (s^c, s^a), the value being $\pm$ must be the same and by the definition of d, we know that s^d as well as s_a^d indicate the part of the step value pair that is not fixed to $\pm$.

Case 1: $s_a^d = +$ and $s^d = \pm$ or $s_a^d = 0$ and $s^d = -$. With $y \in s_b(-\sigma_a^t - 2 + i)$, there exists an orthogonal representation $\mathcal{H}_b$ of G_b fulfilling this step value expression. Let $\mathcal{T}$ be the combined valid ortho-radial representation of $\mathcal{T}_a$ and $\mathcal{H}_b$.

First, suppose $(d, i) = (c, 1)$ and let P be an st-path in $\overrightarrow{G}$. See Figure 4.35a for an example, where the arbitrary st-path P is indicated by the red-dotted line. Then there exists an edge $\vec{e} \in G_b$ contained in P with $\ell_{s_b}(e) = -\sigma_a^t - 2 + i = -\sigma_a^t - 1$. As $\ell(\vec{e_a^t}) = \sigma_a^t$, we know that $\ell(\vec{e}) = \sigma_a^t - \sigma_a^t - 1 = -1$.

Second, suppose $(d, i) = (a, -1)$ and let P be an st-path in $\overleftarrow{G}$. See Figure 4.35b for an example, where the arbitrary st-path P is indicated by the blue-dotted line. Then there exists an edge $\overleftarrow{e} \in G_b$ contained in P with $\ell_{s_b}(e) = -\sigma_a^t - 2 + i = -\sigma_a^t - 3$. As $\ell(\overleftarrow{e_a^t}) = \sigma_a^t + 2$, we know that

$$\ell(\overleftarrow{e}) = \ell(\overleftarrow{e_a^t}) + \mathrm{dir}(\overleftarrow{e_a^t}, P(e_a^t, e), \overleftarrow{e}) = \sigma_a^t + 2 + \ell_{s_b}(e) = \sigma_a^t + 2 - \sigma_a^t - 3 = 2 - 3 = -1.$$

No matter the value of d, there is a negative label in the respective path P while it traverses G_b. Together with s_a^d being $+$ or 0, the step value s^d of $\mathcal{T}$ is $\pm$ or $-$, respectively.

Case 2: $s_a^d = -$ and $s^d = \pm$ or $s_a^d = 0$ and $s^d = +$. Then $y \in s_b(-\sigma_a^t - i)$ holds and there exists an orthogonal representation $\mathcal{H}_b$ of G_b fulfilling this step value expression. Let $\mathcal{T}$ be the combined valid ortho-radial representation of $\mathcal{T}_a$ and $\mathcal{H}_b$.

First, suppose $(d, i) = (c, 1)$ and let P be an st-path in $\overrightarrow{G}$. Then there exists an edge $\vec{e} \in G_b$ contained in P for which $\ell_{s_b}(e) = -\sigma_a^t + i = -\sigma_a^t + 1$ holds. With $\ell(\vec{e_a^t}) = \sigma_a^t$, we know that $\ell(\vec{e}) = \sigma_a^t - \sigma_a^t + 1 = 1$.

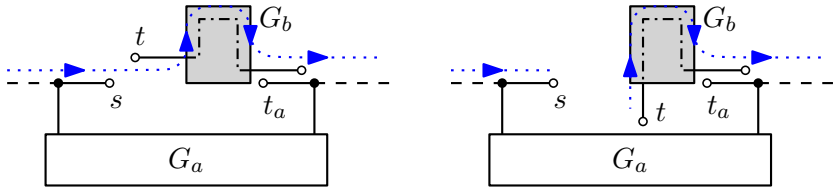

Figure 4.36: Examples of a series-connection containing f_c, where only the st-paths of $\overleftarrow{G_b}$ contain non-zero labels. Both situations result in a step value of $s^a = \pm$.

Second, suppose $(d, i) = (a, -1)$ and let P be an st-path in $\overleftarrow{G}$. Then there exists an edge $\overleftarrow{e} \in G_b$ contained in P for which $\ell_{s_b}(e) = -\sigma_a^t + i = -\sigma_a^t - 1$ holds. With $\ell(\overleftarrow{e_a^t}) = \sigma_a^t + 2$, we know that

$$\ell(\overleftarrow{e}) = \ell(\overleftarrow{e_a^t}) + \ell_{s_b}(e) = \sigma_a^t + 2 - \sigma_a^t - 1 = 2 - 1 = 1.$$

No matter the value of d, there is a positive label in the respective path P while it traverses G_b. Together with s_a^d being $-$ or 0, the step value s^d of $\mathcal{T}$ is $\pm$ or $+$, respectively.

Case 3: $s^d = 0$ and $s_a^d = 0$. Due to $s_a^d = 0$, there exists an st-path P_a of $\overrightarrow{G_a}$ or $\overleftarrow{G_a}$, depending on the concrete value of d that only contains zero-labelled edges. With $s_b^z = 1$ and $\sigma^t = \sigma_a^t$ there also exists an orthogonal representation $\mathcal{H}_b$ of G_b with $\sigma(\mathcal{H}_b) = 0 = y$ and an st-path P_b containing only edges with relative label 0. So the combined valid ortho-radial representation of $\mathcal{T}_a$ and $\mathcal{H}_b$ has the matching st-path $P_a + P_b$ containing only zero-labelled edges. It also has the desired oriented spirality (σ^s, σ^t).

Case 4: $s^d = \pm$ and $s_a^d = 0$. Due to $s_a^d = 0$, we know that $(\sigma_a^s, \sigma_a^t) \in \{(2, -2), (0, 0)\}$. For $\mathcal{T}$ to have the step value $s^d = \pm$, while $s_a^d = 0$, both the positively- and the negatively-labelled edges must be present in G_2.

First, suppose $\sigma^t = \sigma_a^t$ and $s_b^{lr} = 1$. See Figure 4.36a for an example. Then there exists an orthogonal representation $\mathcal{H}_b$ of G_b with $\sigma(\mathcal{H}_b) = 0 = y$ and an edge e with a positive as well as an edge e' with a negative relative label in every st-path. If $(\sigma_a^s, \sigma_a^t) = (2, -2)$, then $\ell(\overleftarrow{e^t}) = 0$ and the only way that $s_a^d = 0$ holds is if $d = a$. For the case $(\sigma_a^s, \sigma_a^t) = (0, 0)$ we similarly know $\ell(\overrightarrow{e^t}) = 0$ and $d = c$. In any case, the labels of the oriented edges e and e' are equal to their relative labels in G_b. Therefore, the combined valid ortho-radial representation $\mathcal{T}$ has the step value $s^d = \pm$ as well as the correct oriented spirality.

Second, suppose $\sigma^t \neq \sigma_a^t$, which implies $y \neq 0$, and $y \in s_b(-\operatorname{sign}(y))$. See Figure 4.36b for an example where $\sigma_a^t = -2$ and $\sigma^t = -3$. If $(\sigma_a^s, \sigma_a^t) = (0, 0)$, it again follows that $\ell(\overrightarrow{e_a^t}) = 0$ and $d = c$. Let P be an st-path in $\overrightarrow{G}$. Then there exists an edge $\overrightarrow{e} \in G_b$ contained in P for which $\ell(\overrightarrow{e}) = \ell(\overrightarrow{e_a^t}) + \ell_{s_b}(e) = -\operatorname{sign}(y)$ holds. With $\ell(\overrightarrow{e^t}) = \ell(\overrightarrow{e_a^t}) + y = y$, the path P contains the edges e and e^t, which combined must have a negative and a positive label. The same holds true for $(\sigma_a^s, \sigma_a^t) = (2, -2)$, only with an st-path in $\overleftarrow{G}$.

Case 5: If none of the above cases apply, then $s^d = s_a^d$ and all the labels for the step value are already contained in $\mathcal{T}_a$. With $y \in s_b(0)$, there exists an orthogonal representation $\mathcal{H}_b$ of G_b such that the combined valid ortho-radial representation has the oriented spirality (σ^s, σ^t).

We now come to the case $a = 2$, where only a rough outline is given on how to adapt the proof for $a = 1$. Let (σ^s, σ^t) be an oriented spirality and (s^c, s^a) be a step value pair and let $((\sigma_a^s, \sigma_a^t), (s_a^c, s_a^a)) \in \mathcal{S}_a$ such that $\sigma^t = \sigma_a^t$, $y = \sigma_a^s - \sigma^s$ and (s_a^c, s_a^a) allows (s^c, s^a). Like for $a = 1$, a valid ortho-radial representation $\mathcal{T}_a$ of G_a following the above structure and an orthogonal representation $\mathcal{H}_b$ with $\sigma(\mathcal{H}_b) = y$ results in a valid ortho-radial representation $\mathcal{T}$

of G with oriented spirality (σ^s, σ^t). To calculate a label of an internal edge in G_b we now calculate it relative from the label of e^s instead of e^t_a. This again results in the desired labels of 1 or -1. See Figure 4.35c for an example where $(d, i) = (c, 1)$ and $\mathcal{T}_a$ only has step value $s^c = +$, while $\mathcal{T}$ has step value $s^c = \pm$. Figure 4.35d depicts the case $(d, i) = (a, -1)$.

Finally, the "$\Longrightarrow$"-direction mostly follows from the fact that in the "$\Longleftarrow$"-direction the step value conditions of G_b for having a positive or negative label in a path was minimal, meaning the step value conditions only implied a label of 1 or -1 for these edges. The existence of an ortho-radial representation of $\mathcal{T}$ with a specific step value pair implies with Lemma 4.51 that the induced representation $\mathcal{T}_a$ has a step value pair that allows the parent's step value pair. A different step value then implies that edges with at least label 1 or -1, depending on the concrete step values, must exist in G_b, which in turn implies the step value conditions. The "$\Longrightarrow$"-direction for the case $s^d = 0$ is a direct implication of the definition of the zero step value since it requires the whole path to have a label of 0. □

The last situation to cover is a $\mathcal{P}$-node containing f_c that is not marked, meaning one if its child nodes still contains f_c. Here, the step value pairs are actually required to imply the existence of a valid ortho-radial representation.

Lemma 4.54. *Let ϕ be a $\mathcal{P}$-node containing f_c with children ϕ_a and ϕ_b where ϕ_a still contains f_c and is orthoradial-plane with structure $\mathcal{S}_a$ and ϕ_b is ortholinear-plane with structure $[s_b, s^z_b, s^{lr}_b]$. Let G be the induced graph of ϕ as well as G_a and G_b be the induced graphs of ϕ_a and ϕ_b. Then G admits a valid ortho-radial representation $\mathcal{T}$ with oriented spirality (σ^s, σ^t) having the rotation combination $[r^s_1, r^t_1, r^s_2, r^t_2]$ if and only if $((\sigma^s_a, \sigma^t_a), (s^c_a, s^a_a)) \in \mathcal{S}_a$ with $\sigma^s_a = \sigma^s + r^s_a$, $\sigma^t_a = \sigma^t - r^t_a$ and the following holds.*

- *If $a = 1$, then $|r^s_1 + r^s_2| + |r^t_1 + r^t_2| + \sigma^t_a - \sigma^s_a \in s_b(0)$ and $s^c_a \sqcup \int(\overline{G_b}) \in \{0, \pm\}$. Moreover, $\mathcal{T}$ has the step value pair*

$$(\int(\vec{e^s}) \sqcup s^c_a \sqcup \int(\vec{e^t}), \int(\overleftarrow{e^s}) \sqcup (s^a_a \sqcap \int(\overline{G_b})) \sqcup \int(\overleftarrow{e^t})).$$

- *If $a = 2$, then $-|r^s_1 + r^s_2| - |r^t_1 + r^t_2| + \sigma^t_a - \sigma^s_a + 4 \in s_b(0)$ and $s^a_a \sqcup \int(G_b) \in \{0, \pm\}$. Moreover, $\mathcal{T}$ has the step value pair*

$$(\int(\vec{e^s}) \sqcup (s^c_a \sqcap \int(G_b)) \sqcup \int(\vec{e^t}), \int(\overleftarrow{e^s}) \sqcup s^a_a \sqcup \int(\overleftarrow{e^t})).$$

Proof. For the "$\Longleftarrow$"-direction, let (σ^s, σ^t) be an oriented spirality, let $r^s_1, r^s_2, r^t_1, r^t_2$ be a rotation combination, let $((\sigma^s_a, \sigma^t_a), (s^c_a, s^a_a)) \in \mathcal{S}$, such that $\sigma^s_a = \sigma^s + r^s_a$ and $\sigma^t_a = \sigma^t - r^t_a$, and let $\mathcal{T}_a$ be a valid ortho-radial representation having the structure-entry above. We make a case distinction over the value a.

Case 1: $a = 1$. We know that an orthogonal representation $\mathcal{H}_b$ of G_b exists with $\sigma(\mathcal{H}_b) = |r^s_1 + r^s_2| + |r^t_1 + r^t_2| + \sigma^t_a - \sigma^s_a$. Let $\mathcal{T}$ be the combined representation of $\mathcal{T}_a$ and $\mathcal{H}_b$. See Figure 4.37a for an example. Then the new face f is created by an anticlockwise st-path of G_a and an st-path of $\overline{G_b}$. So $\mathcal{T}$ is an ortho-radial representation because the rotation of f is

$$\begin{aligned}\operatorname{rot}(f) &= \operatorname{rot}(e^s_2, e^s_1) + \sigma(\mathcal{T}_a) + 4 + \operatorname{rot}(e^t_1, e^t_2) - \sigma(\mathcal{H}_b) \\ &= |r^s_1 + r^s_2| + \sigma^t_a - \sigma^s_a + |r^t_1 + r^t_2| + 4 - \sigma(\mathcal{H}_b) = 4.\end{aligned}$$

The oriented spirality of $\mathcal{T}$ is also $(\sigma^s_a - r^s_1, \sigma^t_a + r^t_1) = (\sigma^s, \sigma^t)$. For $\mathcal{T}$ to be valid, every simple essential cycle in G must be valid. A simple essential cycle contained in G_a is already valid, as $\mathcal{T}_a$ is valid. Any new simple essential cycle C is a concatenation of an

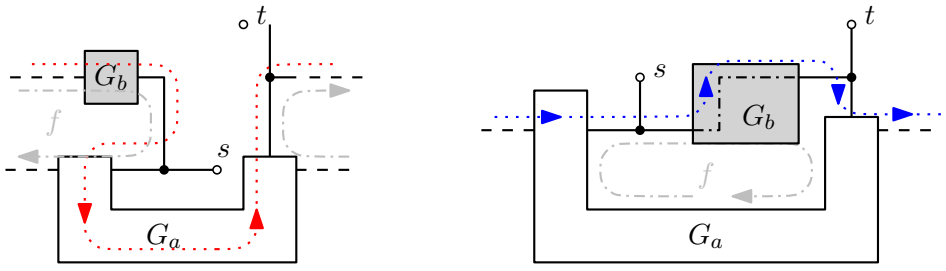

(a) (b)

Figure 4.37: Two parallel compositions of the subgraphs G_a and G_b, where G_a contains f_c, but with a different ordering. On the left, the subgraph containing f_c is G_1 and on the right it is G_2. The gray arrow indicates the rotation of the newly created face f. As $s^c = \pm$ for G_1 on the left, the second subgraph G_2 only requires $-1 \in s(0)$. As $s^a = +$ for G_2 on the right, the subgraph G_1 requires $0 \in s(-1)$.

st-path $P_a \in \overrightarrow{G}^- = \overrightarrow{G_a}$ and an st-path $P_b \in \overleftarrow{G}^- = \overline{G_b}$. Now the step value $s_a^c \sqcup \int(\overline{G_b})$ indicates the step value of the series composition of $\overrightarrow{G}$ and $\overline{G_b}$. If it is the $\pm$ step value (as in Figure 4.37a), then any combination of st-paths P_a and P_b forming a simple essential cycle have somewhere in its path a positively- and a negatively-labelled edge by Definition 4.48. If it is the 0 step value, then either both P_a and P_b have only zero-labelled edges or Lemma 4.16, only using normal instead of relative labels, implies that at least one of the two paths contains both a positively- and a negatively-labelled edge. In any case, every simple essential cycle formed in this way is valid and $\mathcal{T}$ is therefore valid.

Finally, the step value pair of $\mathcal{T}$ is $(s^c, s^a) = (\int(\overrightarrow{G}), \int(\overleftarrow{G}))$ and as ϕ is a $\mathcal{P}$-node, $\overrightarrow{G}$ is the (non-2-legged) series-composition of $e^s, \overrightarrow{G_a}$, and e^t. Lemma 4.51 then implies that

$$\int(\overrightarrow{G}) = \int(\vec{e^s}) \sqcup \int(\overrightarrow{G_a}) \sqcup \int(\vec{e^t}) = \int(\vec{e^s}) \sqcup s_a^c \sqcup \int(\vec{e^t}).$$

Similarly, $\overleftarrow{G}$ is the (non-2-legged) series-composition of e^t, the parallel composition of $\overline{G_b}$ and $\overleftarrow{G_a}$, and then the series-composition of e^s. Again Lemma 4.51 then implies that

$$\int(\overrightarrow{G}) = \int(\overleftarrow{e^s}) \sqcup (\int(\overline{G_b}) \sqcap \int(\overleftarrow{G_a})) \sqcup \int(\overleftarrow{e^t}) = \int(\overleftarrow{e^s}) \sqcup (\int(\overline{G_b}) \sqcap s_a^a) \sqcup \int(\overleftarrow{e^t})$$

Case 2: $a = 2$. We know that an orthogonal representation $\mathcal{H}_b$ of G_b exists with $\sigma(\mathcal{H}_b) = -|r_1^s + r_2^s| - |r_1^t + r_2^t| + \sigma_a^t - \sigma_a^s + 4$ and let $\mathcal{T}$ be the combined representation. See Figure 4.37b for an example. The new face f is created by a reversed clockwise st-path of G_a and an st-path of G_b. So $\mathcal{T}$ is an ortho-radial representation, because the face f has rotation

$$\mathrm{rot}(f) = \mathrm{rot}(e_2^s, e_1^s) - \sigma(\mathcal{T}_a) + \mathrm{rot}(e_1^t, e_2^t) + \sigma(\mathcal{H}_b) = |r_1^s + r_2^s| - \sigma_a^t + \sigma_a^s + |r_1^t + r_2^t| + \sigma(\mathcal{H}_b) = 4.$$

The oriented spirality of $\mathcal{T}$ is also $(\sigma_a^s - r_2^s, \sigma_a^t + r_2^t) = (\sigma^s, \sigma^t)$. Regarding the validity of $\mathcal{T}$, any newly created simple essential cycle C is a concatenation of an st-path $P_a \in \overleftarrow{G}^- = \overleftarrow{G_a}$ and an st-path $P_b \in \overrightarrow{G}^- = G_b$. The validity of such a cycle follows from $s_a^a \sqcup \int(G_b) \in \{0, \pm\}$ similar to the case $a = 1$. The step value pair of $\mathcal{T}$ also follows analogous to case $a = 1$.

Now to the " $\Longrightarrow$ "-direction. Let $\mathcal{T}$ be a valid ortho-radial representation of G with oriented spirality (σ^s, σ^t) and let $\mathcal{T}_a$ be the induced ortho-radial representation of G_a and $\mathcal{H}_b$ be the induced orthogonal representation of G_b. Then $\ell(\vec{e_a^s}) = \ell(\vec{e^s}) + r_a^s = \sigma^s + r_a^s$ and $\ell(\vec{e_a^t}) = \ell(\vec{e^t}) - r_a^t = \sigma^t - r_a^t$. So $\mathcal{T}_a$ has the oriented spirality $(\sigma^s + r_a^s, \sigma^t - r_a^s)$. Now let $a = 1$. With f being the newly created face it follows that

$$4 = \mathrm{rot}(f) = |r_1^s + r_2^s| + \sigma(\mathcal{T}_a) + 4 + |r_1^s + r_2^s| - \sigma(\mathcal{H})$$

and the condition in the statement holds. As $\mathcal{T}$ is also valid, every simple essential cycle C in G is valid. This implies the validity of the induced representation $\mathcal{T}_a$. Let $\mathcal{C}$ be the set of simple essential cycles traversing G_b. Then $C \in \mathcal{C}$ is the concatenation of st-paths $P_a \in \overrightarrow{G}^- = \overrightarrow{G_a}$ and $P_b \in \overleftarrow{G}^- = \overrightarrow{G_b}$. If on the one hand, there exists a simple essential cycle $C^* \in \mathcal{C}$ having only edges with label 0, then there also exist such st-paths in $\overrightarrow{G_a}$ and $\overrightarrow{G_b}$. It follows that $\int(\overrightarrow{G_a}) \sqcup \overrightarrow{G_b} = 0$. If on the other hand, all simple essential cycles in $\mathcal{C}$ contain both a positively- and negatively-labelled edge, then $\int(\overrightarrow{G_a}) \sqcup \overrightarrow{G_b} = \pm$ and in total $\int(\overrightarrow{G_a}) \sqcup \overrightarrow{G_b} \in \{0, \pm\}$. Equality for the step value pair of $\mathcal{T}$ is already shown in the " $\Longleftarrow$ "-direction. The case $a = 2$ for the " $\Longrightarrow$ "-direction follows analogously. □

The following lemma combines the results in Section 4.2 and gives an upper bound to the runtime of creating a structure for a node in the decomposition tree.

Lemma 4.55. *Given a 2-legged series-parallel orthoradial-plane 3-graph $G = (V, E)$ the structure $\mathcal{S}$ of G can be computed in $\mathcal{O}(n^2)$ time.*

Proof. A decomposition tree of G of size $\mathcal{O}(n)$ can be computed in $\mathcal{O}(n)$ time. Lemma 4.37 then implies a runtime of $\mathcal{O}(n)$ for creating a structure of every node that does not contain f_c. For nodes containing f_c, we first limit the possible size of any structure $\mathcal{S}$ of a node. The size of a structure $\mathcal{S}$ is dependent on the number of possible oriented spiralities (σ^s, σ^t). An in absolute terms high value for σ^s requires at least an equal amount of vertices for rotations to somewhere create an edge with a label of the opposite sign. The same holds true for σ^t. Therefore, $\mathcal{S}$ has size $\mathcal{O}(n)$.

For the marked $\mathcal{P}$-node creating f_c, Lemmas 4.47 and 4.52 imply a constant-time algorithm to compute its structure, as only a constant amount of cases have to be checked. For $\mathcal{S}$-nodes, Lemma 4.53 implies a linear-time algorithm to calculate its structure because each structure-entry only takes a constant amount of time to check. For an unmarked $\mathcal{P}$-node containing f_c with induced graph G, let first G_b be its ortholinear-plane subgraph not containing f_c. Calculating which step values $\int(\mathcal{H}_b)$ and $\int(\overline{\mathcal{H}_b})$ are possible over all orthogonal representation $\mathcal{H}_b$ of G_b takes a constant amount of time with Lemma 4.46. Then it also only takes a constant amount of time to check each structure-entry and a structure for the $\mathcal{P}$-node can be calculated in linear time. With the size of the decomposition tree being $\mathcal{O}(n)$, the total runtime is $\mathcal{O}(n^2)$. □

4.3 General Series-Parallel 3-Graphs

In this section, we extend the approach for 2-legged series-parallel plane 3-graph, described in Sections 4.1 and 4.2, to general series-parallel plane 3-graph. The difference between the two is that a 2-legged series-parallel plane 3-graph requires $\deg(s) = \deg(t) = 1$ whereas for general series-parallel plane 3-graph we may have $\deg(s), \deg(t) \in [1, 3]$. General series-parallel 3-graphs are recursively defined by combining single edges in series and parallel-compositions. As a single edge has degree 1 at each terminal and a series-composition does not change the degree of the resulting terminals, we know that the terminals of an SP-graph with a degree other than 1 must have been created at some parallel-composition.

Looking at the subgraphs of this parallel-composition, there are two possibilities. Either the subgraphs have only one edge incident to the terminal or two. If a subgraph has only one edge incident to both terminals of the parallel composition, this subgraph is a 2-legged SP-graph, like the leftmost subgraph of the left parallel-composition in Figure 4.38. If it has two edges incident, like the left child of the middle parallel-composition in Figure 4.38, we can artificially add an extra leg to the terminal of the subgraph to again make it

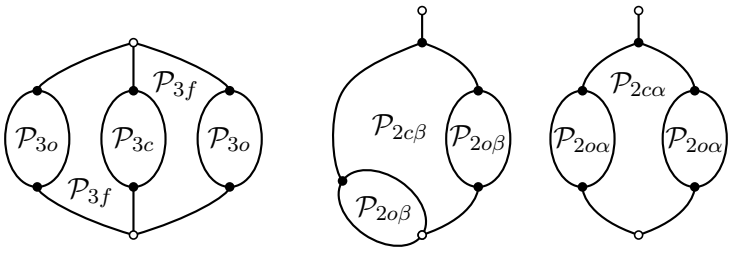

Figure 4.38: The special cases for general series-parallel 3-graphs. A label in some face or subgraph indicates how this case is named if the central face is found in this part of the graph.

2-legged. This artificial leg obviously influences thestructure of the subgraph and therefore special treatment is later required here. Nevertheless, after a single parallel-composition with terminals of degree other than 1, we again only have to handle 2-legged SP-graphs. Therefore, only a few special cases have to be taken into consideration at these parallel-compositions. Further downwards in the composition tree all the results of Section 4.2 about 2-legged SP-graphs apply. Moreover, a single SP-graph can contain at most two such special parallel compositions because at least one of the terminals of a special parallel composition has a degree other than 1 and no further composition is here. This implies that this terminal must also be a terminal of the whole graph, of which only two exist.

As the goal is to find ortho-radial representations, the position of the central face f_c is also important to decide which special case applies in a specific instance. To define all special cases, Figure 4.38 shows parallel compositions with terminals of degree other than 1. A label in some face or subgraph indicates how this case is named if the central face is found in this part of the graph. The subscript of the label encodes the special case as follows. The first digit, 2 or 3, indicates the number of children of the special case. An optional greek letter further subdivides this case, and the final letter is either "c" if f_c is contained in the middle child, "o" if f_c is contained in the left or right child, or "f" if it is contained in a newly created face of the parallel composition. In the case that the parallel composition has two subgraphs we get the following cases. First, it may be that one, or both terminals have a degree of 2 and are therefore simply missing the leg of a 2-legged SP-graph. We call this case $\mathcal{P}_{2\alpha f}$ if the central face is created at the parallel composition, or $\mathcal{P}_{2\alpha 0}$ if the central face is contained in one of the two children. If we have a degree of 3 for some terminal, then one subgraph has twi incident edges to the terminal. Therefore, it must directly start with a parallel composition missing the leg in the subgraph. We call this case $\mathcal{P}_{2\beta f}$ if the central face is created at the parallel composition, or $\mathcal{P}_{2\beta 0}$ if it is contained in a subgraph. If one terminal has degree 3 and the other degree 2, we still use the cases $\mathcal{P}_{2\beta f}$ and $\mathcal{P}_{2\beta 0}$. In the case that the parallel composition has three children, all three subgraphs have to be 2-legged. From this, the cases $\mathcal{P}_{3c}$, where f_c is contained in the central subgraph, $\mathcal{P}_{3o}$, where f_c is contained in one of the outer subgraphs, and $\mathcal{P}_{3f}$, where f_c is one of the two newly created faces, arise. Finally, for a parallel composition with degree 2 at one terminal and degree 1 at the other, as may be the case for $\mathcal{P}_{2\alpha f}$ or $\mathcal{P}_{2\alpha 0}$, there could also be the case that the central face is contained in a serially joined 2-legged SP-graph, connected to the terminal that has degree 1. Here, an artificial leg can be added to make the graph 2-legged without sacrificing equality. This is due to the face that if an orthogonal representation of the special parallel composition exists, then with Lemma 4.7 there also exists one with a non-negative rotation at the terminal with degree 2 by possibly reducing the spirality of a subgraph. And with a non-negative rotation there is always space to add a leg at this terminal. The decomposition tree as defined for 2-legged SP-graphs can still be used for all the special cases by simply marking the non-2-legged $\mathcal{P}$-node with a label indicating

Figure 4.39: Examples of the case $\mathcal{P}_{2\alpha f}$ with degree 2 at some terminal. They take advantage of the fact that a negative clockwise rotation is possible at either s (a) or t (b).

the special case. We now cover a few cases separately and then show that the rest can be reduced to using Lemma 4.54.

First, the case $\mathcal{P}_{2\alpha f}$. At a normal parallel composition of a 2-legged SP-graph, the rotations $\text{rot}(e_1^t, e_2^t)$ and $\text{rot}(e_2^s, e_1^s)$ between the legs of the two subgraphs must always be greater than 0. This is due to the fact that in the middle the leg of the terminal is present. As this leg is missing in the $\mathcal{P}_{2\alpha f}$ case, this rotation can also be negative. See Figure 4.39a for an example where $\text{rot}(e_2^s, e_1^s) = -1$. The following lemma shows that this property is enough to make every such $\mathcal{P}$-node orthoradial-plane.

Lemma 4.56. *Let ϕ be a $\mathcal{P}$-node for which the case $\mathcal{P}_{2\alpha f}$ applies and where its children ϕ_1 and ϕ_2 both are rectilinear-plane. Then ϕ is also orthoradial-plane.*

Proof. As the case $\mathcal{P}_{2c\alpha}$ applies, the parallel connection has degree 2 at either s or t or both and the other terminal has degree 1. If Lemma 4.23 implies the existence of a valid ortho-radial representation using the structures of ϕ_1 and ϕ_2, then G admits the same representation, only without the extra leg at the terminals that now have degree 2.

If Lemma 4.23 does not imply a valid ortho-radial representation, then Equation (4.16) does not hold. Using Lemma 4.20 we know that this is only possible for the step values $[s_1^l, s_1^r, s_1^z] = [0, 0, 1]$ and $[s_2^l, s_2^r, s_2^z] = [x, y, 0]$, $x, y \in \mathbb{N}$ or the inverse assignment. Without loss of generality, let the step values be as they are shown above. Then there exists an OR $\mathcal{H}_2$ of G_2 such that $\sigma(\mathcal{H}_2) = 0$ and every st-path through G_2 has a positive relative label. Moreover, an OR $\mathcal{H}_1$ of G_1 must exist with $\sigma(\mathcal{H}_1) = 0$. Suppose $\deg(s) = 2$ and $\deg(t) = 1$. The two orthogonal representations can be combined into a representation $\mathcal{T}$ of G with rotations $\text{rot}(e_1^t, e_2^t) = 1$ and $\text{rot}(e_2^s, e_1^s) = -1$. The usage of $\text{rot}(e_2^s, e_1^s) = -1$ is possible here, as $\deg(s) = 2$. Figure 4.39a shows this case. We then know that

$$\text{rot}(f_c) = \text{rot}(f_o) = \sigma(\mathcal{H}_1) + \underbrace{\text{rot}(e_1^t, e_2^t)}_{1} - \sigma(\mathcal{H}_2) = 0 + \underbrace{\text{rot}(e_2^s, e_1^s)}_{=-1} = 0$$

and $\mathcal{T}$ is an ortho-radial representation. Now let e_2^s be the reference edge directed such that it points to the outside of G_2 and let $\mathcal{C}$ be an arbitrary simple essential cycle in $\mathcal{T}$. Then $\ell(\vec{e_1^s}) = \text{rot}(e_2^s, e_1^s) = -1$. Let $\overleftarrow{e} \in G_2$ be the edge contained $\mathcal{C}$ that has a positive relative label in $\mathcal{H}_2$. It follows that

$$\ell(\overleftarrow{e}) = \underbrace{\ell(\overleftarrow{e}) + \text{rot}(C[e, e_2^s])}_{=\text{rot}(C)=0} - \underbrace{\text{rot}(C[e, e_2^s])}_{=-\ell_{s_2}(e)<0} > 0$$

Therefore $\mathcal{C}$ contains the positively-labelled edge e and the negatively-labelled edge e_1^s and, as $\mathcal{C}$ was arbitrary, $\mathcal{T}$ must be a valid ortho-radial representation.

Now if $\deg(s) = 1$ and $\deg(t) = 2$, then the same argumentation but with $\text{rot}(e_1^t, e_2^t) = -1$ and $\text{rot}(e_2^s, e_1^s) = 1$ implies the statement as also seen in Figure 4.39b. If both terminals

have degree 2, then one terminal can be selected to have a negative rotation, while the other terminal has a positive one. □

In the case $\mathcal{P}_{2\beta f}$, there exists at least one subgraph missing a leg. This subgraph is then not 2-legged anymore and therefore the results of Section 4.1 can not be used to describe it. But this connection point has a similarity to the series connection in Figure 4.3. There, the problem was that a normal series composition of SP-graphs may leave one child of the 2-legged SP-graph without a leg. The solution was to share the connecting leg between the two subgraphs and when connecting them in series, the two legs get merged into one edge again. The same idea is used here in the case $\mathcal{P}_{2\beta f}$. This results in a parallel composition, where at one, or maybe even both terminals, not a parallel connection but a series one is performed.

Lemma 4.57. *Let ϕ be a $\mathcal{P}$-node for which the case $\mathcal{P}_{2\beta f}$ applies and where its children ϕ_1 and ϕ_2 both are rectilinear-plane. Let G be the induced graph of ϕ and G_1 and G_2 be the induced graphs of ϕ_1 and ϕ_2. Then ϕ is orthoradial-plane if and only if the matching condition holds.*

1. *If $\deg(s) = 1$ and $\deg(t) = 3$, then for the series composition of G_1 and $\overline{G_2}$ one of $s^{lr} = 1$, $s^z = 1$, $-1 \in s(1)$, or $-1 \in s(-2)$ holds.*
2. *If $\deg(s) = 3$ and $\deg(t) = 1$, then for the series composition of $\overline{G_2}$ and G_1 one of $s^{lr} = 1$, $s^z = 1$, $-2 \in s(1)$, or $-1 \in s(-2)$ holds.*
3. *If $\deg(s) = 3$ and $\deg(t) = 3$, then for the series composition of G_1 and $\overline{G_2}$ one of $s^{lr} = 1$, $s^z = 1$, $0 \in s(2)$, or $0 \in s(-2)$ holds.*
4. *If $\deg(s) = 2$ and $\deg(t) = 3$, then for the series composition of G_1 and $\overline{G_2}$ one of $s^{lr} = 1$, $s^z = 1$, $-1 \in s(1)$, $-1 \in s(-2)$, $1 \in s(-1)$, or $1 \in s(2)$ holds.*
5. *If $\deg(s) = 3$ and $\deg(t) = 2$, then for the series composition of $\overline{G_2}$ and G_1 one of $s^{lr} = 1$, $s^z = 1$, $-1 \in s(1)$, $-1 \in s(-2)$, $1 \in s(-1)$, or $1 \in s(2)$ holds.*

Proof. We explicitly prove equality only for the first condition, and then explain how the proof can be adapted to the others.

Case 1: $\deg(s) = 1$ and $\deg(t) = 3$. Let $[s, s^z, s^{lr}]$ be the structure of the series composition H of G_1 and $\overline{G_2}$ with legs e^s and e^t. The idea is to create an orthogonal representation of H and to the connect the legs e^s and e^t as in a parallel composition to create an ortho-radial representation. See for example Figure 4.40a, where an orthogonal representation of H with spirality 0 is wrapped around the center of the ortho-radial grid and connected at e^s and e^t. With $r \in \{0, 1\}$ being the rotation between e^t and e^s, the legs of an orthogonal representation $\mathcal{H}$ of H can be connected with a new leg to form an ortho-radial representation of G if $0 = \text{rot}(f_c) = \text{rot}(f_o) = \sigma(\mathcal{T}) + r$. This implies $\sigma(\mathcal{T}) \in \{0, -1\}$. A simple essential cycle of the ortho-radial representation is then equivalent to an st-path of H. If $s^{lr} = 1$ or $s^z = 1$, then using the respective representations with $r = 0$ obviously results in a valid ortho-radial representation with $e^* = e^s$. The case $s^{lr} = 1$ is shown in Figure 4.40a. Having $-1 \in s(1)$ similarly results in a valid ortho-radial representation with $e^* = e^s$ since every st-path contains the negatively-labelled edge e^t and also an edge with label 1 (see Figure 4.40b). If $-1 \in s(-2)$, using $e^* = e^t$ results in a label of $\ell(\vec{e^s}) = 1$, because r must be 1. Figure 4.40c shows this case. Then every edge e with relative label -2 has normal label $\ell(\vec{e}) = -2 + 1 = -1$ and the representation is again valid.

Conversely, if a valid ortho-radial representation $\mathcal{T}$ of G exists with $x \coloneqq \ell(\vec{e^s})$, then when splitting it up at the leg vertex of s, an orthogonal representation of the series composition

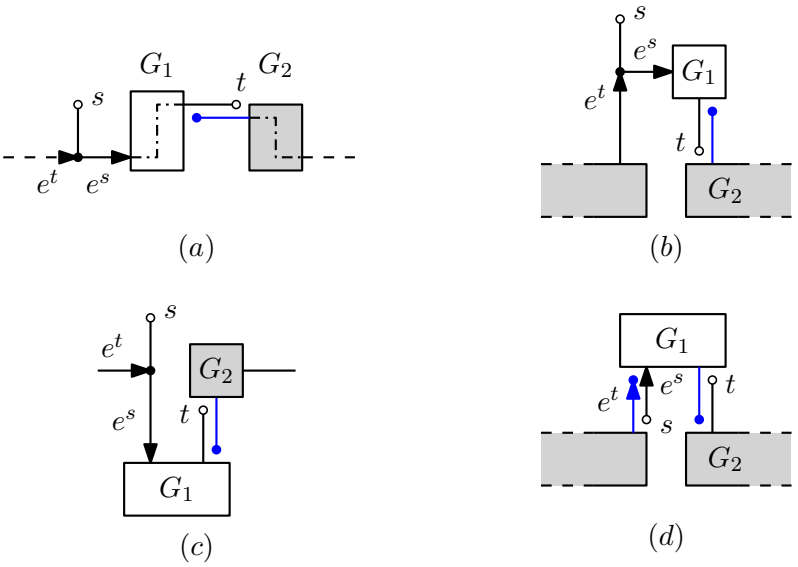

Figure 4.40: Examples of the case $\mathcal{P}_{2\beta f}$. The vertices s and t represent the terminals of the composed graph. After merging, t is contained in G_2 for every example. The blue legs are the artificially added legs used to create a series-composition and the legs e^s, e^t of this series-composition are connected to form an ortho-radial representation. For (d), also these legs get merged, as $\deg(s) = \deg(t) = 3$ in this case.

of G_1 and $\overline{G_2}$ is created. For this representation we know that $\ell_s(e^t) = -r \in \{0, -1\}$. There are now two possibilities.

Case 1a: Every st-path of H contains an edge e_+ with a positive label in $\mathcal{T}$, for which $\ell_s(e_+) = \ell(\vec{e_+}) - x \geq -x + 1$, and an edge e_- with a negative label in $\mathcal{T}$, for which $\ell_s(e_-) = \ell(\vec{e_-}) - x \leq -x - 1$. If $x > 0$, then e^s already has a positive label and $\ell_s(e_-) \leq -x - 1 \leq -2$ implies $y \in s(-2)$ with $y = \ell_s(e^t) \in \{0, -1\}$. Using Lemma 4.32, both cases imply that $-1 \in s(-2)$. If $x = 0$, then $\ell(\vec{e}) = \ell_s(e)$ for every edge $e \in H$, so $\ell_s(e_+) > 0$ and $\ell_s(e_-) < 0$. If also $\ell_s(e^t) = 0$ it follows that $s^{lr} = 1$ and if $\ell_s(e^t) = -1$, it follows that $-1 \in s(1)$. If finally $x < 0$, then $\ell_s(e_+) \geq -x + 1 \geq 2$ and it follows that $y \in s(2)$ with $y = \ell_s(e^t) \in \{0, -1\}$. Using Lemma 4.32 this always implies $-1 \in s(1)$.

Case 1b: There exists a simple essential cycle having only edges with label 0 in $\mathcal{T}$. Then especially $\ell(\vec{e^s}) = 0$ and the corresponding st-path of H therefore also has only edges with relative label 0. This implies $s^z = 1$ for H.

Case 2: $\deg(s) = 3$ and $\deg(t) = 1$. The argumentation of Case 1 can directly be used to show equivalence for this case. Only the series composition H is constructed differently.

Case 3: $\deg(s) = 3$ and $\deg(t) = 3$. For the " $\Longrightarrow$ "-direction, the series composition H of G_1 and $\overline{G_2}$ with legs e^s and e^t can now only be connected with $r = 0$ since also e^s and e^t get merged into a single edge (see Figure 4.40d where the condition $0 \in s(2)$ is used). For the conditions $s^{lr} = 1$ or $s^z = 1$, this is already given as shown in Case 1. For the condition $0 \in s(2)$ and $0 \in s(-2)$ this is also possible since the spirality in both cases is 0. When picking a reference edge such that $\ell(\vec{e^s}) = -1$ for $0 \in s(2)$ and $\ell(\vec{e^s}) = 1$ for $0 \in s(-2)$, then the validity can be shown similar to Case 1. The " $\Longrightarrow$ "-direction follows with the argumentation of Case 1 when using $r = 0$.

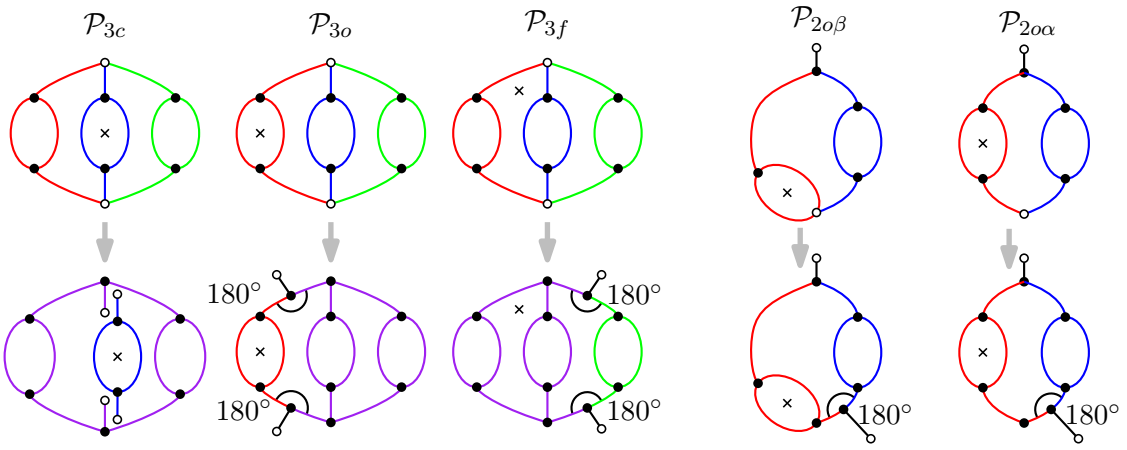

Figure 4.41: For each special case a depiction of how it can be reduced to 2-legged series-parallel 3-graphs.

Case 4: $\deg(s) = 2$ and $\deg(t) = 3$ or $\deg(s) = 3$ and $\deg(t) = 2$. In these cases, the rotation value r may also have the value -1 and the same argumentation as in Case 1, implies the equivalence. □

Any other special case not covered in Lemmas 4.56 and 4.57 can simply be reduced to handling 2-legged series-parallel 3-graphs. For this we define G_l and G_r to be the left and right subgraph of a special parallel composition, and if the composition has three children, then G_c also denotes the central subgraph. Figure 4.41 gives a graphical example for every of the following cases. For $\mathcal{P}_{3c}$, the graph can be split up into two 2-legged series-parallel 3-graphs. One consisting of G_c, where also the central face is contained, and one we call G_j consisting of G_l and G_r joined with a copy of the legs of G_c. If we can create a valid representation for both subgraphs separately and ensure that their legs have opposing orientations, we can merge the legs together to form a valid representation of the whole graph. The new subgraph G_j is again 2-legged but the induced embedding of G_j is not an outer embedding because the legs are incident to the central instead of the outer face. Barth et al. [BNRW21, Lemma 6] have defined so-called flipped representations, which in essence swap the central and inner face in the embedding. The resulting embedding of this process is then again outer and the results of Section 4.1 can be used to find an st-outwards valid ortho-radial representation. When flipping the representation back, the legs point inwards to the center and can therefore be merged again with an st-outwards representation of G_c. Conversely, if a valid ortho-radial representation of $\mathcal{P}_{3c}$ exists, Lemma 4.23 implies that there also exists a valid ortho-radial representation of G_c and the flip of G_j, both of which are st-outwards.

For $\mathcal{P}_{3o}$, where without loss of generality G_l contains f_c, the graph can be split up into the 2-legged series-parallel 3-graphs G_l and one we call G_j consisting of G_c and G_r joined with temporary legs to make it 2-legged. Both graphs can then be connected via a parallel composition. Given a valid ortho-radial representation of this new parallel composition, a representation of $\mathcal{P}_{3o}$ can be created by removing the new legs of the parallel composition and merging the temporary legs of G_j with the ones from G_l. This process is not possible though if the legs of G_l and G_j do not align correctly. But by enforcing an internal angle at the leg-vertices of the new parallel composition of 180°, the legs of G_j and G_l can always be merged, as they have opposite orientations. Then every valid ortho-radial representation of the constructed parallel composition translates to a valid ortho-radial representation of $\mathcal{P}_{3o}$. The angle of 180° can be enforced by considering only the rotation combination $r_1^s, r_1^t = -1$ and $r_2^s = r_2^t = 1$ in Lemma 4.54. Conversely, a valid ortho-

radial representation of $\mathcal{P}_{3o}$ always translates to a valid ortho-radial representation of the constructed parallel composition by subdividing the legs of G_l and adding new legs.

The other cases can be handled similarly. For $\mathcal{P}_{3f}$, where without loss of generality f_c is between G_l and G_c, the graph can be split up into the 2-legged series-parallel 3-graphs G_r and one we call G_j consisting of G_l and G_c joined with temporary legs to make it 2-legged. A parallel composition with a fixed inner angle of 180° can then be used similarly to the $\mathcal{P}_{3o}$-case. For $\mathcal{P}_{2\beta 0}$, every subgraph not being 2-legged gets a temporary leg and if a terminal has degree 2 as in the $\mathcal{P}_{2\alpha 0}$ case, then one of the subgraphs is serially composed with a $\mathcal{D}$-node to represent the possible rotations at the terminal. In both cases the same approach using a parallel-composition with a fixed inner angle of 180° can then be used as in the $\mathcal{P}_{3o}$-case.

The following theorem summarizes the results of this section and gives a polynomial bound to the runtime of creating a bend-free valid ortho-radial representation of a general series-parallel plane 3-graph.

Theorem 4.58. *Given a series-parallel plane 3-graph $(G, \mathcal{E})$, a fixed outer face f_o, and a fixed inner face f_c, a bend-free valid ortho-radial representation of G, if one exists, can be found in $\mathcal{O}(n^2)$ time.*

Proof. The runtime of $\mathcal{O}(n^2)$ to check if a bend-free valid ortho-radial representation exists follows from Lemma 4.55, the fact that Lemmas 4.56 and 4.57 require constant time to compute, and the fact that the other special cases can be reduced to handling 2-legged series-parallel 3-graphs. The actual creation of an ortho-radial representation can then be handled similar to Theorem 4.25. □

5. Conclusion

The TSM-framework of Tamassia [Tam87], created for finding orthogonal drawings of a graph, has been used by Barth et al. [BNRW21] to find ortho-radial drawings instead. In the intermediate step of both approaches, a representation of the drawing must be found that only describes the angles between edges and excludes the concrete lengths of an edge. The definition of orthogonal representations for orthogonal drawings and ortho-radial representations for ortho-radial drawings share many similarities. In the ortho-radial case, the existence of only a so-called valid ortho-radial representation, which adds global conditions for essential cycles, is equivalent to the existence of an ortho-radial drawing. However, efficient algorithms for finding such a valid ortho-radial drawing were not known. In this work we showed that in contrast to orthogonal representations, the problem of finding a bend-free valid ortho-radial representation is NP-complete for general plane 4-graphs. This directly implies that finding an ortho-radial drawing for such graphs is NP-complete as well. Moreover, we have also shown that when restricting the graph to be a series-parallel plane 3-graph, efficient algorithms for finding bend-free valid ortho-radial representations exist. When the graph is restricted further to be a 2-legged series-parallel plane 3-graph, even a bend-minimum valid ortho-radial representation can be efficiently searched for.

Future work can still be put into extending the shown algorithm for series-parallel 3-graphs to a less restrictive class of graphs, like general 3-graphs or series-parallel 4-graphs. Orthogonal representations can in both cases be found using so-called splines [DBLV98][DKLO22], which are a natural extension to the st-paths of 2-legged SP-graphs. It may therefore be possible to also define properties, similar to step values, using these splines, and build up a recursive algorithm. Moreover, it may also be possible to use the concepts introduced in this work and use the branch-width of a graph to formulate a parameterized algorithm on sphere-cut decompositions even for general 4-graphs.

Another point for improvement could be to search for a valid ortho-radial representation over all possible outer embeddings as well as every assignment of the outer and central face of a series-parallel 3-graph. The embedding of an SP-graph with terminals s and t is encoded by the order of child nodes at every $\mathcal{P}$-node in the decomposition tree. By checking all arrangements of subgraphs for each node, one automatically searches over all possible outer embeddings. The open question here is how efficiently one can test all possible assignments of the outer and central face as well as all possible terminals s and t (as these change the decomposition tree).

Finally, this work only gives an approach to find bend-free, and not bend-minimum, valid ortho-radial representations for general series-parallel 3-graphs. It is imaginable that the same concept as in Section 4.1.3 can give a polynomial time algorithm to also find bend-minimum representations for these graphs.

Bibliography

[BBR14] Thomas Bläsius, Guido Brückner, and Ignaz Rutter. Complexity of higher-degree orthogonal graph embedding in the kandinsky model. In Andreas S. Schulz and Dorothea Wagner, editors, *Algorithms - ESA 2014*, pages 161–172. Springer Berlin Heidelberg, 2014.

[BK94] Therese Biedl and Goos Kant. A better heuristic for orthogonal graph drawings. In Jan van Leeuwen, editor, *Algorithms — ESA '94*, pages 24–35. Springer Berlin Heidelberg, 1994.

[BKRW11] Thomas Bläsius, Marcus Krug, Ignaz Rutter, and Dorothea Wagner. Orthogonal graph drawing with flexibility constraints. In Ulrik Brandes and Sabine Cornelsen, editors, *Graph Drawing*, pages 92–104. Springer Berlin Heidelberg, 2011.

[BLR15] Thomas Bläsius, Sebastian Lehmann, and Ignaz Rutter. Orthogonal graph drawing with inflexible edges. In Vangelis Th. Paschos and Peter Widmayer, editors, *Algorithms and Complexity*, pages 61–73. Springer International Publishing, 2015.

[BNRW21] Lukas Barth, Benjamin Niedermann, Ignaz Rutter, and Matthias Wolf. A topology-shape-metrics framework for ortho-radial graph drawing, 2021.

[CK12] Sabine Cornelsen and Andreas Karrenbauer. Accelerated bend minimization. *Journal of Graph Algorithms and Applications*, 16(3):635–650, 2012.

[DBLV98] Giuseppe Di Battista, Giuseppe Liotta, and Francesco Vargiu. Spirality and optimal orthogonal drawings. *SIAM Journal on Computing*, 27(6):1764–1811, 1998.

[DKLO22] Walter Didimo, Michael Kaufmann, Giuseppe Liotta, and Giacomo Ortali. Computing bend-minimum orthogonal drawings of plane series-parallel graphs in linear time, 2022.

[GT97] Ashim Garg and Roberto Tamassia. A new minimum cost flow algorithm with applications to graph drawing. In Stephen North, editor, *Graph Drawing*, pages 201–216. Springer Berlin Heidelberg, 1997.

[GT01] Ashim Garg and Roberto Tamassia. On the computational complexity of upward and rectilinear planarity testing. *SIAM Journal on Computing*, 31(2):601–625, 2001.

[HHT09] Mahdieh Hasheminezhad, S. Mehdi Hashemi, and Maryam Tahmasbi. Ortho-radial drawing of graphs. *The Australasian Journal of Combinatorics [electronic only]*, 44, 06 2009.

[NR20] Benjamin Niedermann and Ignaz Rutter. An integer-linear program for bend-minimization in ortho-radial drawings. In David Auber and Pavel Valtr,

editors, *Graph Drawing and Network Visualization*, pages 235–249. Springer International Publishing, 2020.

[REN06] Md. Saidur Rahman, Noritsugu Egi, and Takao Nishizeki. No-bend orthogonal drawings of series-parallel graphs. In Patrick Healy and Nikola S. Nikolov, editors, *Graph Drawing*, pages 409–420. Springer Berlin Heidelberg, 2006.

[Tam87] Roberto Tamassia. On embedding a graph in the grid with the minimum number of bends. *SIAM Journal on Computing*, 16(3):421–444, 1987.

[TTV91] R. Tamassia, I.G. Tollis, and J.S. Vitter. Lower bounds and parallel algorithms for planar orthogonal grid drawings. In *Proceedings of the Third IEEE Symposium on Parallel and Distributed Processing*, pages 386–393, 1991.

[ZN05] Xiao Zhou and Takao Nishizeki. Orthogonal drawings of series-parallel graphs with minimum bends. In Xiaotie Deng and Ding-Zhu Du, editors, *Algorithms and Computation*, pages 166–175. Springer Berlin Heidelberg, 2005.